DISSERTATION

QUANTIFYING SCALE RELATIONSHIPS IN SNOW DISTRIBUTIONS

Submitted by

Jeffrey S. Deems

Department of Geosciences

In partial fulfillment of the requirements

For the Degree of Doctor of Philosophy

Colorado State University

Fort Collins, Colorado

Summer 2007

COLORADO STATE UNIVERSITY

May 10, 2007

WE HEREBY RECOMMEND THAT THE DISSERTATION PREPARED UNDER OUR SUPERVISION BY JEFFREY S. DEEMS ENTITLED QUANTIFYING SCALE RELATIONSHIPS IN SNOW DEPTH DISTRIBUTIONS BE ACCEPTED AS FULFILLING IN PART REQUIREMENTS FOR THE DEGREE OF DOCTOR OF PHILOSOPHY.

Committee on Graduate Work

_____
Kelly J. Elder

_____
Glen E. Liston

_____
Thomas H. Painter

_____
Steven R. Fassnacht, **Adviser**

_____
Sally J. Sutton, **Department Head**

ABSTRACT OF DISSERTATION

QUANTIFYING SCALE RELATIONSHIPS

IN SNOW DEPTH DISTRIBUTIONS

Spatial distributions of snow in mountain environments represent the time integration of accumulation and ablation processes, and are strongly and dynamically linked to mountain hydrologic, ecologic, and climatic systems. Accurate measurement and modeling of the spatial distribution and variability of the seasonal mountain snowpack at different scales are imperative for water supply and hydropower decision-making, for investigations of land-atmosphere interaction or biogeochemical cycling, and for accurate simulation of earth system processes and feedbacks.

Assessment and prediction of snow distributions in complex terrain are heavily dependent on scale effects, as the pattern and magnitude of variability in snow distributions depends on the scale of observation. Measurement and model scales are usually different from process scales, and thereby introduce a scale bias to the estimate or prediction. To quantify this bias, or to properly design measurement schemes and model applications, the process scale must be known or estimated. Airborne Light Detection And Ranging (lidar) products provide high-resolution, broad-extent altimetry data for terrain and snowpack mapping, and allow an application of variogram fractal analysis techniques to characterize snow depth scaling properties over lag distances from 1 to 1000 meters.

Snow depth patterns as measured by lidar at three Colorado mountain sites exhibit fractal (power law) scaling patterns over two distinct scale ranges, separated by a distinct break at the 15-40 m lag distance, depending on the site. Each fractal range represents a range of separation distances over which snow depth processes remain consistent.

The scale break between fractal regions is a characteristic scale at which snow depth process relationships change fundamentally. Similar scale break distances in vegetation topography datasets suggest that the snow depth scale break represents a change in wind redistribution processes from wind/vegetation interactions at small lags to wind/terrain interactions at larger lags. These snow depth scale characteristics are interannually consistent, directly describe the scales of action of snow accumulation, redistribution, and ablation processes, and inform scale considerations for measurement and modeling.

Snow process models are designed to represent processes acting over specific scale ranges. However, since the incorporated processes vary with scale, the model performance cannot be scale-independent. Thus, distributed snow models must represent the appropriate process interactions at each scale in order to produce reasonable simulations of snow depth or snow water equivalent (SWE) variability. By comparing fractal dimensions and scale break lengths of modeled snow depth patterns to those derived from lidar observations, the model process representations can be evaluated and subsequently refined. Snow depth simulations from the SnowModel seasonal snow process model exhibit fractal patterns, and a scale break can be produced by including a sub-model that simulates fine-scale wind drifting patterns. The fractal dimensions provide important spatial scaling information that can inform refinement of process representations. This collection of work provides a new application of methods developed in other geophysical fields for quantifying scale and variability relationships.

Jeffrey S. Deems
Department of Geosciences
Colorado State University
Fort Collins, CO 80523
Summer 2007

ACKNOWLEDGEMENTS

Firstly, I would like to thank my advisor, Dr. Steven Fassnacht, for the friendship, support, and advice he has provided me for the past several years. We share common ground on many subjects, which enabled us to explore and forge our viewpoints on a diverse array of scientific, cultural, and philosophical topics. I am also most grateful to my committee, Drs. Kelly Elder, Glen Liston, and Tom Painter, whose encouragement and insight have inspired me to push my abilities and to explore new ways to apply myself.

My research was supported by NASA Headquarters under Earth System Science Fellowship Grant NNG04GQ40H, which provided not only financial support, but also the academic independence to pursue a research line of my own choosing. I also owe thanks to the Randy Cook Memorial Scholarship at CSU, which helped defray additional costs.

I would like to extend thanks to the NASA CLPX field crews for excellent field data and adventures. Specific thanks go to Kelly Elder and Gus Goodbody (USDA Forest Service), Don Cline (NOAA/NOHRSC), and Bert Davis (USACE CRREL) for their efforts in planning, organizing, conducting, and funding the stupendous CLPX efforts, upon which my research relied.

To my many friends who sustained and encouraged both my studies and extracurricular pursuits – thank you all for your friendship and partnership, and the tremendous experiences we have shared in the outdoors far and near. Thanks also to my peers, for many insightful and exciting intellectual ramblings on snow and earth systems – those interactions are a big part of what makes science fun!

My family has provided incalculable strength, support, and inspiration, without which I can truly say my education and research effort would not have been possible. Thank

you to my parents, Ward and Nancy, and to my brother Jeremy and sister-in-law Paula – you have all showed me endless love and encouragement, and allowed me to find strengths that I did not know that I had.

And to Claudia, thank you for your love and laughter, and for helping me to maintain a foundation of perspective – on my life, my work, and my heart.

CONTENTS

CHAPTER 1: INTRODUCTION

The spatial distribution of snow in mountain environments represents the time integration of accumulation and ablation processes, and forces mountain hydrologic, ecologic, and climatic systems. Seasonal snow distributions in midlatitude mountain environments exert a strong influence on biogeochemical cycles (Brooks and Williams, 1999), ecological systems (Jones, 1999; Jones *et al.*, 2001), climate patterns (Cohen and Rind, 1991), land-atmosphere interactions (Liston, 1999), and local to regional water budgets. Many studies have observed and modeled the importance of snow on these land-surface processes, from local to global scales (e.g., Liston, 2004), with attendant climatic, biologic, and hydrologic feedbacks. Accurate modeling of the spatial distribution and structure variability of the seasonal mountain snowpack at different scales is imperative for correct simulation of earth system processes and feedbacks.

Snow represents the fundamental water resource in the semiarid western US, providing up to 75% of surface water runoff in a single year. More than 60 million residents of the western United States depend on snowmelt-dominated hydrologic systems to meet municipal, agricultural, and ecosystem demands for water supply (Bales *et al.*, 2006). Fifty to seventy percent of the precipitation in the mountain regions of the western US falls as snow (Serreze *et al.*, 1999), which represents the major storage component of the annual hydrologic cycle in snowmelt-fed river systems. Societal dependence on snowmelt systems has driven the development of an extensive monitoring network of snow courses and automated monitoring stations (SNOTEL) in the western US. Data from these networks are used as indices of runoff volume for water supply, flood, and hydropower operation forecasts, and are based on empirical relationships between the point observations and streamflow (Bales *et al.*, 2006). These forecasting

methods are most successful when the hydroclimatic conditions are within the envelope defined by the period of record. In conditions that are poorly represented historically, such as extreme conditions, forecasting ability decreases substantially (Pagano *et al.*, 2004).

Recent studies showing strong trends in climatic precipitation and temperature signals (e.g. Mote *et al.*, 2005), when combined with the demonstrated sensitivity of western US snowpacks to large snowfall events (Serreze *et al.*, 2001), suggest that forecasting efforts would benefit from distributed measurement of snow volumes and properties to support model simulations. Progress in these areas would allow managers and researchers to build process-based forecasts for hydroclimatic conditions that are not represented in the historical record, and to more readily respond to rapid change in snowpack conditions due to extreme weather events.

1.1 Spatial Snow Data And Variability

Acquiring spatial datasets of snowpack properties in mountainous terrain is challenging due to spatial heterogeneity in the snowpack, the rate of snowpack change, and danger to field workers due to snow avalanches (Elder *et al.*, 1991). While detailed, spatially distributed datasets have been collected for specific research interests, they are limited in spatial and temporal extent. Manual data collection of spatial snow properties entails mostly destructive, spatially limited sampling, and cannot provide exact repetition of sampling at fine time intervals. Furthermore, the complexity of snow system process interactions and poorly understood scaling relationships complicate accurate extrapolation from sparse measurement networks or manual surveys to a spatially distributed datasets.

In contrast, several remote sensing options exist that provide rapid, safe, and non-destructive collection of various spatial snow properties (Dozier and Painter, 2004). Optical imaging sensors have shown value for mapping snow albedo, grain size, and

fractional snow-covered area (SCA) at a variety of spatial and temporal resolutions (Rosenthal and Dozier, 1996; Painter *et al.*, 2003; 2007). Gamma radiation sensors on airborne platforms are currently used operationally for estimating snow water equivalent (SWE) integrated over individual flight lines (Carroll *et al.*, 2001). Passive and active microwave sensors have been the subject of intensive research campaigns in recent years, and show much promise for SWE estimation over large areas (e.g. Cline *et al.*, 2003). Remote sensing data sources can supply snow cover information at broad spatial extents and offer repeat sampling at higher temporal resolution than is feasible with ground-based collection campaigns.

Light Detection And Ranging (lidar) products from airborne sensors provide a unique combination of high-resolution and broad-extent elevation data for terrain and snowpack mapping (Hopkinson *et al.*, 2001; Deems *et al.*, 2006), and provide an excellent source of distributed snow depth, land surface elevation, and vegetation structure and height data (Lefsky *et al.*, 2002). Lidar data may be acquired with high resolution and relatively broad spatial extent, which are properties consistent with the scales of variability in snow. Because of these scale properties, lidar provides the best available method for mapping snow depth distribution and for investigation of process interactions over a range of variability scales relevant to hydrologic interests in mountain environments (10^0-10^4 m).

Efforts to assess or predict snow distributions in complex terrain are heavily dependent on scale effects; measurement or model scales are constrained by field measurements, sensor or computational limitations, and are usually different from scales of process interactions. The pattern and magnitude of observed variability in snow distributions depends on the scale of observation (Blöschl, 1999). In turn, observed characteristics of snow depth distribution are strongly influenced by the scales of variability of driving processes, such as topography, vegetation, and wind. Terrain and vegetation act as roughness elements to modify wind flow and control snow redistribution. Moreover, the length scale over which the surface roughness elements

vary is altered by snow, presenting a feedback loop. As the roughness elements are buried by snow deposition at a given scale, surface roughness decreases and snow deposition may diminish. The complex interactions of precipitation, terrain, vegetation, solar radiation, and wind combine to produce extreme variation in snowpack properties over scale ranges relevant to basin hydrologic interests.

Snow process models are designed to represent processes acting over specific scale ranges. However, since the incorporated processes vary with scale, the model performance cannot be scale-independent. Thus, distributed snow models must be capable of representing the appropriate scales of process interaction in order to produce reasonable simulations of snow depth or snow water equivalent (SWE) variability. Refinement of process understanding and acquisition of distributed snowpack data will require new, high-resolution measurement technologies and innovative analysis methods that address the multiscale complexity of process interactions in complex mountain terrain (Bales *et al.*, 2006).

1.2 Research Objectives

This project attempts to broaden the understanding of seasonal snow process relationships by addressing the seasonal snowpack from the perspective of the mountain snow *system*, a complex nonlinear, dynamic interaction of forcing components (precipitation, wind transport, vertical and horizontal energy fluxes) with terrain and vegetation features. The resulting snow properties, distribution patterns, and patterns of events (i.e. redistribution, avalanching, snowmelt) emerge from the system dynamics. This perspective dictates a characterization of relevant system processes and process interactions at the scale of interest in order to understand or predict the spatial pattern or temporal change of a single variable. This framework is different from, but not exclusive of, the traditional, "reductionist" approach to physical processes, in that interactions on multiple scales are considered, rather than addressing specific process relationships in

isolation and at a particular scale.

The examination of physical processes in a reductionist setting provides quantitative representations of system components and subsequently allows characterization of system dynamics. The systems framework acknowledges that the snowpack properties at any given point in space or time are the result of a combination of processes, some of which are deterministic while others retain a strong degree of "historical and spatial contingency" (Phillips, 2004, p. 40). Therefore, in the systems framework, understanding spatial patterns of snow properties can only be undertaken in conjunction with an investigation into system dynamics and interactions affecting those processes (Phillips, 1999). Further, the components defining the mountain snow system will vary depending on the scale at which the system is defined, as will the variability of emergent system properties or observable variables. Thus any investigation of the mountain snow system must include a characterization of the scale and scaling relationships of its constituent processes.

The objectives of this work are to characterize the scale and scaling properties of snow accumulation and redistribution process interactions with topographic and vegetation patterns, and to use this characterization to investigate the ability of a distributed snow model to represent accumulation patterns produced by multiscale process interactions. This is accomplished by using a combination of field observations of snow properties and meteorological variables, modeled snow accumulation and redistribution processes, and remotely sensed data. The research specifically addresses the following questions: **(1)** Can airborne lidar surveys provide snow depth data with an accuracy, resolution, and extent suitable for addressing seasonal snow process scale questions? **(2)** Is fractal analysis an appropriate method for characterizing snow depth spatial variability and for exploring snow system interactions between terrain, vegetation, weather, and snowpack on the 1 to 1000 meter scale range? **(3)** Are observed scale properties of snow depth spatial pattern consistent, and if so, are they linked to

site-specific patterns of vegetation or topography? **(4)** How well does a physically-based snow process model (SnowModel) represent the scale properties of wind-terrain/vegetation interaction?

Project objectives are investigated via the testing of the following set of hypotheses: *Hypothesis 1:* Snow depth exhibits scale invariance in its spatial variability pattern over specific length scale intervals, as characterized by fractal dimension and power law relationships. *Hypothesis 2:* Spatial variability of snow depth shows a transition from fractal (scale invariant) structure to random (or stochastic) structure at a specific length scale, related to the variation present in the underlying topography and vegetation patterns. *Hypothesis 3:* Modeled variability of the snow transport process at specific length scale intervals will be consistent with the observed spatial snow depth patterns over that scale interval.

1.3 Research Overview

The research objectives and hypotheses outlined above are pursued via three lines of inquiry. First, airborne lidar survey products are examined for their ability to provide adequate data for scale investigations of spatial snow depth distributions. Second, fractal analysis is explored as a model for characterizing and quantifying patterns and scales of spatial variability in snow depth. Third, a distributed seasonal snow accumulation and ablation process model (SnowModel; Liston and Elder, 2006a) is evaluated using fractal techniques.

The research is presented here in the form of four journal articles, that follow a review of scale, spatial variability, and fractal analysis (Chapter 2). Chapter 3 examines airborne lidar as a tool for mapping spatial snow depth values, with specific attention to the optical properties of snow as a laser target. In Chapter 4, fractal analysis techniques are explored as a tool to quantify scales of variability in lidar-derived snow depth distributions. The interannual consistency of these fractal scaling relationships are

examined for two different water years in Chapter 5. In Chapter 6, modeled snow depth distributions from SnowModel simulations are compared with lidar snow depth maps and observed fractal patterns.

This collection of work addresses the above research questions, and provides a new application of methods developed in other geophysical fields for quantifying scale and variability relationships. Future uses and studies of the techniques presented here should result in standardization of these new approaches to spatial variation in snowpack properties, and quantification of scale issues as advocated by previous inquiries.

CHAPTER 2: BACKGROUND

2.1 Scale Concepts

Scale, referring to the characteristic length or time of a phenomenon, observation, or model (Blöschl and Sivapalan, 1995), is a unifying concept across all earth science disciplines, and applies far beyond common application of cartographic representation. Studies of earth systems are concerned with a wide range of physical and temporal scales, from the microscopic biologic interactions to water and energy fluxes of planetary scope.

If a given system is examined at a particular scale, the relevant, driving processes will likely be different from when the same system is viewed at a different scale. In other words, processes and process relationships change with scale, and the characteristic scale of a process is commonly termed the *operational* or *process* scale. Determining the process scale is a critical step, as it dictates observation and modeling scale resolution and extent for explicit treatment of the process variability. This relationship between process, observation, and modeling scale fundamentally controls the ability of a study to detect and detail the constituent processes.

Measurements of the physical environment impose a choice of characteristic *measurement* or *observation scale*, governed by the physical constraints of the measurement technique or instrumentation, as well as duty availability of the instrumentation and available man-hours of sampling teams. The measurement scale must be chosen appropriately to match the operational scale to allow full and explicit treatment of the variability in the observed phenomenon (Blöschl and Sivapalan, 1995; Blöschl, 1999). The *model scale* may be, but is not always, the same as the measurement scale. For example, the variable of interest may be measured by a certain technique

with specific scale characteristics, but the availability of data for representing driving processes may only be available at a coarser resolution or for smaller spatial extents.

The observation scale can be decomposed into components that describe elements of the measurement or modeling scheme, referred to by Blöschl and Sivapalan (1995) as the *scale triplet* (Figure 2.1). An individual measurement or model element is characterized by its *support*, the area or integrating volume for which the measurement is representative. *Spacing* denotes the interval between measurements, and *extent* indicates the overall coverage of the measurement scheme. The observation scale determines what can be learned about the processes of interest. Processes, as seen through the lens of the observation scale, have an apparent scale of operation that results from the superposition of measurement scale on process scale. If the support, spacing, and extent of the measurement or model are appropriate, the observations will be an accurate representation of the true process, and the true variability of the phenomenon will be evident. Any difference between observation and process scales will result in a scale bias, misrepresenting the true magnitude and pattern of variability and allowing potentially improper conclusions about the nature of the process.

Designing a sampling protocol, remote sensing instrument, or model that has scale characteristics that match the phenomenon of interest requires knowledge of the process scales of all relevant components of the system. Conversely, to construct a measurement system with specific scale characteristics, it is necessary to understand the process dynamics at that scale. Any difference between measurement and process

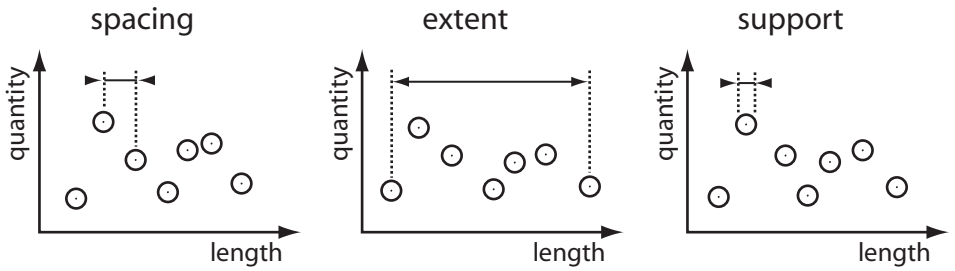

Figure 2.1. The 'scale triplet', which characterizes the scale properties of measurements or models (from Blöschl, 1999).

scale will result in an inaccurate depiction of the true variability. If the spacing is too large, the variability might appear to be noise. If the measurement support is too large, the observed variability will be smoothed and therefore too low. Improper spatial extent could result in the appearance of spurious trends or a reduced range in variation. Blöschl (1999) describes a scale mismatch as a 'filtering' of the true variability, potentially quantifiable by the ratio of measurement and process scales.

The changes in variability with scale are manifested through changing degrees of organization and random behavior of observed variables. Organization refers to regularity, often of a complex nature, and implies an origin in system dynamics – as a property that emerges from complex nonlinear or feedback interactions – rather than simple cause-and-effect relationships. Randomness describes variation that is unpredictable in detail, but has definable statistical properties. Different degrees of organization or randomness will 'emerge' from system process interactions dependent on scale. In this context, there may be preferred scales where a given system exhibits a large degree of organization, and may yield to reductionist investigations, with deterministic process relationships being discernable (Phillips, 1999). Between these orderly scale regions will likely exist scale ranges where system dynamics produce no organized pattern or relationship. This scale dependence presents a challenge when investigating spatial phenomena, as observation scales must be chosen to reflect natural scales of organized behavior.

While much of the body of knowledge in mountain hydrology has been gleaned through 'reductionist' examinations of single variable interactions and empirical relationships, it has become clear over recent decades of research that no phenomenon can be totally isolated from processes that operate over multiple scales. Indeed, as multiscale connections affecting a given system are considered, the problem of even defining the relevant 'system' becomes overwhelming. However, it is also true that not all processes or scales are relevant to the system of interest at the scale of interest,

allowing the system to be constrained. Thus a critical task is the identification of relevant processes at all relevant scales of operation and observation, and, in parallel, the identification of critical scales where processes or process interactions change.

Several studies refine this system characterization into a series of cumulative challenges that must be addressed in order to properly address scale issues (Blöschl and Sivapalan, 1995; Phillips, 1999; Hageli and McClung, 2004). First, the characteristic time and space scales of relevant natural processes must be identified. This step has seen significant attention from investigations of mountain hydrologic components in the past two decades (e.g., Bales *et al.*, 2006). Geostatistical techniques such as autocorrelation or variogram analysis are commonly used to quantify spatial variability through metrics such as correlation length. These techniques were designed to quantify variation that is explicit to the scale of measurement, and thereby predict values at non-measured locations at the same scale. However, from a system perspective the ability to predict conditions at different scales is more relevant to the task of defining and characterizing processes across the scale spectrum (Herzfeld, 1993).

Second, once process scales are known, the scale ranges over which process relationships (and thus spatial pattern) are consistent must be determined. Perhaps more importantly, knowledge of these scaling ranges will identify scales at which the process interactions change – potentially critical scales from both a process knowledge perspective as well as for measurement or model interests (Mark and Aronson, 1984; Vedyushkin, 1994).

Third, any measurement or modeling scheme that is developed must have scale characteristics that closely match the process scale in order to avoid misrepresentation of process variability. Parameters such as model or sensor resolution, study extent, and sample spacing require consideration. After quantifying process scales, identifying homogeneous scale ranges, and defining the measurement scale triplet, any scale bias due to differences between observational and process scale can be quantified. Additionally, it

is important to consider which variable is appropriate to measure at the scale of interest, and best represents the primary mode of variation due to process interactions at the scale of interest.

Though it is useful to conceptualize these challenges as discrete, in effect they are but different facets of the fundamental scale problem. To develop a scale-appropriate measurement scheme and rectify its scale bias requires knowledge of both characteristic process scales and the scale ranges of consistent process behavior.

Though some process relationships can be quantified in a reductionist setting, it is rare that simple, low-dimensional simulation can produce the spatial pattern complexity observed in natural systems. However, the results of process interactions are manifested in the spatial patterns of the observed variables. Changes in process dynamics with temporal or spatial scales will result in different observed spatial patterns. Therefore, metrics describing pattern complexity can be used to identify process scales and scales where process dynamics change character.

Additionally, Phillips (1999) raises the issue of scale linkage. Efforts to define a system of interest, and thereby exclude processes that operate on fundamentally different time or space scales, invariably encounter the challenge of characterizing the nature and extent of cross-scale linkage. This issue feeds directly into practical problems of upscaling and downscaling from existing data or models. That climate dynamics can be functionally excluded from snow microstructure investigations may be self-evident, but effects of orographic enhancement of precipitation are not as easily separable from wind redistribution, despite reasonably clear scale distinctions between the two processes.

Hierarchy theory was pioneered in the field of ecology, in part, to address this very problem (O'Neill *et al.*, 1989; Allen and Hoekstra, 1992; Levin, 1992). Hierarchy theory holds that a complex, hierarchical system is composed of distinct, relatively independent levels, each with a characteristic temporal and spatial scale. This hierarchical structure is advantageous to the investigator, as it limits the number of system processes requiring

consideration to those operating on very similar scales as the phenomenon in question. Processes at larger levels will manifest themselves as low-frequency trends, while constituent, fine-scale processes will appear as noise. Another advantage is introduced by O'Neill *et al.* (1989) as a *constraint envelope*, wherein the behavior of a system is constrained by the physics of constituent processes at a lower hierarchy, and by environmental limits imposed by the next higher level. In a snow hydrology context, catchment-scale snow distribution processes are limited by the physics of snowpack processes, such as the bonding of snow grains, and are constrained at a higher level by broad-scale processes such as the synoptic weather behavior or topographic position.

The formalism of hierarchy theory offers a fine organizing construct, yet the problem of defining characteristic process scales and consistent scaling ranges is simply relabeled as a problem of defining the scale limits of each hierarchical level. Further, implicit in the hierarchy framework is the notion that each hierarchical level is relatively isolated from higher and lower levels. The problem of characterizing the number, direction, and magnitude of the connections between hierarchical levels is part of the scale linkage issue discussed above, and depends partly on the definition and scale characterization of each level. Phillips (1999) argues that hierarchy theory is useful as a conceptual framework or organizing construct, but is not practical to implement operationally.

Optimal sampling, measurement, and modeling snow distributions requires knowledge of accumulation and ablation process interactions, and how those process relationships change with scale. Delineation of these snow process scale relationships will allow selection of observation scales that match operational scales, i.e. resolutions and extents that permit explicit measurement or modeling of the primary sources of variability in the distribution (Blöschl, 1999; Bales *et al.*, 2006).

2.2 Spatial Variation and Geostatistics

The concept of spatial variation is often distilled as Tobler's First Law of Geography:

"Everything is related to everything else, but near things are more related than distant things" (Tobler, 1970). Traditional geostatistical methods developed for estimating local values from sample data can be used to characterize spatial variability, and include spatial covariance, variogram analysis, and spectral analysis (Webster and Oliver, 2001). These methods build upon Tobler's fundamental tenet by quantifying the spatial pattern of variability of an observed property over a scale range from the minimum sample separation to the distance at which the variable becomes spatially independent. This quantified variability can then be used for spatial estimation based on a finite number of data points.

Geostatistics is based on treating a spatial variable as a random field, defined as having a continuous spatial distribution, but with a structure too complex to be represented by a deterministic mathematical function. In this context, the spatial variation is partially random, or more precisely stochastic, as a given value cannot be calculated precisely from nearby measurements. This construct is usually implemented by describing the variation as having deterministic and stochastic components. The deterministic component can be modeled using a trend surface, for example, while the stochastic component can be modeled as random deviations from that surface. These deviations have spatial structure which can be characterized by the variogram (Webster and Oliver, 2001).

This stochastic treatment is used while recognizing that the processes generating the apparently random component of variation are likely deterministic, but are too complex to be represented explicitly. This treatment is a practical solution to distributing values from limited spatial datasets. However, in many cases, the random behavior is a function of the scale of observation. Changing the scale of observation will reveal a different pattern of variability that may be more resolvable and potentially subject to explicit treatment.

It is common to model variability that occurs at scales larger than the scale of interest

with a deterministic relationship, and subsequently model the remaining, small-scale variability as a random variable. The small-scale variability is described using the experimental variogram, which is then fit with a model function. These steps help to narrow the model scale and minimize the number of processes represented. However, from a system perspective, there are two problems with this type of geostatistical approach. First, fitting a trend surface removes information regarding the contribution of larger-scale processes to the local variability. Second, there is no physical basis for the model functions fit to the experimental variogram.

Though certainly valuable for interpolation, geostatistical techniques are not designed to examine process relationships at multiple scales simultaneously. Due to stationarity assumptions and/or removal of large-scale trends, standard geostatistical measures may provide a filtered estimate of spatial variability over a narrow scale band. To properly address scale issues, or to define a hierarchical system framework, techniques are needed that are sensitive to multiscale process contributions to observed variability. The fractal model may be an appropriate tool for describing scale relationships in snow system processes. Fractal analysis builds on standard geostatistical techniques that quantify spatial variability, can describe ranges of consistent process dynamics, and can identify critical scales at which process dynamics change.

2.3 Fractal Methods for Characterizing Variability and Scale

Following the systems paradigm, when examining the spatial or temporal variability of a phenomenon it is useful to employ measures that include some information related to the dynamics of the system as a whole. Systems exhibiting chaotic or complex, nonlinear behavior in their constituent dynamics often show organization into fractal, or scale-invariant properties in their observable characteristics (Phillips, 1999). The fractal paradigm holds that variability exists at a range of scale, and provides means to quantify the relationship between variability at different scales (Blöschl and

Sivapalan, 1995). In this interest, the fractal model has been applied to a wide variety of geophysical and geographic investigations, including geomorphic evolution of landscape features, earthquake magnitudes, variation in soil properties, precipitation patterns, and classification of remote sensing images, among many others (Lam and DeCola, 1993). For example, some hydrologic systems, consisting of complex terrain, hydraulic, biologic, and climatic interactions, organize into dendritic drainage patterns, with similar branching structures across a range of scales (e.g., Tarboton *et al.*, 1988). Both the range of scales over which the branching structure is applicable and the complexity of the drainage system can be characterized by fractal analysis.

For snow system interests, several factors indicate that a fractal model could be an appropriate tool for characterizing spatial snow properties. Many of the driving processes or system components relevant to basin scale snow distributions have been shown to exhibit fractal characteristics, including small-scale wind turbulence (e.g., Poveda-Jaramillo and Puente 1993), topography (e.g., Mark and Aronson, 1984; Klinkenberg and Goodchild, 1992), vegetation surface roughness (e.g., Pachepsky and Ritchie, 1998), and forest pattern (e.g., Vedyushkin, 1994). Tabler (1980) demonstrated that snowdrifts in the lee of snow fences maintain a consistent geometry over a range of scales from 10 cm to 10 m, which indicates a self-similar scaling of wind deposition patterns.

Several investigations have specifically examined fractal properties of snow distributions. Shook and Gray (1994) linked the fractal distribution of ablation season snow patch sizes to a fractal distribution of SWE within the snowpack. Two previous studies have calculated fractal dimensions from survey transects of snow depth. Shook and Gray (1996) found fractal scaling over a scale range from one meter up to a 'cutoff length' of 30-500 m, beyond which the distribution appeared random. Kuchment and Gelfan (2001) also noticed power law behavior in snow depth data, though there appears to be the potential for a multifractal treatment of their distributions (defined below).

The fractal dimension (D) (Mandelbrot, 1983), is a measure of the complexity of

a feature, and may provide a robust parameter for comparing the patterns of spatial variability between multiple surfaces (snow depths, topography, or vegetation). Fractal dimension is consistent with Euclidean dimension (i.e. a line has $D = 1$, a plane has $D = 2$, and a volume has $D = 3$) but can be non-integer, and is a measure of the irregularity or roughness of the structure. For example, a drainage network with $D = 1.8$ would be so intricate as to be nearly plane-filling (Burrough, 1993).

There are several methods by which fractal dimension may be calculated, and the choice of method should be consistent with the goals of the investigation and therefore the type of metric required (Carr and Benzer, 1991). Geometric methods, such as the divider (for linear features) or box-counting methods (for surfaces), produce a fractal dimension that describes the morphologic complexity of the feature. The divider technique was used by Mandelbrot (1983) to demonstrate the concept of fractal geometry as embodied by the problem of estimating the length of the coastline of Britain. As the coastline is measured with rulers (dividers) of shorter and shorter length, the length of the coast appears to increase exponentially. The measured length (L) is related through a power function to the ruler length (r) through the fractal dimension:

$$L = r^{D}(N + f/r), \tag{2.1}$$

where N is the number of measurements and the remainder f is any fraction of the ruler length (Carr and Benzer, 1991).

For a linear feature (or curve), D will have a value between 1 and 2, with smooth features closer to 1, and very complex features closer to 2. A surface feature can have dimensions between 2 (perfectly planar) and 3 (space-filling). This morphologic fractal dimension is distinct from stochastic fractal measures, wherein the behavior of the variable of interest is related to that of a random noise.

Spectral analysis or variogram analysis are used for calculating fractal dimensions that describe the stochastic nature of a feature, and thus examine statistical self-similarity (Phillips, 1986; Carr and Benzer, 1991). Stochastic fractal dimensions characterize the variability of a feature relative to the variation exhibited by a Brownian noise,

and therefore quantify the ratio of large- and small-scale variability. Brownian noise is a stochastic function useful for describing highly irregular variable fluctuations. A Brownian function is non-differentiable and non-stationary, but is continuous and the differences in values offset by a consistent lag are normally distributed. If *Y(x)* is a Brownian function at position *x*, the difference

$$Y(x_i) - Y(x_j), \tag{2.2}$$

has a normal Gaussian distribution with zero mean and a variance equal to the lag (Burrough, 1983a; Phillips, 1986; Carr and Benzer, 1991). Additionally, for a Brownian function the expected value of the squared difference between the two values $Y(x_i)$ and $Y(x_j)$ at locations x_i and x_j is proportional to their separation distance (lag). Specifically, the values are proportioned via the Hurst exponent *H*:

$$E[(Y(x_i) - Y(x_j))^2] \propto |x_i - x_j|^{2H} \ , \quad 0 \le H \le 1 . \tag{2.3}$$

The value of *H* is 0.5 for a Brownian function. By allowing *H* to vary between 0 and 1, Mandelbrot (1983) created a class of *fractional* Brownian functions describing the range of motions from white noise ($H = 0$) to smooth, differentiable curves ($H = 1$). The value of *H* describes the correlation of neighboring points. When $H > 0.5$, values are positively correlated, or persistent. For $H < 0.5$, neighboring values will tend to be negatively correlated, or antipersistent.

By substituting the lag h_{ij} for $x_j - x_i$, Eq. (2.3) can be rewritten:

$$E[(Y(x_i) - Y(x_j))^2] \propto |h_{ij}|^{2H}, \qquad 0 \le H \le 1 . \tag{2.4}$$

The relationship described by Eq. (2.4), i.e. the variance of a spatial variable as a function of separation distance, can be quantified by the semivariogram. The semivariance γ (Webster and Oliver, 2001) is defined as:

$$\gamma(h_{ij}) = \tfrac{1}{2} (E[(Y(x_i) - Y(x_j))^2]. \tag{2.5}$$

Therefore:

$$\gamma(h_{ij}) \propto 2 \ |h_{ij}|^{2H}, \qquad 0 \le H \le 1 . \tag{2.6}$$

If the variogram is plotted in log-log space, $log(\gamma(h_{ij}))$ *vs.* $log(h_{ij})$, any linear (power law) segments can be fitted with a power function of the form:

$$\gamma(h_{ij}) = a(h_{ij})^b. \quad (2.7)$$

From Eq. (2.6), the slope b of the plot is equal to $2H$ (Carr and Benzer, 1991). Gao and Xia (1996) show that for a surface feature $D = 3 - H$. Since $b = 2H$, by substitution:

$$D = 3 - b/2. \quad (2.8)$$

Thus the fractal dimension of a surface can be estimated through variogram analysis.

A debate exists regarding the accuracy of D values estimated by various fractal analysis methods. Carr and Benzer (1991) note that fractal dimensions derived from spectral analysis are sensitive to the size of the analysis window used (Parzen window). They conclude based on this sensitivity that the variogram method is superior for estimating the stochastic fractal dimension. Other work has indicated that both the variogram and spectral methods produced biased fractal dimension estimates (e.g. Wen and Sinding-Larsen, 1997; Lam *et al.*, 2002). Several studies have found that the variogram method has a minimum bias when H values are close to 0.5 ($D_{surface} = 2.5$; Gallant et al., 1994; Wen and Sinding-Larsen, 1997). Sun *et al.* (2006) suggest that some reports of poor D estimates from the variogram method are due to using random subsets of the data for computational expediency, thus treating the computed fractal dimension as a random variable. Others have recommended the use of log-width variogram bins to provide more accurate least-squares fits in log-log space (Klinkenberg and Goodchild, 1992). It is well-established, in any case, that comparisons of D values for discriminating multiple datasets should be done using a consistent methodology, to eliminate inconsistencies caused by the different fractal analysis techniques.

Most geographical features are not self-similar across all scales, but rather their power law exponent changes with scale (e.g., Mark and Aronson, 1984). By treating a variable as a *multifractal* rather than a monofractal, the feature can be conceptualized as a series of superposed fractal sets, with fractal regions separated by clear scale breaks. A cascade

process describes a generalized scale invariance, whereby there is a multiplicative modulation of smaller-scale processes by larger-scale processes (Blöschl and Sivapalan, 1995). These cascade processes produce multifractal patterns recognizable by multiple superimposed power-law scaling functions (Herzfeld, 1993). The multifractal model is consistent with the 'nested variogram' concept described in the context of snow hydrology by Blöschl (1999):

> "… there is a discontinuous variogram exhibiting steps of the form of [a power law]. This variogram exhibits a number of preferred scales (i.e. the λ_i) each of which may represent one physical process. For example, the process scale of crystal growth may be λ_1 = 1 mm, that of wind drift at hillslopes may be λ_2 = 1 m, that of solar radiation effects at hillslopes of different aspects may be λ_3 = 100 m, and that of different climatic conditions may be λ_4 = 10 km. The combined nested variogram … then is a combination of the effects of the individual processes" (p. 2160-61).

Using the (multi)fractal variogram analysis, scale ranges can be identified within which the variable of interest exhibits fractal behavior, and the fractal dimension estimated. This technique provides a powerful method to quantify hierarchical scaling relationships across a span of length scales, and to thereby identify regions of consistent process behavior and scales (or scale breaks) at which process relationships change character (Mark and Aronson, 1984; Emerson et al., 1999). The specific scales at which the fractal character of a feature changes are important thresholds that indicate a shift in process dynamics. This scaling information informs the development of measurement schemes and process models, by identifying both optimal scales for addressing variability explicitly and ranges within which spatial fields can be rescaled.

From the perspective of hierarchy theory the multifractal scale breaks have a

straightforward interpretation: they indicate scales at which process dynamics change and therefore define the length scales of hierarchy transition (Vedyushkin, 1994). Thus, scaling characteristics described by fractal analysis can potentially be used to delineate hierarchy levels, and fractal descriptions of driving variables may be able to aid in describing the full suite of process interactions over the level(s) of interest.

The observed fractal scaling relationships are also likely to vary with time, highlighting the importance of temporal scale. Blöschl (1999), for example, examined three different time series of fractal scaling patterns in snow covered area (SCA) images. Though the fractal scaling exponent showed little change through time, towards the end of the ablation season the exponent value decreased, potentially indicating a shift in process dominance from long-range to short-range as the SCA pattern increased in complexity.

Temporal changes in the spatial scaling relationships are not likely to occur smoothly, due to thresholds in snow cover processes. For instance, the burial of topographic or vegetative roughness elements as the seasonal snowpack accumulates could lead to a relatively sudden change in SCA or snow depth variability, due to a temporal change in process interactions. Patchy snow covers have dramatically different energy exchange dynamics from continuous snow covers (e.g., Shook and Gray, 1994; Liston, 1995; Essery *et al.*, 2006). The complete burial of surface roughness elements would represent a fundamental shift in the state of the snow system along with a commensurate shift in process dominance from, in some environments, energy balance to wind redistribution effects. This effect can be tested using time series datasets, as in Blöschl (1999), or by using a distributed snow model, provided that the model can adequately simulate process-driven scaling patterns.

2.4 Model Scale and High Resolution Datasets

Distributed snow process models are widely used for estimating or predicting snow distributions and melt volumes, and are powerful tools for investigating process relationships. Model structure and spatial and temporal resolution are usually dictated by a combination of modeling goals, available data, and computing power. Input needs for distributed models are increasingly met using remote sensing data, in both initialization and assimilation roles (e.g. Cline *et al.*, 1998; Molotch *et al.*, 2004; Dressler *et al.*, 2006; Liston, *et al.*, 2007). As snow process models grow more powerful and are able to simulate processes at higher resolutions, it becomes increasingly important that the scale and scaling properties of all relevant processes, data streams, and model elements are known.

Verification of distributed snow process models is frequently performed using a water budget approach, by comparing modeled SWE to basin outflow volumes. However, due to potentially offsetting errors, it is possible to achieve a satisfactory simulation of runoff volume with poor process representation. Further, a one-dimensional performance metric such as runoff volume does not provide any information with which to improve process representations, and thereby broaden a model's applicability to other locations or conditions (Blöschl and Sivapalan, 1995).

Over the past decade or so, many investigations have used spatial patterns of state variables such as SCA, SWE, or snow depth, for model verification (e.g. Blöschl *et al.*, 1991; Davis et al., 1995; Hiemstra *et al.*, 2005). Distributed evaluation techniques require substantial verification datasets, and more significantly, the scale properties of the verification data should be consistent with those of the model, and, by extension, of the modeled processes.

Specification of the scale triplet for measurement and modeling has been advocated for estimating scale bias when the process scale characteristics are known or can be reliably estimated (Blöschl, 1999). However, if snow properties display a multifractal

nature, it is likely that certain measurement or model scales are not compatible with some process scales. For example, if a process scale break occurs at a particular lag distance, models with resolutions greater than the scale break length are not able to represent process relationships that exist below the scale break. The fractal analysis methodology outlined above, and examined in more detail in the following chapters, can identify the critical scales represented by scale breaks on multifractal variogram plots, and thereby inform development of measurement schemes and model structure.

Conventional measurements of spatial snow cover variables exhibit combinations of coarse resolution, restricted extent, or large measurement integrating volumes. Standard methods for measuring snow depth and SWE rely on intensive field surveys or a combination of ground data and low spatial and/or temporal resolution products from airborne or space borne platforms (*i.e.* gamma, passive microwave). Manual snow surveys, for example, have high precision corresponding to individual measurements, but the spatial extent and resolution that are safely and efficiently achievable are limited (Elder, *et al.*, 1991). SWE retrieval products from operational microwave remote sensing technologies provide large spatial extents, but are constrained by sensor resolution and complicated emission, attenuation, and backscatter responses to snow properties (Sokol *et al.*, 2003). The USDA Natural Resource Conservation Service Snow Telemetry network (SNOTEL) and similar remote sensor arrays have high temporal resolution, and large spatial extent when treated as a network (e.g., Fassnacht *et al.*, 2003), but provide little spatial information at the basin scale (Molotch and Bales, 2005; Bales *et al.*, 2006). These and other measurement scale issues limit the investigation of process scale relationships, and bias or hamper operational decision-making or modeling efforts dependent on spatially explicit snow cover information.

Quantification of scale relationships in support of snow science interests requires datasets that minimize scale filtering imposed by measurement scale issues. The ideal dataset would have high spatial resolution, a large spatial extent, a small sensor footprint,

integrating volume, or measurement cross-section, and the ability to adjust temporal resolution to respond to important events (Bales *et al.*, 2006). Airborne laser scanning (lidar) surveys provide this combination.

The availability of lidar snow depth datasets will undoubtedly allow stringent testing of snow models. The high resolution and broad extent provided by lidar allows characterization of snow depth patterns across a wide scale range, and will provide superb verification datasets with which to examine the process representation in distributed snow process models. It is possible that, as these or other high resolution data become more readily available and are increasingly used to validate spatial models, significant process representation problems due to spatial or temporal scale issues will be revealed. This can only be viewed as a natural and beneficial progression in the ability to understand, simulate, and predict complex snow system processes, one that has occurred recently in the global climate modeling community, for example (Le Quéré, 2006).

Geographic phenomena commonly exhibit differing amounts and patterns of variability depending on the scale of observation. By examining the appropriate variable using a measurement scale commensurate with the true process scale, the true variability of the variable can be examined. In practice, measurement and model scales are determined in large part by technological, physical, or financial constraints, and do not match process scales. It is therefore critical to develop a fundamental understanding of process scale characteristics for more accurate and efficient observation and simulation of snow properties and distributions. The following chapters detail the use of airborne lidar data, fractal analysis, and a distributed snow process model to aid in quantifying scale relationships in spatial snow depth distributions.

CHAPTER 3:
LIDAR MEASUREMENT OF SNOW DEPTH:
ACCURACY AND ERROR SOURCES

3.1 Introduction

Airborne laser scanning (lidar) is a remote sensing tool with the ability to retrieve surface elevations at high spatial resolutions, in rough terrain and in heavily forested regions (Reutebuch *et al.*, 2003). Differencing lidar maps from two dates allows the calculation of snow depth at horizontal spatial resolutions close to 1 m, and over spatial extents compatible with basin-scale hydrologic needs (Hopkinson *et al*., 2004; Miller *et al*., 2003; Deems *et al.*, 2006). The spatial resolution and coverage, repeatability, and sub-canopy mapping capability of airborne lidar offer a powerful contribution to research-oriented and operational snow hydrology and avalanche science in mountain regions.

Knowledge of spatial snowpack properties in mountain regions, especially snow water equivalent (SWE) is critical for accurate assessment and forecasting of snowmelt timing (Luce *et al*., 1998), snowmelt volume (Elder *et al*., 1991) and avalanche hazard (Conway and Abrahamson, 1984; Birkeland *et al*., 1995), for initialization of synoptic and global-scale weather and climate models (Liston, 1999; Groisman and Davies, 2001), and for investigations of ecologic dynamics and biogeochemical cycling (Jones, 1999; Brooks and Williams, 1999). Snowfall and wind interact with terrain and vegetation to create highly variable patterns of snow accumulation. These complex interactions produce a snow cover that is challenging to sample and model (Elder *et al*., 1991). The seasonal snow system and its spatial distribution at multiple scales is coupled

to hydrologic, atmospheric, and biologic systems through dynamic forcing of runoff characteristics, heat and energy fluxes, soil moisture distributions, and growing season duration (Jones *et al*., 2001), greatly influencing energy, water, and biogeochemical cycling in mountain and earth surface systems.

Manual sampling of snow depth is expensive, time-consuming, potentially dangerous to field crews. Avalanche starting zone depths and runout volumes are particularly difficult to sample, presenting an obvious need for remote sensing technologies. Further, the intervals over which snow depth can be feasibly measured are limited to spacings and extents that likely do not capture the full variability at the slope or basin scale. Lidar altimetry is a data acquisition tool that can provide high spatial point densities over extents compatible with both avalanche research and catchment-scale hydrologic needs.

Calculation of snow depth from lidar data requires two data collections, one each for snow-free and snow-covered dates, followed by differencing the snow surface and bare-ground elevations (Hopkinson *et al*., 2004; Miller *et al*., 2003; Deems *et al*., 2006). Lidar-derived digital elevation models (DEM) have been shown to have accuracies as great as ± 10 cm RMSE, even in densely forested areas (Kraus and Pfeifer, 1998; Reutebuch, *et al.*, 2003). The snow depth calculation procedure effectively involves the creation of two DEMs, plus interactions of the laser light with the snow surface. Additionally, snow depth mapping in mountain terrain involves consideration of laser scanning geometry relative to steep slopes and with the potential for dramatic variations in aircraft flying height. These factors, if not accounted for, produce the potential for large accuracy variations in lidar-based snow depth measurements.

The science of airborne lidar mapping is evolving, and the body of work concerning suitability and error sources for natural resource applications continues to grow. However, the available sensors and proprietary processing techniques are not standardized, making an understanding of each instrument, processing step, and range of potential error sources critical for successful application of airborne lidar mapping

for snow science interests. This paper seeks to explore error sources and magnitudes involved in snow depth mapping using lidar, and to provide recommendations for successful employment of this powerful technology for scientific and operational snow hydrology and avalanche science needs.

3.2 Lidar Altimetry and Snow Depth Calculation Techniques

3.2.1 Lidar altimetry

Lidar is a ranging instrument, and measures target distance by calculation of the elapsed time between emitted and return laser signals. The position of the aircraft platform is established by way of Differential Global Positioning System (GPS) triangulation, and platform orientation (roll, pitch, yaw) determined via an inertial navigation system (INS) link (Figure 3.1). Once the platform geometry and the geometry of the scanner system are known, the time interval between laser pulse emission and return is used to determine the three dimensional locations of the laser point measurements. Each of these geometric components has the potential to introduce error into the final elevation measurement. Further, complex topography and multiple reflections may induce additional measurement errors.

The emitted laser pulse diverges as it travels away from the source. Modern sensors have divergence angles in the range of 0.3-1 mrad, which produces a ground spot radius of 0.3 to 1 m at a flying height of 1000 m above ground level (Baltsavias, 1999). The beam width allows portions of the laser spot to be reflected by several targets, resulting in multiple returns per pulse (Figure 3.2). Newer lidar systems have the ability to record first, last, or several return pulses, allowing mapping of vegetation height, structure and/or understory in addition to enhancing the ability to map sub-canopy terrain. Other sensors, called ‘waveform-recording’ sensors (Lefsky *et al*., 2002) offer the capability to record a time series of return intensity from each pulse. These sensors utilize a larger

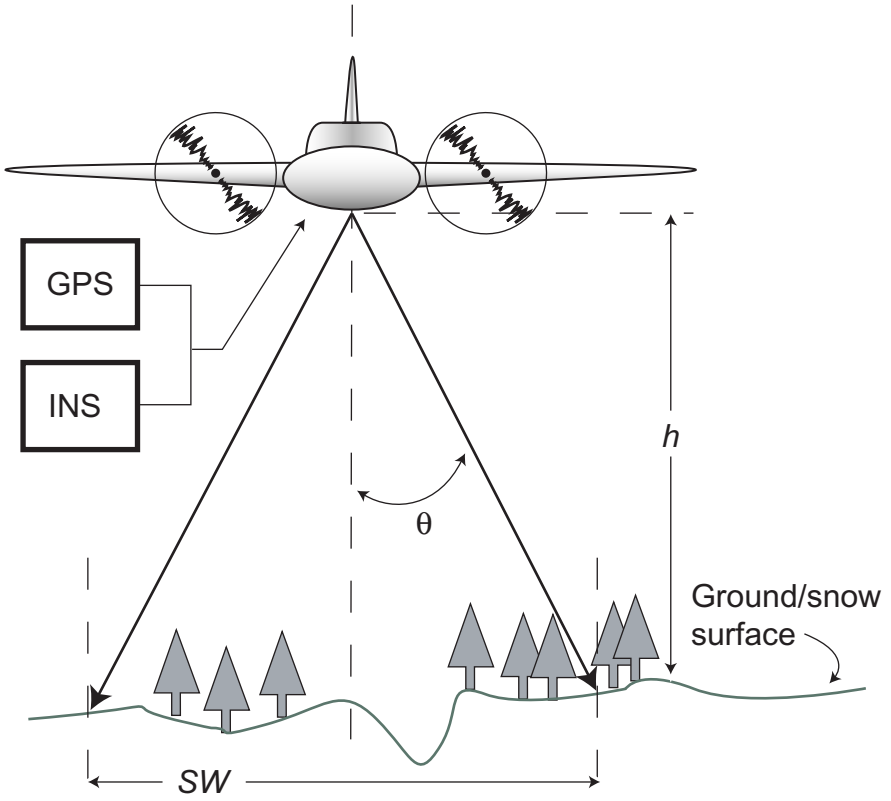

Figure 3.1. Lidar system geometry: scan angle (θ), platform height (h), and swath width (SW) are shown. GPS and INS systems are on the platform and time-synchronized with the laser scanning system.

laser footprint (on the order of 25 m), and are most useful for studying forest canopy structure. Waveform-recording sensors, because of the large footprint, do not provide sufficient spatial resolution for snow depth mapping at the catchment scale. The spatial resolution of the point data is often quantified as the average point density per square meter, or by an average point spacing, though occasionally it is represented as the smallest elevation contour interval that can be mapped from the data. Factors influencing the spatial point density at ground level include the scan pattern, scan rate, swath width, pulse rate, and aircraft height (Baltsavias, 1999).

Several scan patterns are currently in use, and more complex scan patterns are being developed for acquisition of specific point densities or spatial coverages. The most common are parallel or Z-shaped bidirectional scans. Palmer (elliptical) scans are also in use, which provide fore and aft pointing angles in addition to the across-track directions

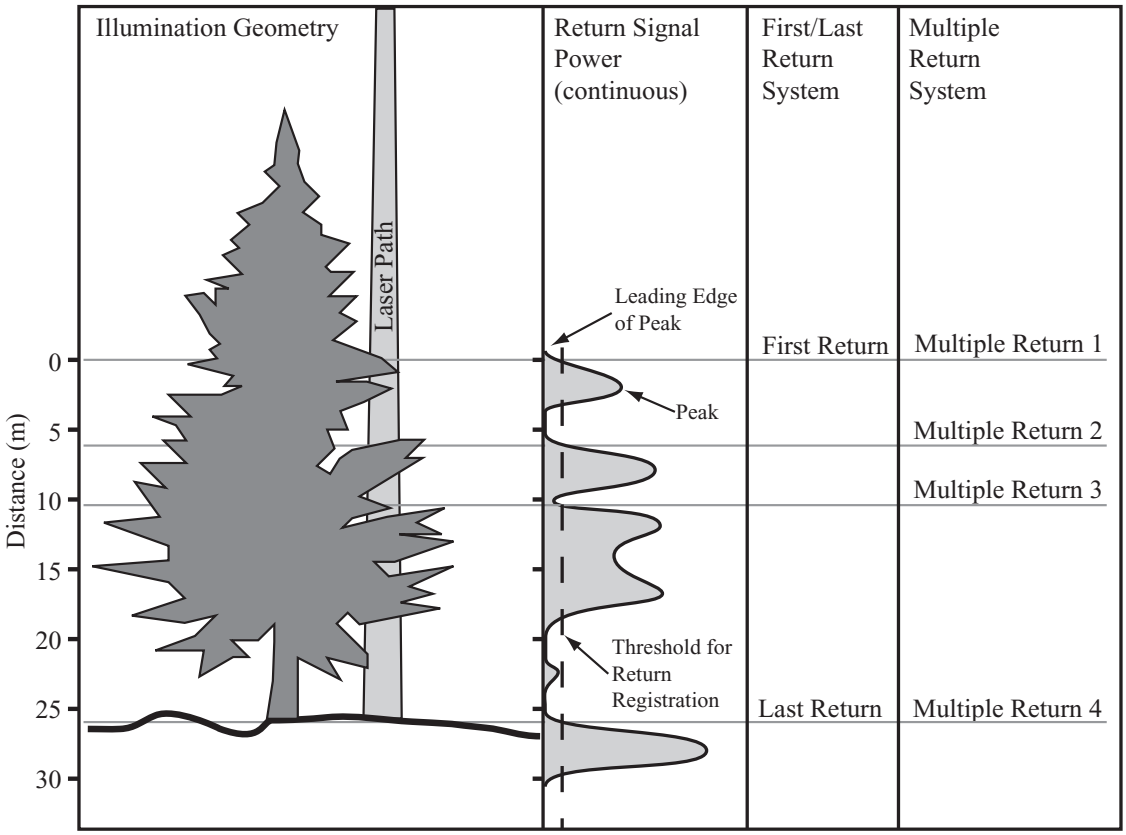

Figure 3.2. Laser illumination and return signal recording. Portions of the emitted laser pulse are reflected by different targets, resulting in multiple return signals for each pulse. Different Lidar systems have different return signal recording capabilities. (after Lefsky et al., 2002)

achieved by the bidirectional scan patterns, and therefore provide more opportunities for canopy penetration. Scan angles of ± 15° are sufficient for penetration of all but the most dense conifer canopies in mountain regions (Romano, 2006).

The laser pulse rate is the primary determinant of across-track point spacing, and on older lidar systems can be a limiting factor. Newer systems can achieve pulse rates of 100 kHz, allowing for very dense laser shot patterns (Optech, Inc., 2006). The scan rate is the angular velocity of the oscillating mirror that directs the outgoing laser pulse, and combines with the pulse rate to determine minimum across-track point spacing. Common scan rates are in the 30 Hz range, and are usually secondary in importance to pulse rate in determining point spacing (Wehr and Lohr, 1999).

Along-track point spacing is controlled by the aircraft ground speed and the period

of a single scan, with the maximum occurring coincident with the edge of the field of view. Adjacent swaths are overlapped to provide additional point density along the swath margins (Wehr and Lohr, 1999). In practice, ground speed and scan period are constrained so that the along-track spacing is consistent with the across-track spacing.

The width of the scanned swath is of primary importance for mission planning purposes. Wider swaths allow greater areal coverage with fewer flight strips, and therefore can significantly decrease the data collection cost. Swath width depends primarily on the scan angle of the scanner system and the aircraft flight height. Increasing swath width via aircraft height comes at the expense of laser point spacing and/or range accuracy. At larger scan angles, the probability of canopy penetration decreases, with possible reductions in achievable ground point spacing.

The collected data, after georegistration, are represented as (x,y,z) points. The raw data must be filtered in order to ensure that all points belong to the surface of interest, i.e. the canopy, ground or snow surface. Most filtering algorithms are proprietary to laser mapping contractors, which creates a potential source of data problems that are opaque to the data user. Most filtering is done via automated algorithms that are monitored manually (Wehr and Lohr, 1999). Once the point data are filtered and a satisfactory collection of surface points has been obtained, the snow-free ground elevations can be subtracted from the snow-covered elevations to derive snow depth.

3.2.2 Snow Depth Calculation

The two datasets consist of (x,y,z) points, and the likelihood of ground and snow points existing at exactly the same (x,y) location is quite small, which precludes a point-to-point subtraction. The most efficient method of subtracting the two datasets is to convert the bare-earth elevations to a grid dataset and subsequently extract the grid values below each snow surface elevation point measurement (Deems *et al.*, 2006). The creation of the grid dataset, or DEM, involves interpolation, and thus induces some

error. However, due to the high spatial resolution of the point data, a simple interpolation scheme, such as inverse-distance-weighting, can be employed with minimal introduced error. Terrain with significant vertical displacements, such as cliff bands, may present challenges to DEM generation by simple interpolation, however GIS techniques, such as barrier delineation, can be used as necessary.

The grid element size should be of similar magnitude to the average point spacing of the filtered elevation point dataset in order to minimize scaling concerns and smoothing. In general, a small number of nearest neighbors should be used to interpolate each grid value, in order to minimize smoothing errors. The highest degree of smoothing will occur in areas of lower point density, such as where heavy forest cover exists.

3.2.3 Integration with Other Sensors

High-resolution orthophotography is often acquired concurrently with the lidar data, and its use during the filtering process can greatly improve data quality. The snow-covered orthophotos will also show snow drift and scour features, enabling a qualitative assessment of the final snow depth map. In areas or seasons with partial snow coverage, snow-covered area products, such as the MODSCAG fractional snow cover maps (Painter *et al.*, 2006) could be used for mission planning to constrain flight lines to areas having snow cover.

3.3 Error Sources in Lidar Mapping

A significant body of literature is emerging as applications for lidar technology are developed. Much work has been done to quantify errors imparted by systematic sources such as global positioning and inertial navigation systems, laser system calibration, and scanning geometry. However, as snow depth mapping application evolves, there is a need to quantify potential errors due to interactions of the laser light with the snow surface. In the following, error sources common to most laser mapping applications are

reviewed. For more detail, the reader is referred to Baltsavias (1999), Wehr and Lohr (1999), and Hodgson and Bresnahan (2004). Lidar sensing of the snow cover involves the additional complication of the volumetric reflection of laser light by the near-surface snow layers.

3.3.1 Positioning and Inertial Navigation Systems

The GPS and INS systems provide positional and platform orientation data from which the location of the laser sensor can be derived, and thus the locations of the ranged ground elevations can be determined precisely (Wehr and Lohr, 1998). The GPS and INS systems must be time-rectified with the laser scanner, so that all laser range measurements are tied to the appropriate positional data.

Differentially-corrected GPS is required to achieve sub-decimeter positional accuracy, on a par with the laser range accuracy. Differential correction necessitates a nearby ground reference GPS station, either a permanent station or a portable unit located on a surveyed point or triangulation benchmark. The time series of airborne GPS locations is then corrected using the time series offsets recorded by the ground station. Error magnitudes due to GPS/INS are typically on the order of 6-8 cm.

3.3.2 Flight Planning

Flight planning is critical to mission success, minimizing cost, and data accuracy, especially in rough terrain. Terrain geometry (slope magnitude and aspect relative to the flight line) interacts with the laser scan angle to affect the laser angle of incidence at a given ground surface location. Proper flight planning will minimize the number of points collected with poor geometry.

Positional error due to terrain slope occurs via two mechanisms. First, errors in the horizontal (x,y) directions will induce an apparent error due to the uncertainty of the planimetric position of the measured elevation (Figure 3.3a). This effect of vertical error dependence on horizontal accuracy can cause the measured point to appear above or

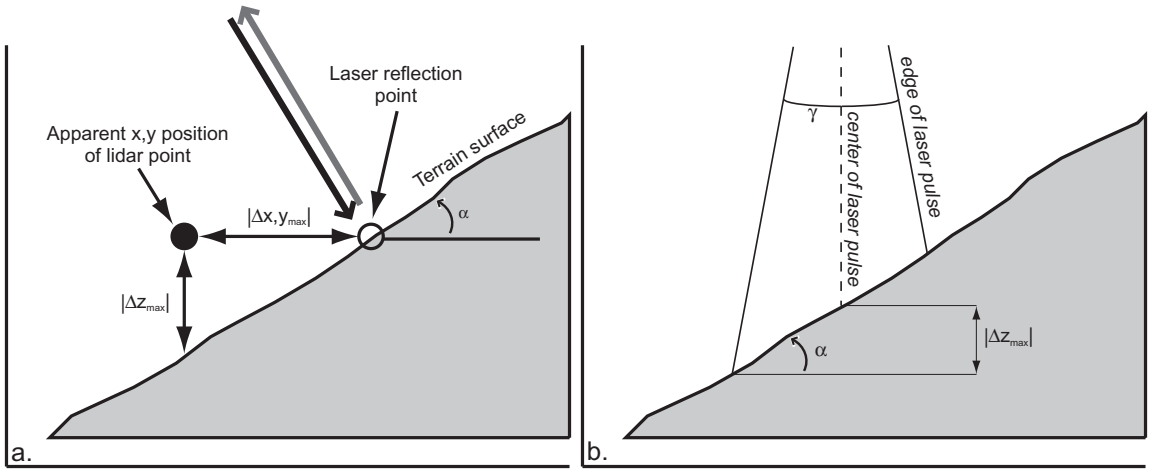

Figure 3.3. Errors induced by terrain slope. a) vertical error induced by horizontal errors (after Hodgson and Bresnahan, 2004). b) 'time-walk' vertical error induced by laser spot spread over inclined terrain (after Baltsavias, 1999). α = slope angle; γ = laser beam divergence; Δz_{max} = maximum elevation error; $\Delta x,y_{max}$ = maximum horizontal error.

below the actual terrain surface due to errors perpendicular to the contour line direction (Hodgson and Bresnahan, 2004).

The second slope-induced error is due to the spreading of the laser spot on the inclined surface (Figure 3.3b). This effect will spread the time distribution of the returned pulse, increasing the 'rise time' for the return to reach the intensity threshold for return signal registration, and thus increasing the recorded range distance. For a 45° slope with a flight height of 1000 m, this 'time-walk' effect can induce a vertical error of close to 50 cm (Baltsavias, 1999). Errors of this magnitude would reduce the value of airborne lidar for avalanche investigations. It is therefore critical that the flight planning account for areas of steep terrain by modeling the laser and terrain geometry and orienting flight lines to minimize the number of nadir laser shots on steep slopes.

3.3.3 Vegetation

The ability of lidar to map both forest canopy and ground surface elevations in one survey is one of the more attractive features of the technology. Accurate sub-canopy mapping is contingent on a sufficient number of laser shots reaching the ground and returning to the sensor directly. The number of successful ground hits, and therefore the

final surveyed point density, decreases inversely with canopy cover density. Reutebuch *et al.* (2003) compared lidar and manually surveyed elevations in several areas with open, forested, and forested with understory cover types. They showed that the decrease in ground point density is relatively minor, with point spacings on the order of 1 point/m^2 in old growth Douglas Fir forest. The accuracy of the measured point elevations was degraded slightly by the forest or understory due to reduction in the return signal strength, but again this effect was shown to be relatively small – on the order of 10 cm.

The specific relationship between point density and canopy density is determined by the forest cover type (and therefore canopy and understory structures), the laser pulse rate, and the scan angle of the laser sensor. The effects of canopy screening are minimized by increased pulse rates and decreased scan angles. Higher pulse rates (on the order of 50 – 100 GHz) provide a larger number of laser shots per square meter and thus an increased probability of successful canopy penetration. Smaller scan angles increase the probability of canopy penetration by reducing the number of individual trees that a single laser shot must penetrate (see Figure 3.1). However, sub-canopy elevation mapping has been shown to be of comparable accuracy to that in open areas. Indeed, in snow-covered landscapes, the effects of understory vegetation buried in snow combined with the high reflectivity of the snow surface allow for increased accuracy for the snow-covered acquisitions compared to snow-free periods.

3.3.4 Post-processing

After data collection, the 'point cloud' of raw lidar return points are classified as 'terrain' or 'non-terrain' returns. This process is usually highly automated, with several steps requiring interaction from a technician. The classification can be accomplished using any number of (usually proprietary) algorithms, but commonly involves segregating terrain points through an iterative process that evaluates the deviation of individual points from a surface generated from nearby points. Classification thresholds

based on these deviations are somewhat subjective, requiring manual supervision using ancillary data such as digital orthophotos or existing, lower-resolution DEMs.

Misclassification of points can induce errors in the final elevation surface. Because the error magnitude depends on many factors, including the type of filter used, the accuracy of the measured elevation, the elevation of the vegetation above the terrain surface, and the terrain geometry, the contribution of classification errors to the overall surface accuracy will vary widely. It is clear, however, that successful application of classification algorithms is critical to the accuracy of the final elevation surface or snow depth map.

3.4 Snow Surface Interactions

Most lidar acquisitions are performed with a Nd:YAG laser centered at wavelength $\lambda = 1064$ nm with a full-width half-max (linewidth) of ~1 nm (Roth, 2007). At this wavelength, ice is moderately absorptive and therefore snow reflectance is sensitive to grain size. The optical properties of ice are described by the complex refractive index, *m:*

$$m = n + ik \tag{3.1}$$

where n is the real part (that describes refraction) and k is the imaginary part (that describes absorption). At $\lambda = 1064$ nm, k has value of approximately 2×10^{-6}. An understanding of the sensitivity of the transmission at this wavelength to snow grain size and snow liquid water content is important for assessment of the associated uncertainties in snow depth retrievals.

The literature on measurements and modeling of snow transmission is sparse. Beaglehole *et al.* (1998) measured the spectral transmission of solar radiation in snow in six bandpasses from 350 to 900 nm. At 900 nm, they found that the transmission of snow at 2 cm depth was 0.03 and at 4 cm depth the transmission was 0.006. At this wavelength $k \sim 4.1 \times 10^{-7}$, whereas at 1064 nm k is order 10^{-6}, which means that the absorbing path length is smaller. We can therefore consider that the same attenuation of radiation

(scattered + absorbed) comes at a shallower depth (order 1 cm). These measurements were made for fine grain snow that had a small absorbing path length but a larger optical depth for a given snow depth than the case for coarser grains.

Given the lack of measurements of transmission for varying grain sizes at a wavelength of 1064 nm, we are compelled to make the reasonable assumption that 97% of scattering or absorption occurs in the top 1 cm of the snowpack, and therefore the overwhelming proportion of the lidar return from the snowpack comes from the top 1 cm. However, this assumption should be checked with further measurements given that geometric effects in the near-surface layers can contribute to non-exponential decay of radiation (Warren *et al.*, 2006).

Snow impurities will have little effect on the transmission of radiation at this wavelength given that the contrast in k for ice and impurities is relatively small and the proportion of ice is vastly greater than most impurity concentrations (Warren, 1982). Liquid water content should have a similar effect as a coarsening of grain size, whereby the optical depth of the snowpack decreases (increasing transmission) but the absorbing path length increases (decreasing transmission). Therefore, given the bounding measurements discussed above, in these cases we estimate that 97% of attenuation occurs in the top 1 cm of the snowpack.

These measurements and discussion strongly suggest that the backscattered laser signal at the 1064 nm wavelength will come from within the top 1 cm of the snowpack, independent of snow physical properties. Therefore, the sensitivity of the lidar range accuracy to scattering depth is below that of the range sensitivities to scanning geometry and GPS or INS errors.

3.5 Recommendations for Lidar Snow Surveys in Mountainous Areas

Much of the potential for error in surface elevation measurement exists in the geometric relationships between the aircraft dynamics, the scanning system, and the

irregular ground surface. Careful flight planning is critical to minimizing these errors. Lidar contractors use flight planning models to constrain many of the laser geometry parameters, but we recommend that investigators seeking lidar acquisitions be proactive and involved in both the mission planning and post-processing operations.

For snow depth mapping in mountainous, forested terrain, high laser pulse rates (~ 50 kHz) and scan angles on the order of ±15° each side are desired to minimize slope-induced errors and to maximize canopy penetration and thereby maximize ground/snow surface point densities. Flight lines require careful planning so that laser shot/slope angle geometry remain favorable – i.e. obtuse, down-slope shots are minimized. In very complex terrain, significant swath overlap may be required to ensure that the planned point spacing is achieved.

Flight planning requirements for complex mountain terrain, especially the potential for complicated flight lines, are likely to significantly increase flight time and data acquisition costs over survey criteria that are adequate for flat, unvegetated sites. However, to fully utilize the accuracy and spatial resolution potentials of lidar technology, maximum accuracy should be the goal.

Current cost for lidar acquisition is prohibitive for many operational and research budgets. Some cost-saving measures, such as coincident data collection or flight dates for nearby projects, may be available and can significantly decrease aircraft flight time. Further, demand for lidar data is growing, and more lidar survey units are in operation; data collection costs are dropping, and are likely to decrease further as competition increases and as data processing techniques become more efficient.

3.6 Conclusions

Airborne lidar surveying is seeing increased attention as a data source for high-resolution terrain mapping. Repeat surveys that include one snow-free collection and one or more snow-covered collections allow the calculation of snow depth over sizeable

geographic areas with 1-2 m horizontal spacing and decimeter-scale vertical accuracy. Data resolution and accuracy of this scale provides numerous advantages over manual survey or larger-footprint sensors.

Lidar surveying is an evolving field, with rapid advances in technology and processing techniques. The availability of lidar contractors and high-quality scanners and processing routines has increased significantly in recent years. Lidar snow depth surveying has potential to be an important tool for snow hydrology and avalanche science applications, and is sure to have a significant impact on spatial snow science in the years to come.

CHAPTER 4:
FRACTAL DISTRIBUTION OF SNOW DEPTH FROM LIDAR DATA

4.1 Introduction

Knowledge of the spatial distribution of snow in mountain regions is critical for accurate assessment and forecasting of snowmelt timing (Luce et al., 1998), snowmelt volume (Elder et al., 1991) and avalanche hazard (Conway and Abrahamson, 1984; Birkeland et al., 1995), for initialization of synoptic and global-scale weather and climate models (Liston, 1999; Groisman and Davies, 2001), and for investigations of ecologic dynamics and biogeochemical cycling (Jones, 1999; Brooks and Williams, 1999). The interactions of snowfall and wind with terrain and vegetation create highly variable patterns of snow accumulation. These complex interactions present formidable sampling and modeling problems for characterizing spatial snow properties (Elder et al., 1991). The seasonal snow system and its spatial distribution at many scales is dynamically linked to hydrologic, atmospheric, and biologic systems through forcing of runoff characteristics, heat and energy fluxes, soil moisture distributions, and growing season duration (Jones et al., 2001), greatly influencing processes governing energy, water, and biogeochemical cycling in mountain and earth surface systems.

The nature of the process interactions creating spatial snow distributions are complex and the observed variability changes with the scale of observation (Blöschl, 1999); scale is thus central to any assessment of the spatial distribution of snow. Investigations have shown that spatial snow distributions in a variety of environments exhibit fractal characteristics (Shook et al., 1993; Shook and Gray, 1996; Shook and Gray, 1997; Kuchment and Gelfan, 1997; Granger et al., 2002; Litaor et al., 2002). Fractal

distributions indicate self-similar properties over multiple scales, and may provide a theoretical basis for sampling, modeling, and rescaling spatial snow data, and for understanding the underlying process interactions. In this study, snow depth, topography, and vegetation topography data are examined for fractal characteristics and consistencies in scaling characteristics among the three datasets.

4.2 Background

4.2.1 Scale and Snow Measurement

It is difficult to obtain measurements of snow depth distribution over a large area at a resolution that approximates the true variability present (Blöschl, 1999). Manual data collection, via snow stakes or probes is labor-intensive, expensive, and potentially dangerous in steep mountain environments. Airborne and satellite remote sensing methods have been used effectively for estimation of snowpack properties such as snow-covered area and albedo (Dozier and Painter, 2004), but are not yet to the point where they provide real-time operational estimates of snow depth or water equivalent on the scale of individual catchments (Marchand and Killingtveit, 2004). Recently, the use of high-resolution airborne laser altimetry (lidar – Light Detection and Ranging) has been explored for fractal analysis of terrain and vegetation patterns (Pachepsky et al., 1997; Pachepsky and Ritchie, 1998) and for gathering spatial snow depth data (Hopkinson, et al., 2001; Miller et al, 2003). Pachepsky et al. (1997) and Pachepsky and Ritchie (1998) used fractal analysis techniques to study spatial patterns in terrain and vegetation distributions derived from lidar data, but did not examine snow distributions. Hopkinson et al. (2001) and Miller et al. (2003) focused on the utility of lidar altimetry for measuring snow depth, but did not analyze spatial snow distributions. This study builds on the previous work, using fractal analysis to examine spatial patterns and scaling in lidar-derived snow depth distributions.

Snow properties vary over multiple scales, from microscopic crystal morphology and grain bonding to landscape-scale patterns of accumulation and ablation. The amount of variability at each scale is controlled by the process interactions governing snow accumulation, metamorphism, and ablation; as the process interactions change with scale, so too does the variability in the snow cover. As with many Earth-surface phenomena, ordered behavior may be found at some scales, while others show incomprehensible complexity (Phillips, 1999). Identification of 'natural' scales of observation or modeling can lead to better assessment of snow distributions or more effective models. It is important to describe scaling properties of snow depth variation and to identify scales where process interactions change in order to more effectively characterize and model spatial patterns in the snow cover.

Orographic effects on precipitation, dominant at the mountain-range scale, have been observed over elevation changes as small as 50 m (Barry, 1992). However, local-scale (1-1000 m) snow depth variability in mountain environments is dominated by wind redistribution of snow (Elder et al., 1991; Blöschl and Kirnbauer, 1992; Winstral et al., 2002). Wind redistribution coincident with or subsequent to a precipitation event can quickly alter accumulation patterns. This superposition of accumulation processes leads to a dependence on both orography (terrain) and roughness element (vegetation) distribution (Elder et al., 1991. Therefore, the scaling properties of the wind/terrain/vegetation interactions are a critical focus for understanding patterns of snow accumulation over different scales.

Efforts to model the snow depth or snow water equivalent (SWE) distributions resulting from this complex system, while undoubtedly successful, show that there is still progress to be made. Snow distributions have been modeled extensively using terrain components as predictors in diverse model types including simple linear regression, binary regression trees (Elder et al., 1995), and geostatistical methods (e.g. Balk and Elder, 2000), predicated on the wind/terrain interactions that govern

snow redistribution and the relative ease with which terrain can be modeled. Various methods of parameterizing terrain have been explored, including using 'curvature' (the first derivative of slope or aspect) (e.g. Blöschl et al., 1991; Liston and Sturm, 1998), shelter from versus exposure to wind (e.g. Purves et al., 1998), and characterization of upwind and downwind terrain features (e.g. Winstral and Marks, 2002; Winstral et al., 2002). The work of Winstral et al. (2002) confirms the notion that a terrain parameter most suited for addressing snow accumulation addresses the upwind terrain features that directly modify the wind field on the 10-100 meter scale. They demonstrated that a 'wind exposure index' can identify areas of convergent and divergent wind flow, and consequently predict areas of snow scour and deposition.

Winstral et al. (2002) also state that the relatively low portion of the snow depth variance explained by the terrain parameters could be related to differences in process and model scales. This issue, treated in detail by Blöschl (1999), is a critical problem for the development and testing of spatial snow accumulation and melt models. The true spatial variability is never fully knowable, and our assessment and characterization of it is limited by the scales at which we observe snow properties, and the scale at which we model them.

Measurement of spatial phenomena is in essence a filtering of the actual variability on the ground, as the resolution at which measurement occurs is usually different from the actual process scale (Blöschl, 1999). Depending on the true nature of the spatial phenomenon, sampled variability may be either smoother or rougher than what exists on the ground. To assess this scaling effect induced by the data collection, we must therefore know the process scale. The most common method used to estimate the process scale is calculation of the correlation length from a variogram. The correlation length is the lag distance (length) beyond which there is no correlation between adjacent points. In practice, the correlation length is defined as the scale where the semivariance reaches 95% of the spatial (sill) variance, and only exists for stationary (constant mean) or locally

stationary processes where the variogram has a well-defined sill (Webster and Oliver, 2001).

The correlation length, while useful for discriminating autocorrelated from uncorrelated scale regions, cannot describe any scaling relationships at longer or shorter scales. The slope of a log-log variogram, and therefore its fractal dimension, may provide an important alternative to the correlation length (Blöschl, 1999). Fractal analysis performed on a variogram, in addition to identifying important breaks in scale analogous to the correlation length, can also characterize the scaling properties of the spatial distribution in question. Further, if the fractal dimension changes with scale (i.e. the phenomena is multifractal), the length scale of the changes can point to important changes in the process relationships that create the spatial pattern in question.

Other studies have found self-similar, or fractal, behavior in snow properties. Tabler (1980) demonstrated consistent wind drift geometry over several orders of magnitude, from centimeter-scale models to drifts behind four-meter snow fences. This scale invariance suggests that wind-induced patterns of snow accumulation may exhibit scaling properties over a significant scale range, with important implications for analyzing the spatial distribution of snow in mountain environments. Shook et al. (1993) found that patchy snow covers show fractal scaling in the area/frequency relationships of snow and snow-free patches. They attributed this effect to a fractal distribution of snow-water equivalent (SWE). Shook and Gray (1996) analyzed snow depth transects in southern Saskatchewan, and found that snow depth shows a fractal distribution over lengths from 1 to around 30 m, with spatially random behavior at longer distances. Subsequently, Shook and Gray (1997) used fractal distributions to model snow covers in an effort to supplement available field data for snowmelt model development. They also describe the fractal nature of patchy snow covers, and note that the fractal patches arise from the fractal spatial distribution of SWE. Blöschl (1999) examined snow-covered area data from diverse sources across a wide range of scales, and showed that power-law fractal

patterns could exist over several scale regions covering multiple orders of magnitude. Kuchment and Gelfan (1997; 2001) demonstrated fractal behavior in both linear snow course and spatially aggregated snow course data, and used the fractal scaling relationships to estimate spatial snow depth variability at different scales. Granger et al. (2002) also examined patchy snow covers, and found the patch length/area relationship to be fractal. In contrast to previous work, the rich spatial coverage of the lidar dataset used in this study allows a more robust spatial analysis than transect data. Furthermore, the areal coverage of the data allows an analysis of directionality in the spatial patterns of snow depth.

4.2.2 Fractals, and Fractal Measurement

The spatial distribution of snow depth is the result of the complex interactions of many physical processes. Some of the interactions are highly nonlinear or chaotic, producing a pattern with such complexity that it appears random. Such stochastic variation is often treated with geostatistical methods, employing the variogram and correlation length, as described above. Geostatistical techniques characterize a spatially varying phenomenon as a random field, that is the sum of a mean value and a random component (Webster and Oliver, 2001) where the spatial pattern is comprised of random deviations from the mean value. The random characterization neglects any spatial structure that may exist in the random component.

Treating snow depth in the above manner implicitly limits the explainable variability by defining the scale at which the mean value is computed, and does not allow for multiscale effects arising from process interactions over multiple length and time scales. A fractal analysis, conversely, allows for stochastic structure within the random component of the distribution, and explicitly allows multiple scales of variability. Scale invariance, or fractal geometry, has been observed in snow distribution patterns (Shook and Gray, 1996; Kuchment and Gelfan, 1997; Granger et al., 2002) over specific scale ranges.

A fractal is a structure that has infinite detail – i.e. more detail is resolved as the scale of observation is reduced (resolution increased). The structure is therefore *self-similar* – small parts of the structure have the same shape and/or statistical properties as the whole. Mathematical fractals display perfect self-similarity. In practice, no perfect natural fractals have been found, though numerous natural systems show fractal properties over distinct scale windows. Fractal concepts have seen numerous applications in the Earth Sciences, including coastline geometry (Mandelbrot, 1983; Phillips, 1986), earthquake size distribution (Turcotte and Huang, 1995), landslide magnitude (Malamud and Turcotte, 1999), and precipitation events (Peters and Christensen, 2002).

A fractal is quantified by its Hausdorff-Besicovich, or fractal, dimension (*D*). Fractal dimensions are consistent with Euclidean (topological) dimensions, but are non-integer. The fractal dimension of a linear feature has a value between 1 and 2, with numbers near 1 indicating a smooth line, and values near 2 describing a nearly plane-filling object. Similarly, surface features have *D* values between 2 and 3, with low values being close to planar, and high values being nearly volume-filling. Indeed, a fractal is defined as a feature whose Hausdorff-Besicovich dimension exceeds its topological dimension (Mandelbrot, 1983; Lam and DeCola, 1993). *D* therefore is an index of the complexity or roughness of the feature or distribution in question (Turcotte and Huang, 1995; Gao and Xia, 1996).

Natural features most often exhibit fractality only over a specific range of scales (Mark and Aronson, 1984; Gao and Xia, 1996). Often features will have one or more scale windows over which they exhibit fractal self-similarity, with a distinct fractal dimension characterizing each window. This multifractility is not unexpected, as different driving processes are likely to become dominant at different scales in any given system (Blöschl, 1999; Phillips, 1999). These 'scale breaks' can be identified by a change in the fractal dimension value, and can indicate important changes in process or process interactions.

Complex, nonlinear systems have been shown to produce fractal distributions, indicated by power-law behavior in size-frequency relationships (Malamud and Turcotte, 1999). Turbulent wind fields behave chaotically, with vortices resulting from the nonlinearities of viscous fluid dynamics in the near-surface atmosphere (Poveda-Jaramillo and Puente, 1993). Therefore, in environments where wind plays a significant role in the spatial distribution of snow, snow depth is expected to show a fractal distribution over scales from 1 cm to 1000 m, where wind redistribution dominates.

If the spatial distribution of snow depth has fractal characteristics, the spatial distribution has a structure that produces similar statistical snow depth distributions at multiple scales, allowing spatial pattern characteristics to be transferred from one scale to another using a scaling parameter (Kuchment and Gelfan, 1997). Fractal analysis can also provide information about the scale, scope, and resolution of modeling and field sampling efforts, as well as reveal any particular scale ranges over which snow depth distributions can be up- or down-scaled. Knowledge of the spatial scales over which a phenomenon shows a fractal distribution also exposes scales at which important changes in governing processes occur (Burrough, 1981).

4.2.3 Objectives

Previous analyses applying fractal techniques have important ramifications for up- and down-scaling of snow depth distributions, sampling design, and the appropriate resolution of snow accumulation models. This study builds on these previous efforts, using high-resolution, spatially extensive data that allow a detailed analysis over a large area and in multiple directions. We examine the fractal characteristics of snow depth distributions and the associated terrain and vegetation patterns. lidar-derived snow depth, topography, and vegetation topography datasets from three study sites are subjected to variogram analysis to look for fractal patterns and scale limits to fractal behavior. The variogram analysis is next restricted to 16 compass directions to examine anisotropy

in the datasets. The fractal characteristics of snow depth, topography, and vegetation topography are then compared to look for any scaling characteristics consistent among the three datasets.

4.3 Study Areas

This study uses data from the 2003 NASA Cold Land Processes Experiment in Colorado, at the Buffalo Pass, Walton Creek, and Alpine Intensive Study Areas (Cline et al., 2001; Figures 4.1 and 4.2). The Buffalo Pass site is characterized by dense coniferous forest interspersed with open meadows, low rolling topography, and deep snowpacks. The Walton Creek site provides a broad meadow environment, interspersed with small, dense stands of coniferous forest, low rolling topography, and deep snowpacks. The Alpine study site contains alpine tundra, with some subalpine coniferous forest, and is generally north-facing with moderate relief (Cline et al., 2003). Buffalo Pass and Walton Creek are in a similar synoptic-scale terrain position, receiving high annual snowfall, while the Alpine site receives lower annual precipitation totals and has greater wind exposure above treeline.

The three study areas provide a variety of terrain and vegetation environments,

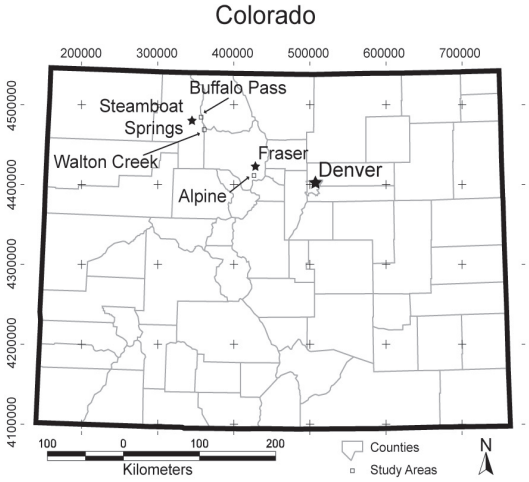

Figure 4.1. Locations of the Buffalo Pass, Walton Creek, and Alpine NASA CLPX Study areas.

a.

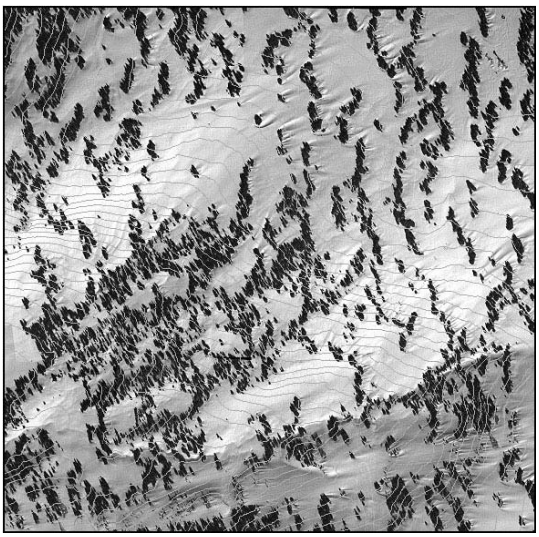

b.

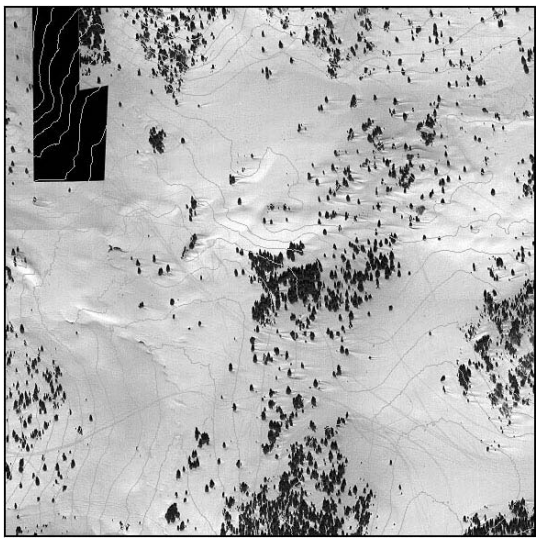

c.

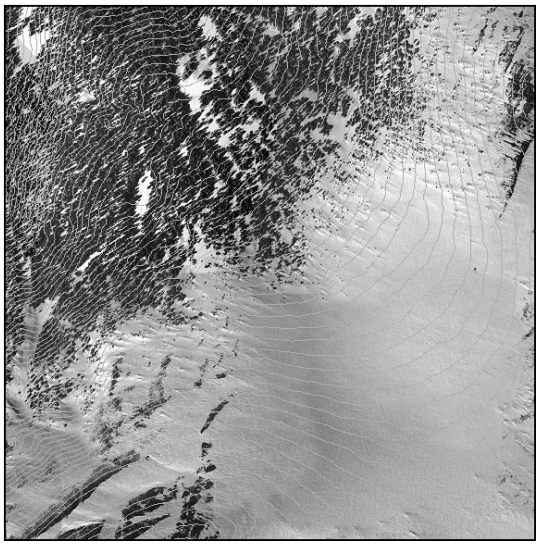

Figure 4.2. NASA CLPX ISA orthophotos. Contour interval is 5 meters. Photos were captured on April 9, 2003, concurrent with lidar data acquisition. a. Buffalo Pass: Dense coniferous forest interspersed with open meadows and ribbon forest; low rolling topography with deep snowpacks; b. Walton Creek: Broad meadow interspersed with small, dense stands of coniferous forest; low rolling topography with deep snowpacks; c. Alpine: Alpine tundra, with some subalpine coniferous forest; generally north-facing with moderate relief (Cline, et al., 2003).

from low to high relief, and from alpine tundra to subalpine forest of varying density. Field observations indicate that snow distributions at all sites are dominated by wind redistribution and wind interaction with terrain and vegetation patterns. Wind direction frequency distributions, calculated from meteorologic data collected at each of the study sites for a period of 1 October 2002 through the lidar flight date of 9 April 2003 (Elder and Goodbody, 2004), indicate that winds of speeds greater than 5 m s^{-1} (at 10 m height) are confined to narrow direction bands (Figure 4.3).

4.4 Methods

4.4.1 Lidar Altimetry

Lidar altimetry is used for many applications, including terrain modeling and forest structure mapping. Lidar altimetry offers the ability to process multiple laser returns to get bare ground or snow and canopy height information. The data used here have 1.5 meter nominal horizontal spacing between data points, and a 0.15 m vertical

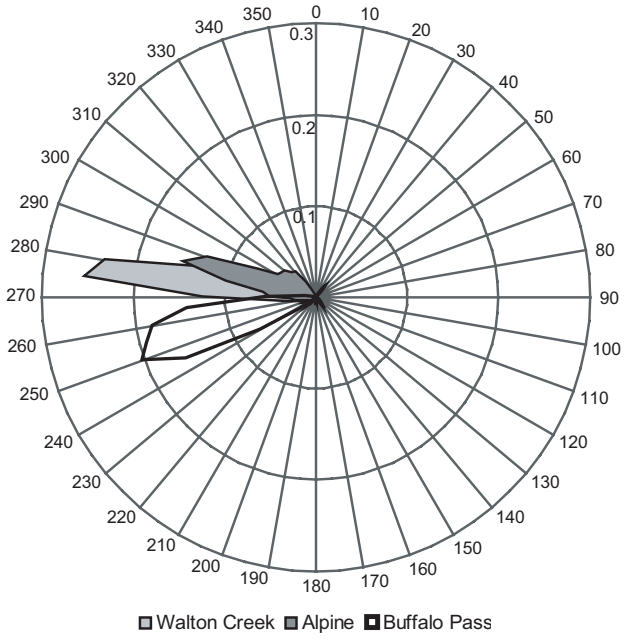

Figure 4.3. Wind direction frequency for a threshold wind speed of 5 m s^{-1}. Snow transporting winds are confined to relatively narrow direction bands; anisotropy in the snow depth, terrain, and vegetation topography fractal dimensions is consistent with these dominant wind directions.

measurement tolerance. Positioning data were collected using a combination of Global Positioning System and inertial navigation system technologies. The raw data were normalized using ground control points, and then post-processed to remove redundant data points and noise (Miller, 2003).

Two lidar datasets are used for this study – one acquired on 9 April 2003 and the other on 19 September 2003. The last-return signal from the September mission provides ground surface ('bare earth') elevations, the September first-return data measure the terrain-plus-vegetation (vegetation topography) elevations, and the April last-return data provide snow surface elevations. A 1 m resolution DEM was produced from the bare earth point data using inverse-distance-weighting interpolation. The DEM elevations were then subtracted from the snow surface elevation points, producing a dataset of snow depth point estimates. The point datasets of snow depth, bare earth elevations, and vegetation topography were used for the variogram fractal analysis.

4.4.2 Variogram Fractal Analysis

Omnidirectional and directional semivariograms, $\gamma(r)$, are estimated using 50 log-width bins:

$$\gamma(r_k) = \frac{1}{2(N_k)} \sum_{i=1}^{N_k} \{z_i - z_j\}^2 \qquad (4.1)$$

where r is the lag distance of bin k, N is the total number of pairs of points in the k^{th} bin, and z_i and z_j are the snow depth values at two different point locations i and j. Log-width distance bins are used to provide equal bin widths when the variograms are transformed to log-log space. Log-width bins also allow for a greater bin density at short lag distances than would linear-width bins, which aids in resolving the variogram structure at short length scales; therefore log-width bins allow a more precise power law fit than would standard linear distance bins. The variograms were restricted to a maximum distance of

1100 m, the diameter of the largest circle that could be fit within the mapped area, which helps avoid directional bias (Mark and Aronson, 1984). Additionally, any non-stationarity in the data was not removed, though that is standard practice in a geostatistical analysis. In fractal analysis, the fractal dimension is an index of the relative balance of long- and short-range processes, and removing large-scale trends would bias the calculated fractal dimensions toward short-range variability (Klinkenberg and Goodchild, 1992).

The variograms are log-transformed to allow identification of regions that can be described by a power-law. Linear regions in each log-log variogram are identified visually, and each straight section is fit with a power function of the form:

$$\gamma(r) = ar^b \tag{4.2}$$

by varying coefficients a and b to minimize the squared residuals.

The fractal dimension (D) is estimated from the slope (power) of the log-log variogram by (Gao and Xia, 1996):

$$D = 3 - b/2 \tag{4.3}$$

When breaks in slope are observed in the log variogram plots, the scale break length is determined from the intersection of the two fitted power law curves. It is recognized that, rather than a discrete break, the slope changes continuously from one linear segment to another. It should be noted, however, that this change in slope occurs over a relatively short scale range. The power-law relationships display very good fits with the transition region included in the power-law segments (R^2 based on the log data greater than 0.90). Solving the two power-law equations to derive a single break point provides a consistent measure that is comparable between datasets. Shook and Gray (1996) used a similar methodology, though they assumed that the longer-range sections approached a completely random spatial distribution (flat slope, $D = 3$). Their technique results in slightly larger estimates of the scale break distance than the technique used here. Our methods likely produce a more conservative estimate of the scale break location.

4.5 Results

4.5.1 Snow Depth

All three datasets show strong power-law distributions over two segments, separated by a relatively distinct scale break (Figure 4.4). The short-range window is characterized by fractal dimensions of approximately 2.5, while at longer distances the *D* values approach 3, indicating nearly spatially random distributions (Table 4.1).

The directional variograms (Figure 4.5, a and b) show short-range *D* values that are smaller parallel to the dominant wind direction, showing smoother (i.e. autocorrelated) patterns with the wind and rougher patterns normal to the wind (see Figure 4.3). The long-range, directional *D* values (Figure 4.5b) show the opposite pattern of the short-range values, namely that the smallest fractal dimensions are found perpendicular to the dominant wind direction.

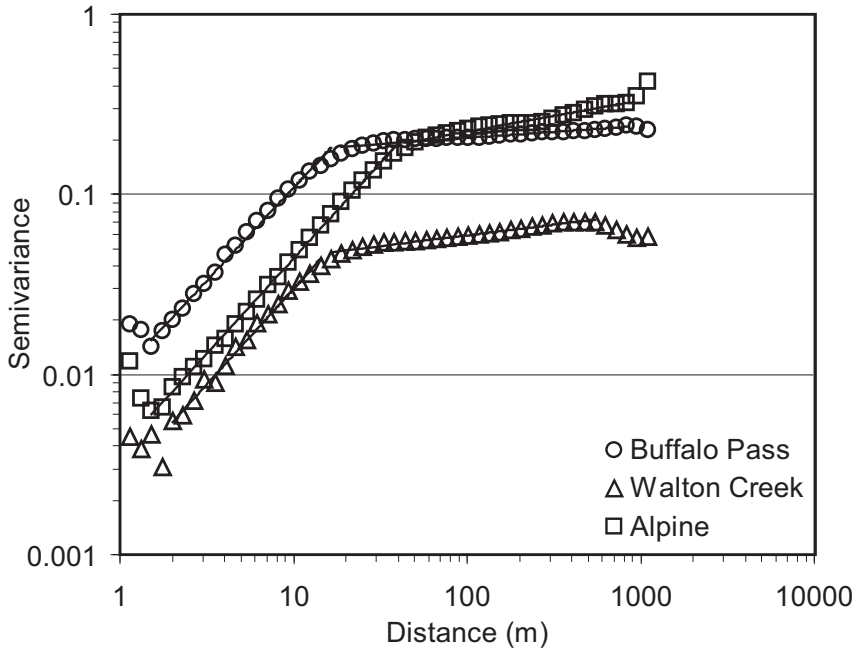

Figure 4.4. Snow depth log-log variograms. Log-linear segments indicate self-similar, fractal distributions. At each site, a short-range fractal segment ($D \approx 2.5$) is separated by a break point from a long-range fractal segment ($D = 2.91 – 2.97$). The length of the scale break varies depending on the site (see Table 2).

Table 4.1. Snow depth fractal dimensions (*D*) and scale break lengths, and vertical relief for the three study sites.

	Walton Creek	Buffalo Pass	Alpine
Short-range *D*	2.47	2.48	2.47
Long-range *D*	2.94	2.97	2.91
Scale Break Length (m)	15.5	16.5	40.3
Vertical Relief (m)	98	184	339

4.5.2 Bare Earth Topography

The topography datasets show power-law behavior over several orders of magnitude, from around 10 m to over 1000 m (Figure 4.6; Table 4.2). The power-law fits are strong, with R^2 values greater than 0.90. The Buffalo Pass and Alpine variograms plots are nearly coincident, with very similar *D* values. The Walton Creek terrain data show a much higher fractal dimension than the other two sites, indicating a much higher relative roughness. The small scale terrain variations are large relative to the overall relief of the area. In contrast, the Buffalo Pass and Alpine sites have a large-scale relief that is large relative to the small scale terrain roughness.

The directional terrain variograms show strong anisotropy (Figure 4.7). The smallest *D* values, and thus the smoothest relative roughness, are found parallel to the direction of maximum relief.

4.5.3 Vegetation Topography

The Buffalo Pass and Walton Creek vegetation topography data show similar scale breaks, at 50 and 60 m, respectively, while Alpine has a scale break at 30 m (Figure 4.8; Table 4.3). At scales below the break, the fractal dimensions are consistent between sites, varying from 2.81 to 2.86. Beyond the scale break, the distributions are virtually identical to the pattern in the bare earth topography data.

The directional variograms show that the short range *D* values have little variation

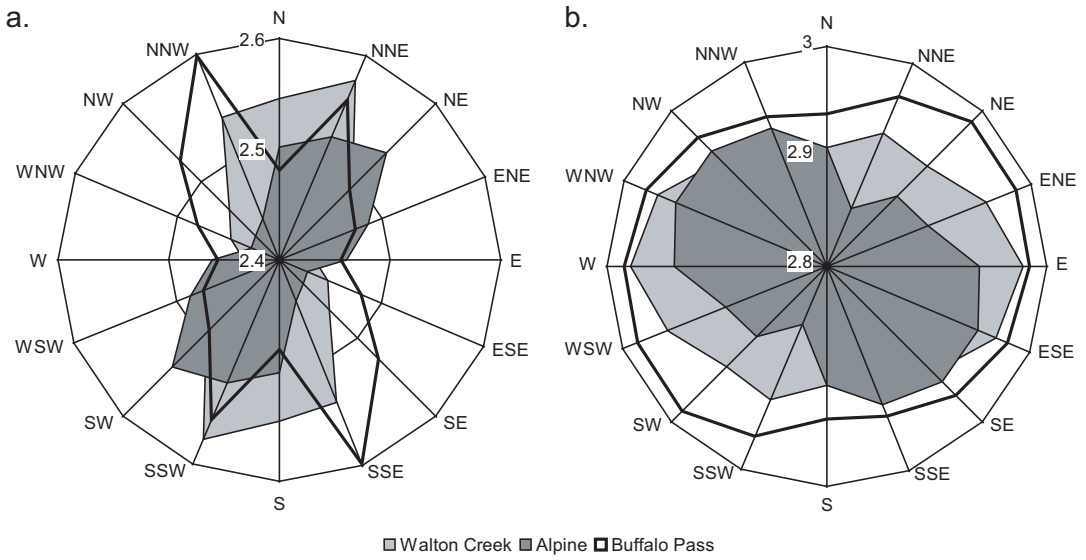

Figure 4.5. Snow depth fractal dimensions by azimuth. Strong anisotropy is present in both the short-range (a) and long-range (b) fractal windows. At short ranges, higher *D* values are found normal to the dominant snow-transport wind direction (see Figure 6). Long-range *D* values show the opposite relationship. Buffalo Pass shows its smallest fractal dimension in a north-south orientation, coincident with the direction of ribbon forest orientation in that area.

with direction, with the exception of a decrease in *D* values in the north/south direction at Buffalo Pass, likely the effect of the ribbon forest orientation at that site (Figure 4.9a; Figure 4.2a). The long-range fractal dimensions show strong anisotropy, with directional patterns very similar to the bare earth terrain data (Figure 4.9b).

4.6 Discussion

The results of the fractal analysis show that the snow depth and terrain datasets are well described by the fractal model over specific scale intervals. The fractal dimensions obtained are consistent with previous studies, as are the scale windows over which snow depth exhibits fractal behavior. There is distinct anisotropy in the fractal dimensions. Topography and vegetation topography also fit the fractal model well; vegetation topography shows a scale break at a scale magnitude compatible with that observed in the snow depth data, while bare earth topography shows no scale break within the range of scales available in the data.

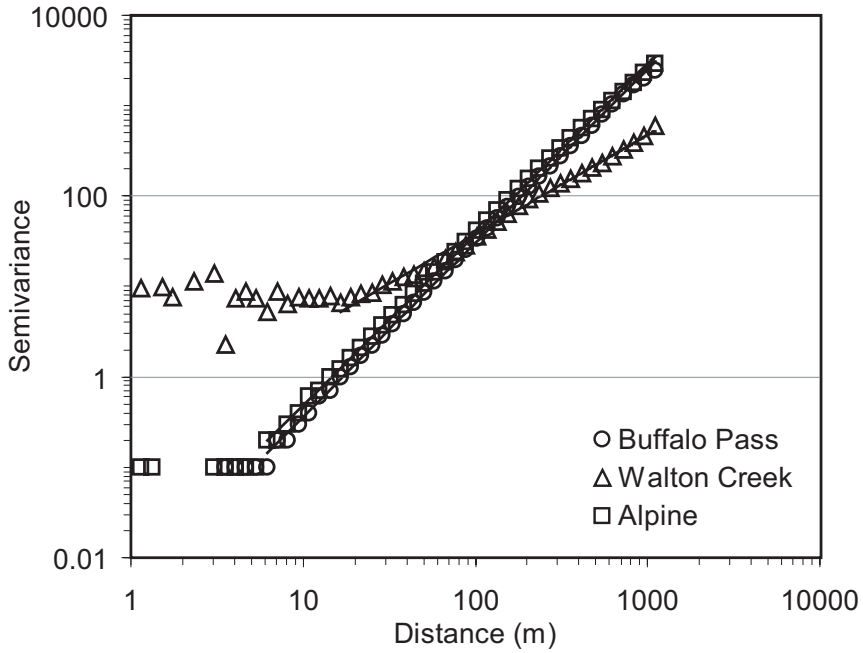

Figure 4.6. Bare earth topography log-log variograms. Fractal distributions of a single *D* value are observed over nearly the entire scale range available. Walton Creek has a higher fractal dimension than Buffalo Pass and Alpine, produced by its higher relative terrain roughness (high short-range/long-range variability ratio).

4.6.1 Omnidirectional Distributions

The scale break observed in the snow depth distributions indicates a change in the process dynamics controlling snow accumulation. The spatial and/or functional relationships between wind, terrain, and vegetation, which combine to produce the snow distribution patterns observed at a particular scale, are substantially different when observed at resolutions above and below the scale break. The values of the snow depth fractal dimensions on either side of the scale break lend insight into how the resulting patterns are different, and may guide investigation into the actual process dynamics.

The short-range snow depth *D* values are nearly identical at all three sites, indicating

Table 4.2. Bare earth terrain fractal dimensions (*D*) for the three study sites.

	Walton Creek	Buffalo Pass	Alpine
D	2.45	2.04	2.06

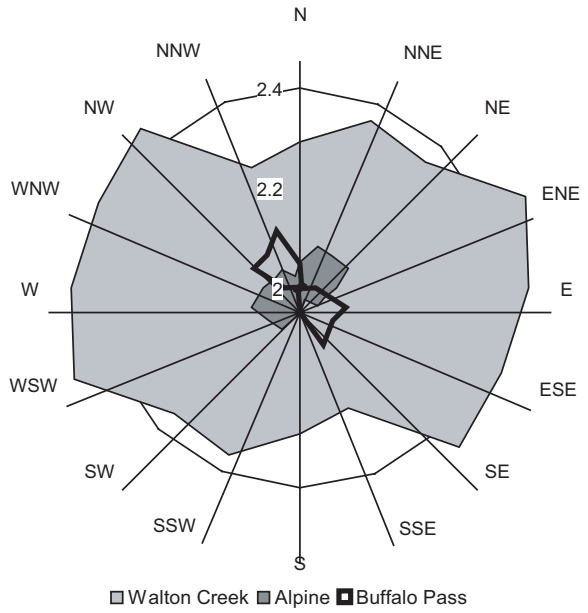

Figure 4.7. Bare earth topography fractal dimensions by azimuth. Lower fractal dimensions are found in directions parallel to the large-scale terrain trend.

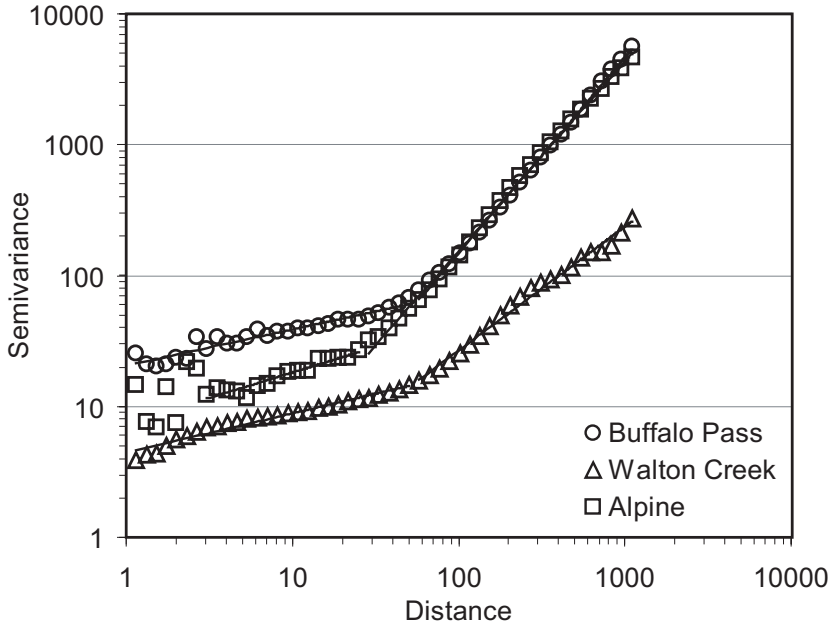

Figure 4.8. Vegetation topography log-log variograms. Two fractal windows are observed, separated by a scale break at 20-40 m; the large-scale window appears nearly identical to the bare-earth terrain variograms, indicating the dominance of the terrain signature at scale lengths greater than the scale break. The small-scale window is dominated by the vegetation distribution.

Table 4.3. Vegetation topography fractal dimensions (*D*) and scale break lengths for the three study sites.

	Walton Creek	Buffalo Pass	Alpine
Short-range *D*	2.85	2.86	2.81
Long-range *D*	2.53	2.25	2.28
Scale Break Length (m)	52.7	55.9	30.8

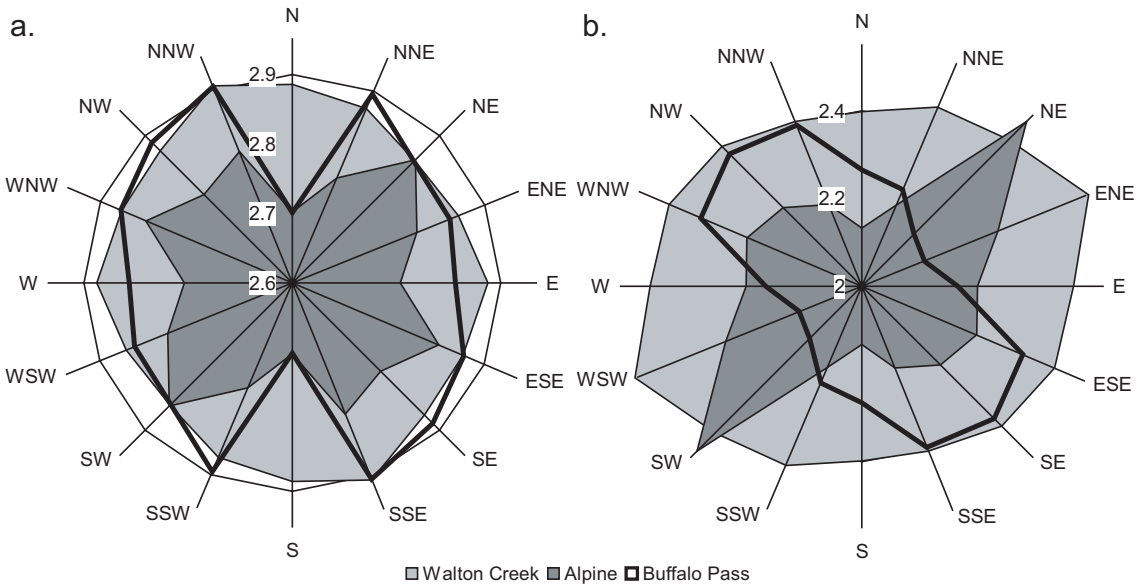

Figure 4.9. Vegetation topography fractal dimensions by azimuth. Short-range (vegetation signal) *D* values are nearly isotropic, except for Buffalo Pass; the decrease in *D* in the north-south direction is likely due to the presence of ribbon forests. The long-range *D* values are very similar to the terrain values, as the similarity between the terrain and vegetation topography omnidirectional variograms would suggest.

that the process interactions producing the snow depth patterns are essentially equivalent in all three areas. This similarity in *D* values also implies that the physical characteristics that differ between sites are insignificant in determining the snow depth patterns over short distances. Fractal dimensions have been used to differentiate features that are formed by different process interactions (Burrough, 1993); the spatial organization indicated by the fractal distribution may be characteristic of snow accumulation patterns in wind-dominated areas when observed over a square-kilometer extent. The snow depth *D* values of 2.5 indicate that at length scales below the scale break, variation due to short-range processes, such as snow drifting around individual trees, is balanced by

variation caused by longer-range process influences such as the direction of wind flow above the canopy (Burrough, 1993; Kuchment and Gelfan, 1997; Blöschl, 1999). At distances longer than the scale break, the snow depth fractal dimensions vary from 2.91 (Alpine) to 2.97 (Buffalo Pass). The high *D* values indicate that the distribution in this upper fractal window is dominated by high-frequency variations (relative to the power-law region). Though the patterns approach spatially random distributions, the spatial structures indicate fractal distributions. The high values suggest, however, that spatial interpolations from sparsely distributed data points may not be appropriate.

The fractal dimensions of the different scale windows have important ramifications for spatial modeling and mapping. In order to interpolate a surface from point observations, the parameter variability as a function of the distance from a data point must be known or estimated. If the spatial distribution is dominated by short-range variation (high *D* value), then the point values are essentially independent, and the variable is probably better characterized as a random distribution. The fractal dimensions calculated for snow depth suggest that this is the case at length scales longer that the scale break. However, at length scales shorter than the scale break, the *D* values indicate a near equal balance of long and short-range variation – more spatial structure (Burrough, 1993). Spatial interpolation may therefore be reasonable over the scale range below the break point.

The vegetation topography dataset represents the surface roughness elements that wind and blowing snow interact with directly. The bare earth topography certainly influences snow accumulation, predominately through flow concentration and separation, and orographic precipitation mechanisms. However, snow depth variability is dominated by blowing snow/vegetation interactions across a wide range of scales dependent on vegetation characteristics interacting with local topography. Therefore, the scaling properties of the vegetation topography dataset are critical to investigating scale characteristics of snow depth.

The vegetation topography data show a scale break at the same order of magnitude as snow depth, though at a slightly longer absolute range. This scale break indicates a switch from a pattern dominated by short-range vegetation variability to one predominately influenced by longer-range variations in terrain. A pattern change in the interaction of terrain and vegetation processes would no doubt influence the patterns of snow deposition and redistribution observed at scales straddling the scale break. All three sites show a scale break separating a scale region of high-frequency variability from a region of terrain-influenced low-frequency variability.

The bare earth terrain shows no scale break over the scale range available in the data. Other studies have shown that terrain patterns in a wide variety of physiographic environments typically exhibit a scale break at lengths around 1.5 to 2 kilometers (e.g. Klinkenberg and Goodchild, 1992; Mark and Aronson, 1984), which is larger than the size of the study area used here. An analysis of vegetation height data (vegetation topography with bare earth terrain subtracted), also does not display a scale break. That the vegetation topography data do show a sharp break in slope, while the individual terrain and vegetation height datasets do not, indicates that a process interaction changes at that particular length scale.

Kuchment and Gelfan (2001) analyzed spatial patterns of snow depth from transect data at slightly longer scales than presented here, and so were unable to resolve any scale breaks that may be present in the 10-50 m range. However, for longer length scales they produced fractal dimensions of 1.82-1.93, similar to those found in this study (linear transects will have a fractal dimension between 1 and 2, and adding 1 to the D value will give the equivalent fractal dimension for a surface). Their study sites were diverse, varying from low to high relief, and steppe to forest to tundra environments. Shook and Gray (1996) also used transect data to compute fractal dimensions and scale breaks (cutoff lengths, in their study), with results (D = 1.53, scale break at 30-500 m) similar to those obtained here. The fractal slope at distances longer than the scale break was

also nearly random (D = 1.94). In both of the above studies, the terrain and vegetation in the study areas were significantly different from the sites used here. The consistency of results between all three studies suggests that the spatial properties of snow depth can be consistent across different environments, given a strong dependence on wind redistribution.

Shook and Gray (1996) demonstrated differences in the scale break length between sites, and showed a dependence of scale break distance on topographic relief. Our results follow a similar scale break pattern, with the scale break distances increasing with the overall study area relief (Table 4.1). However, there are several other differences between the three study areas that could impact the scale break location. For instance, the forest structure is dramatically different at each site, with dense stands and open meadows at Walton Creek, sparse stands and ribbon forests at Buffalo Pass, and dense subalpine adjacent to treeless tundra at the Alpine site. Notably, the Buffalo Pass and Walton Creek snow depth scale breaks are essentially equivalent, while the scale break at Alpine is at a much longer distance. This implies a regional difference, perhaps related to the vegetation/terrain interaction. The vegetation topography scale breaks are also nearly identical at Buffalo Pass and Walton Creek, and are at the same order of magnitude as the snow depth scale breaks. These corresponding scale features indicate that the vegetation/terrain interaction at Buffalo Pass and Walton Creek exhibit similar scaling properties, and that the scale patterns of vegetation topography are qualitatively related to the regional differences in scale break length. Therefore the scale break differences cannot be solely related to relief effects, though the influence of broad-scale terrain trends is undoubtedly important.

The fractal spatial distribution of snow depth at short scales suggests that rescaling of observed distribution patterns would be possible as long as the resolutions or grid sizes of the original and rescaled patterns both fall within the same fractal window. For example, a spatial distribution with a 30 m resolution could be rescaled to a 10 m resolution at

the Alpine site, but not at either Rabbit Ears site. The scale window extent also has implications for sample design. It is likely that as sample spacing is increased toward the upper limit of the scale window, the fractal slope and the location of the scale break will become progressively less resolvable, and therefore representation of the spatial structure will become increasingly poor. On the other hand, if resolutions above the scale break are desired, the data suggest that upscaling from 1000 m resolution is possible, allowing for less expensive data collection at coarser resolutions. However, since the D values in the upper scale range are very high, the spatial distribution of snow depth is nearly random. Investigations conducted at resolutions in this range would provide information on the magnitude of snow depths, but will show very little spatial structure.

4.6.2 Directional Distributions

The large volume of data present in the lidar datasets enables an investigation of directional anisotropy in the magnitude of the fractal dimensions. The snow depth data show opposite patterns between the short-range *D* values and the long-range *D* values; the process change that occurs at the scale break appears to alter the relationships producing the directional fractal dimension patterns.

For distances shorter than the scale break, snow depth fractal dimensions are larger in directions normal to the prevailing wind. These length scales are of a magnitude consistent with snow drifts behind trees and small terrain features. A depth transect at the 1-15 m scale measured across a series of drifts would show a higher roughness (negative correlation) than a transect lengthwise along an individual drift, and thus a higher fractal dimension (e.g. see the drift patterns in Figure 4.2a). At longer length scales, the largest snow depth *D* values occur parallel to the dominant wind direction. The large-scale trends are influenced by large terrain trends, such as those produced by orographic precipitation or lee slope drifting, and thus would exhibit maximum roughness in the direction consistent with the dominant wind-steering terrain feature.

The terrain data show anisotropy that is also similar to, and likely induces, the dominant wind direction at each site. The lowest fractal dimensions are found parallel to the direction of maximum relief at each site, implying a lower roughness in this direction. Despite this directional variation, the *D* values are relatively small in all directions, indicating that the high persistence and the dominance of low-frequency variability in the terrain data are relatively consistent in all directions.

The vegetation topography data are essentially isotropic at scale ranges shorter than the scale break. The exception is Buffalo Pass, which shows a distinct decrease in fractal dimension in the north/south direction. This anisotropy is likely due to the presence of north/south oriented ribbon forests in the northeast quadrant of the study site (Figure 4.2a). For scale lengths longer than the scale break, vegetation topography shows anisotropy very similar to the terrain data. This similarity is not surprising, as the terrain variability is dominating the vegetation topography fractal signal in this scale window.

As with the omnidirectional results, the anisotropic behavior of the snow depth spatial distributions could be important for measuring and modeling snowpacks. Sampling schemes could have varying spatial resolutions dependent on orientation to dominant wind patterns. Models representing accumulation processes, especially wind, may also require parameters that change with direction. A better understanding of the actual process dynamics that cause the scaling features and directional anisotropy is required if these concepts are to aid practical application of measurement and modeling of snowpack processes.

4.7 Conclusions

The complex process interactions that produce the spatial distribution of snow in mountain environments change with scale. Sampling, modeling, and prediction efforts therefore require an assessment of the scaling properties of snow distributions in order to capture and represent natural variability in the snow cover. Fractal analysis techniques

applied at the local scale (1-1000 m) show promise for identifying scales at which snow-related processes or process interactions change, and for finding scale regions over which rescaling of measured or modeled distributions may be reasonable.

Snow depths, as derived from lidar altimetry surveys, show two distinct scale regions with fractal distributions, separated by a scale break. At small distances, the fractal dimensions are close to 2.5 for all study sites, indicating rich spatial complexity and a balance between high- and low-frequency variations. At larger distances, snow depth shows a very high fractal dimension (> 2.9), approaching a spatially random distribution. The length of the scale break between fractal windows appears to vary with overall terrain relief; longer break distances are found in higher-relief terrain. These results are consistent with previous studies in diverse environments; however it is important that relief is not the only characteristic that varies between sites, and other factors, such as local snowfall characteristics, could also be influencing the scale break length.

Terrain and vegetation interactions also show fractal distributions over distinct scale regions, with vegetation effects dominating at small distances and terrain effects dominating at large distances. The length of the scale break separating the two fractal regions in the terrain/vegetation distributions is of the same order of magnitude as the scale break observed in the snow depth data, which indicates that the process change revealed in the vegetation/terrain data potentially influences the scaling behavior of snow depth patterns.

The snow depth fractal dimension varies with direction, and shows a strong qualitative relationship to prevailing winds and large-scale topographic orientation. The anisotropy indicates that directionality of controlling processes must be considered in pattern-analysis application or in sampling design. Terrain and vegetation topography fractal dimensions are also anisotropic; the directional variation appears to be related mainly to the terrain orientation, though the Buffalo Pass site shows some variation in the vegetation distribution associated with the presence of ribbon forests.

Efforts to assess, model, and predict spatial snow distributions are increasingly needed for water supply estimation, river forecasting, and avalanche danger evaluation. In order to improve these efforts, the behavior of controlling process interactions at different scales must be addressed. The fractal techniques presented here provide important measures of process change scales and scaling behavior in snow distributions. Investigations of multi-scale spatial patterns as applied in this study offer a necessary perspective on snow system behavior across multiple process regimes, and can distinguish scales where ordered pattern exists from scales where disorder dominates. Quantifying system interactions at multiple scales is critical for understanding the complex relationships between wind, terrain, vegetation, and snow distributions.

CHAPTER 5:
INTERANNUAL CONSISTENCY IN FRACTAL SNOW DEPTH PATTERNS AT TWO COLORADO MOUNTAIN SITES

5.1 Introduction

Many hydrologic (Luce *et al.*, 1998; Elder *et al.*, 1991), ecologic (Jones, 1999; Brooks and Williams, 1999), and climatic (Liston, 1999; Groisman and Davies, 2001) investigations require that spatial distributions of snow amounts be known or estimated. In complex, mountainous terrain, precipitation and snow redistribution amounts and patterns are often highly variable and difficult to measure. The complex interactions of snowfall and wind with terrain and vegetation present formidable sampling and modeling problems for characterizing spatial snow properties (Elder *et al.*, 1991; Winstral *et al.*, 2002; Erickson *et al.*, 2005). However, since seasonal snow and its spatial distribution at many scales is dynamically linked to hydrologic, atmospheric, and biologic systems through forcing of runoff characteristics, heat and energy fluxes (Liston, 1999), soil moisture distributions (Sturm *et al.*, 2001), and growing season duration (Jones *et al.*, 2001), the ability to measure and model snow distributions is critical to understanding and representing the processes governing energy, water, and biogeochemical cycling in mountain and earth surface systems.

The nature of the process interactions creating spatial snow distributions are complex and the observed variability changes with the scale of observation (Blöschl, 1999). Scale is thus central to any assessment of the spatial distribution of snow. Recent work has shown that spatial snow distributions in a variety of environments exhibit fractal characteristics (Shook *et al.*, 1993; Shook and Gray, 1996; Shook and Gray, 1997;

Kuchment and Gelfan, 1997; Granger *et al.*, 2002; Litaor *et al.*, 2002; Deems *et al.*, *2006*). Fractal distributions indicate self-similar properties over multiple scales, and provide a theoretical basis for sampling, modeling, and rescaling spatial snow data, and for understanding the underlying process interactions.

Deems *et al.* (2006) examined snow depth, topography, and vegetation topography for fractal scaling characteristics at three locations. Snow depth at all sites was found to show two distinct regions of fractal scaling separated by a scale break, where process dynamics appear to change character. The lag distance of the scale break varied among the sites, but is consistently longer where the overall relief of the study area is higher, as found by Shook and Gray (1996). The fractal dimensions of each scale range were very consistent between sites, suggesting that the scaling properties in the snow depth distributions are consistent among different physiographic and vegetation covers within the same snow climate. Additionally, the fractal distributions were shown to be anisotropic, with directional patterns related to the dominant wind direction at each site.

In this study, a second lidar data acquisition allows an investigation of interannual consistency in the observed fractal distributions and scaling features at two of the sites used in the previous study. Consistency between different snow seasons with differing accumulation characteristics would indicate that the scaling characteristics are intrinsic to the specific site, and are relatively insensitive to variations in weather patterns. A robust estimation of scaling characteristics for a single site would allow more efficient and accurate sampling design, data interpolation, and rescaling of existing data.

5.2 Study Areas and Snow Seasons

5.2.1 Study Areas

Two sites from the NASA Cold Land Processes Experiment in Colorado, the Walton Creek and Alpine Intensive Study Areas (Cline *et al.*, 2001; Figures 5.1, 5.2), were used

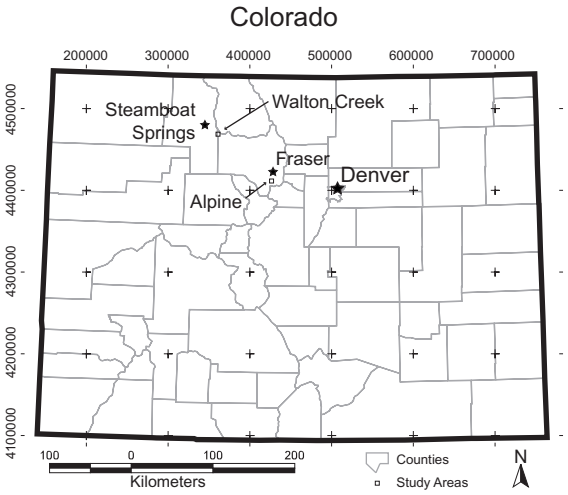

Figure 5.1. Locations of the Walton Creek and Alpine NASA CLPX Intensive Study Areas.

in this study. The moderate-elevation Walton Creek site, in the Yampa River Basin, is characterized by a broad meadow environment, interspersed with small, dense stands of coniferous forest, low rolling topography, and deep snowpacks. The high-elevation Alpine study site, in the Upper Colorado River Basin, contains alpine tundra, with some subalpine coniferous forest, and is generally north-facing with moderate relief (Cline *et al.*, 2003). Walton Creek receives high annual snowfall and calm to moderate winds, while the Alpine site receives lower annual precipitation totals and has greater wind exposure above treeline.

The two study areas provide a contrast of terrain and vegetation environments, from low to high relief, and from alpine tundra to subalpine forest of varying density. Field observations indicate that snow distributions at both sites are dominated by wind redistribution and wind interaction with terrain and vegetation patterns. Wind direction frequency distributions, calculated from meteorological data collected at each of the study sites for both snow seasons in this study (Goodbody *et al.*, 2006), indicate that winds of speeds greater than 5 m s^{-1} (at 10 m height) are confined to narrow direction bands (Figure 5.3).

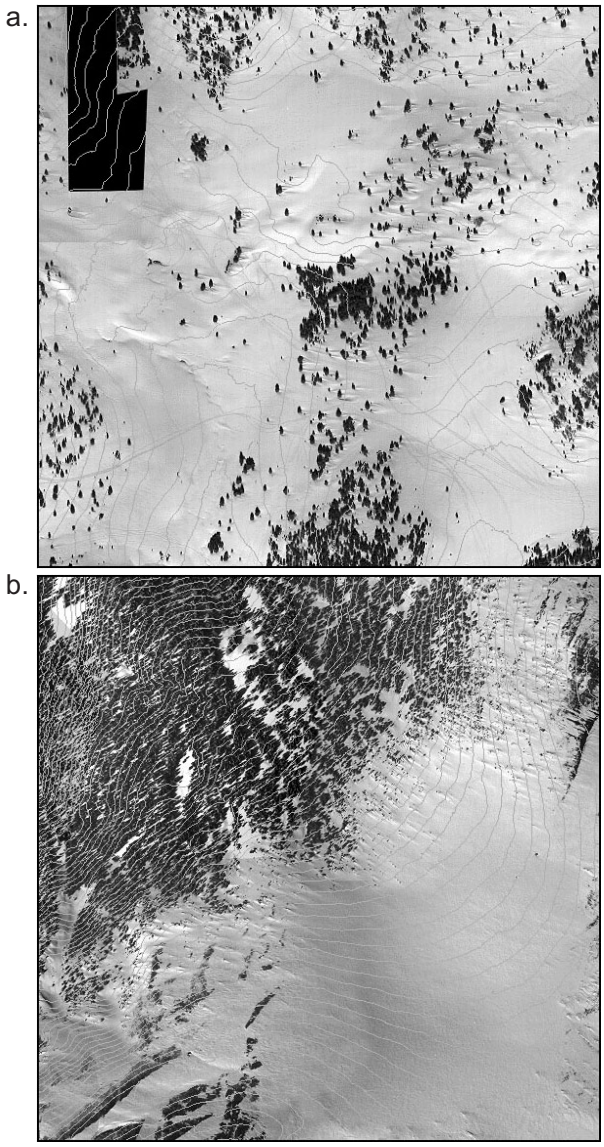

Figure 5.2. NASA CLPX ISA orthophotos captured on 9 April, 2003, concurrent with lidar data acquisition. Contour interval is 5 meters. a. Walton Creek: broad meadow interspersed with small, dense stands of coniferous forest; low rolling topography with deep snowpacks; b. Alpine: alpine tundra, with some subalpine coniferous forest; generally north-facing with moderate relief (Cline, *et al.*, 2003).

5.2.2 2003 and 2005 Snow Seasons

The snow season evolution for the 2003 and 2005 snow seasons can be characterized through micrometeorological data collected at each CLPX study site as well as data from nearby USDA Natural Resource Conservation Service Snow Telemetry (SNOTEL) sites. These data allow an interannual comparison of precipitation amounts and wind redistribution, two major controls on spatial snow accumulation patterns at slope to basin scales.

The Yampa River Basin as a whole experienced very similar season total SWE and precipitation accumulation in 2003 and 2005, as did the Upper Colorado Basin. As

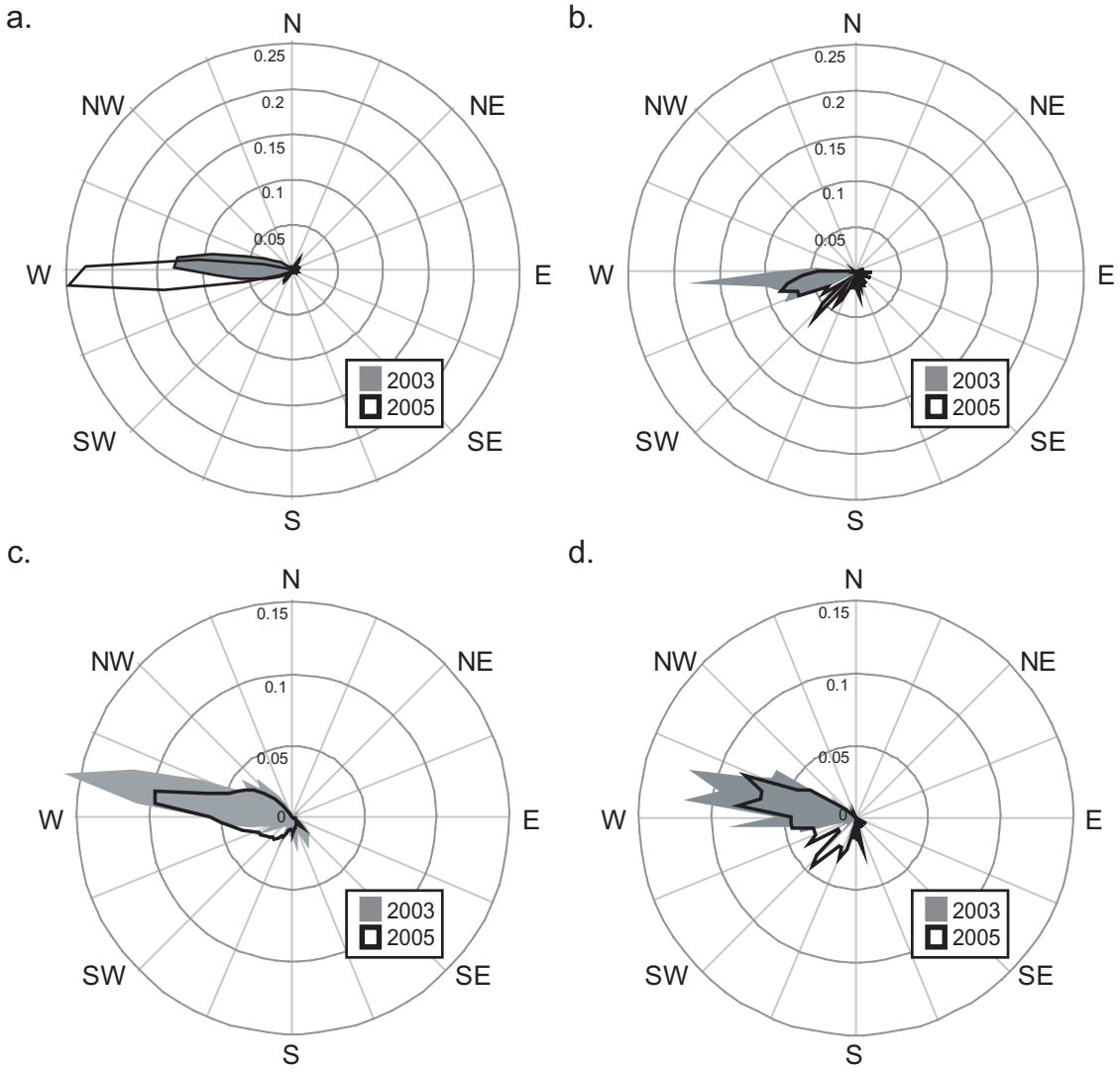

Figure 5.3. Wind direction frequency distributions. a. Walton Creek, winds greater than 5 m/s; b. Walton Creek, winds during or within 1 day of precipitation events; c. Alpine, winds greater than 5 m/s; d. Alpine, winds during or within 1 day of precipitation events.

of 1 April in both 2003 and 2005, the Yampa River Basin was at 90 and 89 percent of average SWE, respectively, while the Upper Colorado River Basin showed a 98 percent of average snowpack in both years. Total precipitation for the Yampa (Upper Colorado) Basin was reported as 92 (97) percent of average in 2003 and 88 (94) percent in 2005. The basin-wide percent of average values show that at the scale of synoptic weather patterns, both 2003 and 2005 snow years were near the 30-year average. This scale of comparison gives a qualitative indication that the storm patterns in the region, which

exert a control on the dominant wind direction during snowfall events, were substantially similar in both years.

1 April SWE values from the individual SNOTEL stations located near the study sites also show similar values for both years, though with greater variation than the basins as a whole. Relative to the entire basins, the Rabbit Ears and Berthoud Pass Summit SNOTEL sites showed higher SWE accumulations in 2003 and lower SWE in 2005 relative to the 30-year mean for each site. As might be expected, there is more year-to-year variation in individual station data than in the basin-wide aggregate data.

Figure 5.4 shows daily SWE observations from the nearby SNOTEL sites for both 2003 and 2005. The curves for both years are similar at both sites, with lower SWE totals in 2005 and complete depletion by early to mid-June. The difference in SWE amounts between years at Berthoud Pass Summit appears to be due mainly to a precipitation event in mid-March 2003 – a large, easterly, upslope storm that did not reach far enough to the west to affect the Rabbit Ears site.

Individual storms assume a greater importance in areas that routinely experience shallow snowpacks, like the above-treeline region at the Alpine site, as a single storm can multiply the existing snow totals several-fold (Serreze *et al.*, 2001). In deeper-snowpack environments, such as the Walton Creek site, a single storm snowfall total is usually a much smaller percentage of the snowpack (Figure 5.5a). This factor is critical when examining the measurements taken in two different years, as a change in measurement date by only a few days can dramatically affect the observed distribution. This fact is well-demonstrated by the snow depth time series from the Alpine study site (Figure 5.5b). Both years show an extremely temporally variable snowpack, though for any given day of the water year, the 2005 snowpack tended to be deeper. Notably, both series show a large storm occurring late in the season, which significantly changed the snow depths for several days. However, each lidar dataset was acquired several days post-storm, when snow depths were much lower, and of similar magnitude. Therefore, though the

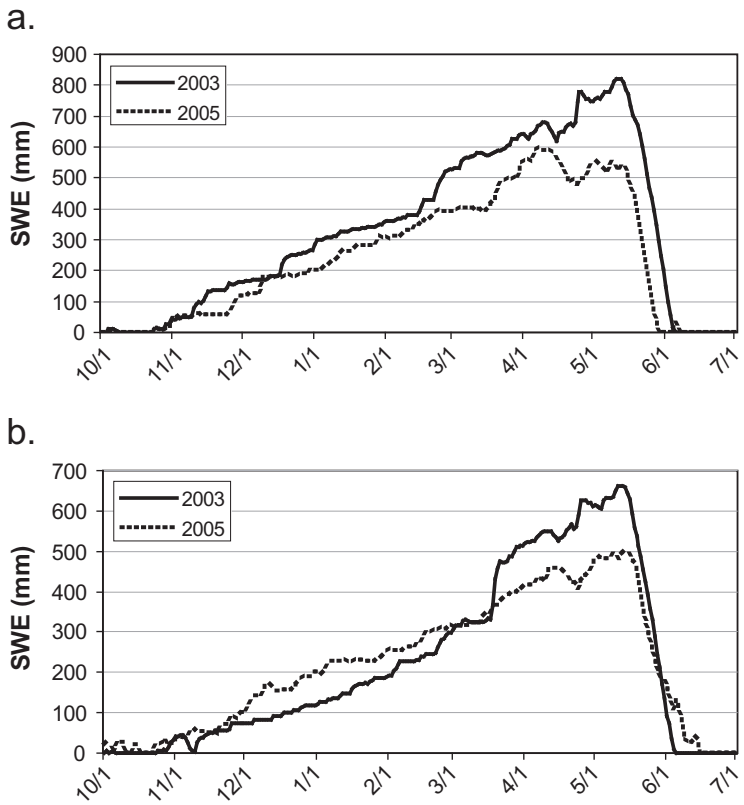

Figure 5.4. Daily SWE observations from a. Rabbit Ears and b. Berthoud Pass Summit SNOTEL sites.

snow distributions at the Alpine site appear similar in magnitude between years, different measurement dates may have produced very different results. Measured distributions at the Walton Creek site, by contrast, are not as sensitive to acquisition date.

The other major weather variable that drives snow distributions is wind. Wind speeds above a transport threshold value can redistribute significant volumes of snow. Figure 5.3 (a-d) shows the frequency distributions of wind direction for both years at both sites, for wind speeds greater than 5 m/s, and for wind during or just after precipitation events. The distributions show little difference in the direction of peak wind frequency between years at each site. The 2005 data show an increase in the frequency of southwesterly winds associated with precipitation events at both sites, making the distributions slightly bimodal. However, the dominant precipitation wind direction is consistent between years. Overall, the two snow depth datasets obtained for each site represent spatial snow distributions at near maximum accumulation in two very similar snow years.

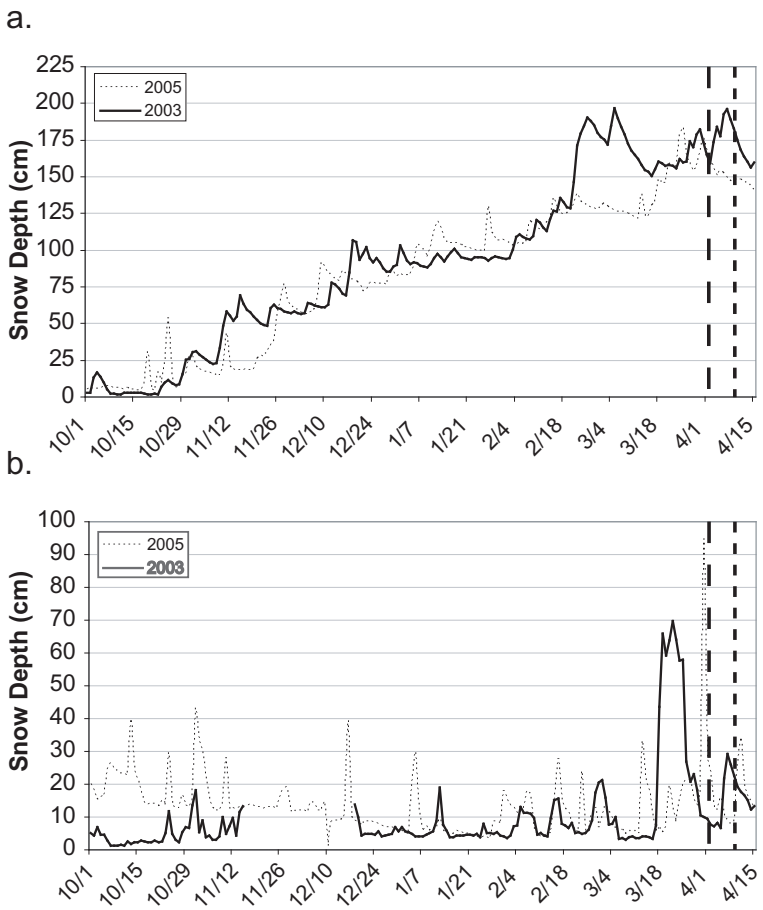

Figure 5.5. Daily snow depth observations collected at micrometeorological stations near the center of each study site. a. Walton Creek; b. Alpine. Vertical lines indicate dates of lidar data acquisition: dashed is 2005, dotted is 2003.

5.3 Methods

5.3.1 Lidar Altimetry

Lidar altimetry is used for many applications, including terrain modeling and forest structure mapping. Lidar altimetry offers the ability to process multiple laser returns to get bare ground or snow and canopy height information. The data used here have 1.5 m nominal horizontal spacing between data points, and 0.05 m vertical measurement tolerance. Positioning data were collected using a combination of Global Positioning System and inertial navigation system technologies. The raw data were normalized using ground control points, post-processed to remove redundant data points and noise, and

finally classified as ground or vegetation points via a proprietary morphological filter (Miller, 2003).

Three lidar datasets from each site were used for this study – one acquired on 9 April 2003, the second on 19 September 2003, and the third on 1 April, 2005. The last-return signal from the September 2003 mission provides ground surface ('bare earth') elevations, the September first-return data measures the terrain-plus-vegetation (vegetation topography) elevations, and the April 2003 and 2005 last-return data provide snow surface elevations. A 1 m resolution DEM was produced from the bare earth point data using inverse-distance-weighting interpolation. The DEM elevations were then subtracted from the snow surface elevation points, producing datasets of snow depth point estimates. The point datasets of snow depth, bare earth elevations, and vegetation topography were used for the variogram fractal analysis.

5.3.2 Variogram Fractal Analysis

Fractal dimensions are calculated using variograms, which show the amount of variance between samples as a function of their distance scale of separation. Omnidirectional and directional semivariograms, $\gamma(r)$, are estimated using 50 log-width bins:

$$\gamma(r_k) = \frac{1}{2(N_k)} \sum_{i=1}^{N_k} \{z_i - z_j\}^2 \tag{5.1}$$

where r is the lag distance of bin k, N is the total number of pairs of points in the k^{th} bin, and z_i and z_j are the snow depth values at two different point locations i and j (Webster and Oliver, 2001). Log-width distance bins are used to provide equal bin widths when the variograms are transformed to log-log space. Log-width bins also allow for a greater bin density at short lag distances than would linear-width bins, which aids in resolving the variogram structure at short length scales; therefore log-width bins allow a more

precise power law fit than would standard linear distance bins (Klinkenberg and Goodchild, 1992). The variograms were restricted to a maximum distance of 1100 m, the diameter of the largest circle that can be fit within the mapped area, which helps avoid directional bias (Mark and Aronson, 1984). Additionally, any non-stationarity in the data was not removed, though that is standard practice in a geostatistical analysis. In fractal analysis, the fractal dimension is an index of the relative balance of long- and short-range processes, and removing large-scale trends would bias the calculated fractal dimensions toward short-range variability (Klinkenberg and Goodchild, 1992).

The variograms are log-transformed to allow identification of regions that can be described by a power-law. Linear regions in each log-log variogram are identified visually, and each straight section is fit with a power function of the form:

$$\gamma(r) = ar^b \tag{5.2}$$

by varying coefficients a and b to minimize the squared residuals. The fractal dimension (D) is estimated from the slope (power) of the log-log variogram by Gao and Xia (1996):

$$D = 3 - b/2 \tag{5.3}$$

When breaks in slope are observed in the log variogram plots, the scale break length is determined from the intersection of the two fitted power law curves. It is recognized that, rather than a discrete break, the slope changes continuously from one linear segment to another. It should be noted, however, that this change in slope occurs over a relatively short scale range. The power-law relationships display very good fits with the transition region included in the power-law segments (R^2 based on the log data greater than 0.90). Solving the two power-law equations to derive a single break point provides a consistent measure that is comparable between datasets. Shook and Gray (1996) used a similar methodology, though they assumed that the longer-range sections approached a completely random spatial distribution (flat slope, $D = 3$). Their technique results in slightly larger estimates of the scale break distance than the technique used here. Our

methods likely produce a more conservative estimate of the scale break location.

The 2003 and 2005 snow depth datasets were compared to examine the consistency of the spatial snow depth distributions from year to year. Due to a problem with aircraft equipment during the 2005 mission, full coverage of the Alpine site was not obtained. Therefore, the 2005 Alpine variograms were compared with 2003 Alpine variograms computed from both the full dataset and a dataset clipped to match the extent of the 2005 data.

5.4 Results and Discussion

5.4.1 Omnidirectional Variograms

Three variogram features were examined for interannual consistency in the spatial snow depth distributions: overall semivariance, the lag distance of the scale break, and the slopes of the power-law fractal segments. Results are consistent between years at both sites, showing only a change in the overall magnitude of the variability at all lag distances, with essentially no changes in the spatial structure or fractal scaling properties.

The Walton Creek omnidirectional variograms are nearly identical between seasons (Figure 5.6a). The scale break lag distance and the fractal slopes are the same, indicating that the spatial distribution of snow depths had the same structure in both years, with virtually identical scaling properties and relative amounts of short-range and long-range variation (Table 5.1). The only difference is a slightly higher overall semivariance in 2005. This difference could be explained by the lower overall snow depth in 2005 (see Figure 5.5), which would have masked less of the terrain and vegetation roughness and produced a larger variance magnitude, though with the same spatial structure. The accumulation and wind redistribution history certainly differ between years, as suggested by the slightly higher proportion of storm winds from the southwest during 2005. The interannual consistency in fractal dimensions and scale break distance demonstrates that

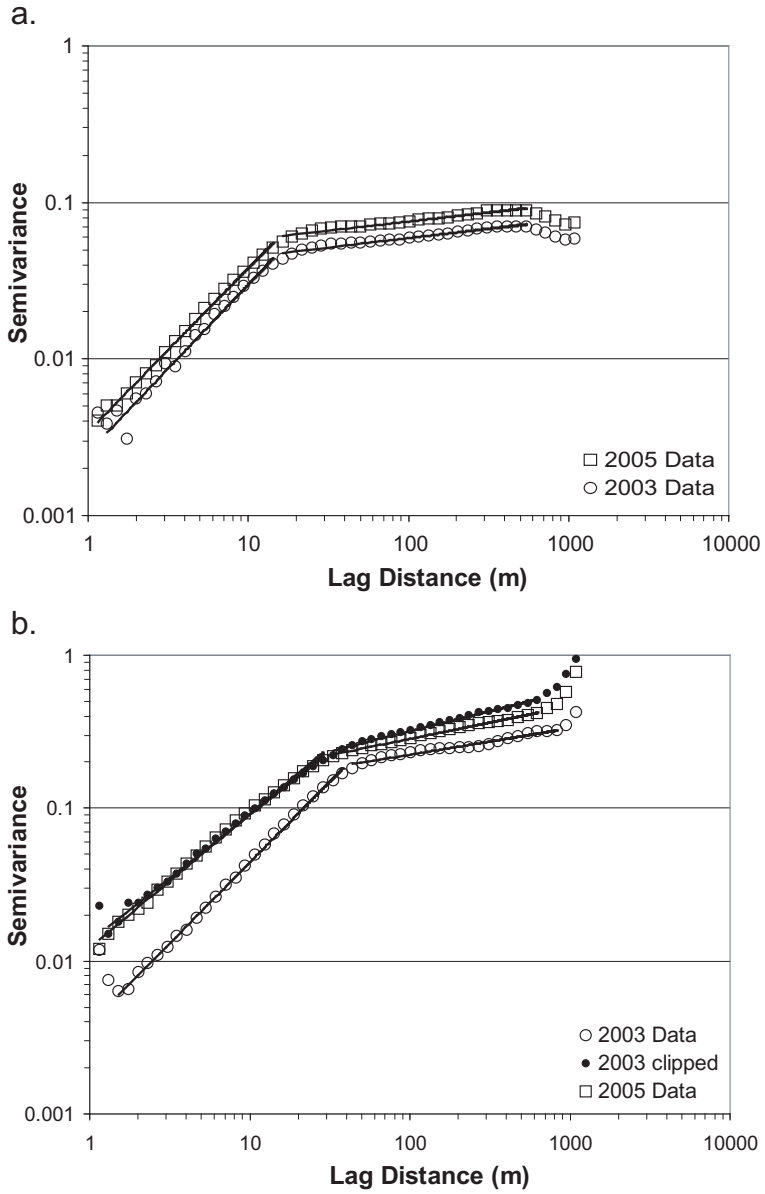

Figure 5.6. Omnidirectional log-log variograms for a. Walton Creek and b. Alpine.

Table 5.1. Short- and long-range fractal dimensions for the two study sites for both years. *D* values from the clipped 2003 dataset are shown for Alpine.

	2003		2005	
Study Site	Short-range	Long-range	Short-range	Long-range
Walton Creek	2.46	2.94	2.48	2.94
Alpine	2.58	2.87	2.56	2.89

the process interactions that create the spatial snow depth pattern are identical in each year. Any differences in the spatial snow depth patterns are not sufficient to disrupt the overall scaling relationships created by the snowfall/wind/terrain/vegetation interactions over the 1-1000 m scale range.

When the Alpine variograms from 2003 and 2005 are compared, the initial result indicates that there is a change in the distribution (Figure 5.6b). However, since an equipment issue precluded data collection for the entire site in 2005, the spatial extent of the 2003 data must be clipped to match that of the 2005 data for the comparison to be valid. Areas of different size will contain different elevation and vegetation distributions – different distributions of the roughness elements that control the pattern of wind redistribution. Therefore, unless the roughness elements have similar distributions, areas of different extent could be expected to have different spatial snow distributions. Previous studies have shown a qualitative relationship between scale break distance on the overall relief of the study area (Shook and Gray, 1996; Deems *et al.*, *2006*). The clipped Alpine extent has a smaller overall relief than the full study area (298 m versus 339 m), and also a shorter scale break length, which is consistent with the prior findings.

When the 2005 Alpine variogram is compared to the variogram from the clipped 2003 dataset, the distributions are essentially identical – they have the same fractal slopes,

similar scale break lag, and same overall variance magnitude. Thus the scaling characteristics of the snow distributions in the two years were consistent on the dates sampled, indicating consistent process relationships despite differences in the snowfall and wind history between the two years. Low snow depths and wind exposure make the Alpine site more sensitive to the date of sampling than the Walton Creek site. It is possible that if either sampling date (2003 or 2005) had been closer to the large spring snowstorm, the resulting spatial scaling patterns might be different. However, based on the snow depth time series, the sampling dates appear to be a good representation of 'normal' conditions at the Alpine site.

5.4.2 Directional Variograms

Snow depth fractal dimensions at the Walton Creek site are virtually identical between years for all directions, and for both the short- (1.5 - 15 m) and long-range (15 - 550 m) fractal segments (Figure 5.7a). Two conclusions can be drawn from this. First, there appears to be no difference between years in the anisotropy of the process relationships that determine the snow depth pattern and pattern scaling relationships. This is supported by the similarity between the wind direction frequencies (Figure 5.3 a,b). Assuming that any changes in the vegetation (and topography) are insignificant over two years, interannual differences in the wind history will exert a dominant influence on differences in snow redistribution. Therefore, any differences in the wind direction frequencies, such as the slightly higher proportion of southwest winds associated with 2005 precipitation events, are not sufficient to substantially alter the overall scaling pattern.

Second, in practical application, any sampling or interpolation scheme designed to capture the anisotropy evident in the short lag distances would be applicable to both snow seasons. Measured or modeled spatial distributions could be rescaled using anisotropic scaling factors, and the results indicate that the same anisotropic rescaling methods might be applicable to the data from both years.

At the Alpine site, the anisotropy is also similar between years, though slightly more variable than at Walton Creek (Figure 5.7b). Two directional features are notable: first, short-range fractal dimensions are much higher in the SSW-NNE direction, which is perpendicular to the dominant wind direction. Second, the short- and long-range fractal dimensions are the same in the SSW-NNW direction. In other words, there is no scale break perpendicular to the dominant wind direction, and the snow depth distribution scales continuously from 1.5 to about 270 m. In this direction, there is virtually no change in elevation (see Figure 5.2b). Since the only variation along an elevation contour is in the vegetation pattern, there is no process change at any lag distance within the range of scales represented in the data, and hence no scale break.

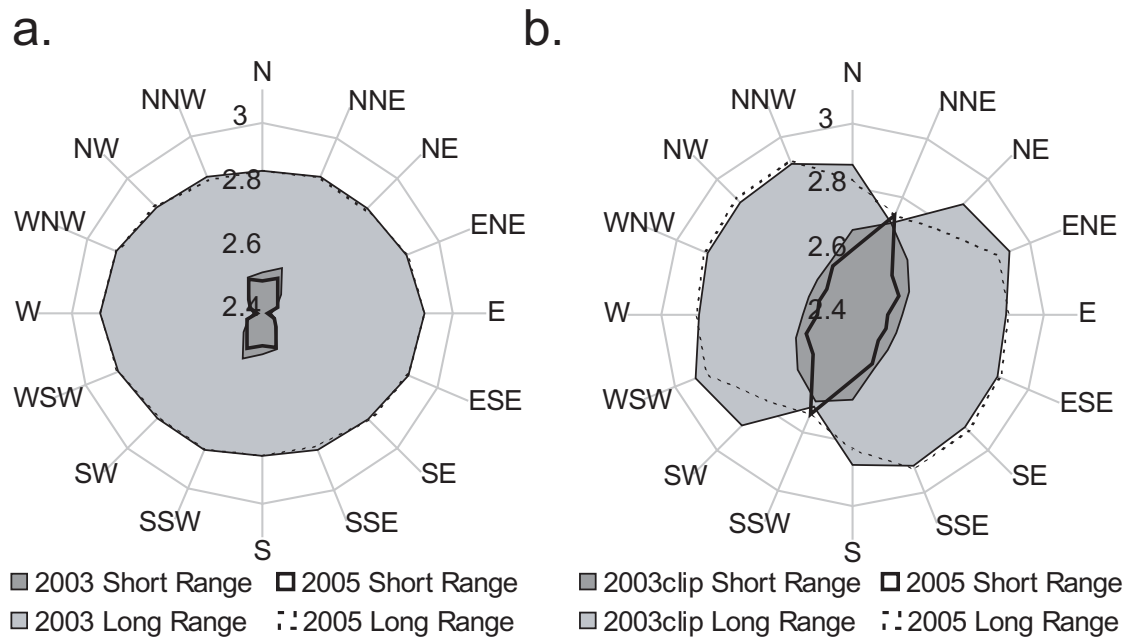

Figure 5.7. Fractal dimensions by azimuth for a. Walton Creek and b. Alpine.

The wind direction frequencies at Alpine are consistent between years (Figure 5.3 c,d), such that the process relationships that determine snow distributions, vegetation, topography, and wind, are equivalent. As with the Walton Creek site, there is a slight increase in the proportion of southwesterly winds associated with precipitation events in 2005, which seems to have had little impact on the both overall and directional spatial distributions.

It is instructive to consider the time of year that data were collected. Both years were sampled near 1 April, the date often used to represent maximum accumulation. By the latter part of the accumulation season, the storm sequence is likely to have produced a spatial snow distribution that is consistent with the dominant storm track and wind direction. Were this same analysis conducted for 1 January data acquisitions, for example, very different distributions might be expected, with spatial patterns more sensitive to variations in early-season snowfall. It is possible, therefore that late-season spatial scaling relationships are more interannually robust than those observed earlier in the year.

5.5 Conclusions

Snow depth spatial patterns and scaling behavior are compared for two years using snow depth datasets derived from airborne lidar measurements at two midlatitude, mountainous sites. Both omnidirectional and directional analyses show strong interannual consistency for two years with significantly different accumulation histories. The spatial distributions differ slightly in overall variance, but the fractal dimensions over two distinct scale regions and the length of the scale break that separates the scale regions are nearly identical.

These results demonstrate interannually consistent process relationships among the major driving factors controlling snow accumulation and redistribution, namely precipitation, wind, vegetation, and topography. The snow seasons that produced the observed snow distributions were similar at the regional, basin, and individual site scales, according to data from nearby SNOTEL sites and micrometeorological data collected onsite. However, significant differences in the temporal accumulation patterns exist between years. The results suggest that the observed scaling properties of the snow depth distributions are characteristic of the site locations and are relatively insensitive to interannual variation in snow accumulation. The interannual consistency in the scaling characteristics indicate that the fundamental process relationships producing spatial snow depth patterns at these sites are consistent year to year. The scaling properties of snow distributions produced by substantially deeper or shallower snow years, or at times earlier in the accumulation sequence, remain to be investigated.

CHAPTER 6:
FRACTAL ANALYSIS AND MULTISCALE PROCESS MODELING OF SNOW DEPTH DISTRIBUTIONS

6.1 Introduction

Spatial snow depth distributions in mountain environments exhibit variability on multiple scales due to complex, multiscale process interactions (e.g., Blöschl, 1999; Liston, 2004; Deems *et al*., 2006). Snow accumulation and redistribution processes operate over a range of spatial and temporal scales, with terrain and vegetation patterns providing the underlying physical structure determining the exact scale relationships between orographic-driven precipitation (e.g., Roe, 2005), wind redistribution (e.g., Liston and Sturm, 2002; Winstral *et al.*, 2002), and radiative and turbulent transfer components of the energy balance (e.g., Marks and Dozier, 1992; Liston, 1995; Luce *et al.*, 1999). These interacting processes combine to produce snow distributions with a complex spatial pattern that presents significant sampling and modeling challenges (Elder *et al.*, 1991).

Spatially explicit snow process modeling can provide estimates of distributed snow depths or water equivalents to supplement or substitute for manual or remote sensing surveys. Process models also offer the opportunity to quantitatively explore relationships among driving variables. The accuracy of modeled snow distributions depends on the physical and scale validity of the modeled representation of snow processes. Further, physical processes and their interactions change character with scale. Ideally, snow process models should not only contain realistic simulations of physical systems, but should also be capable of dynamic scaling of process interactions.

This scale-appropriate combination would be a significant advance not only in the ability of models to represent observed snow distribution patterns, but also to perform in situations outside the range of historical conditions, for example where changing climate drives local shifts in wind patterns. In order to provide this 'scale dynamism', model representations must be built upon quantifiable process-scale relationships of the natural system.

Additionally, it is difficult to validate simulations of complex spatial snow distributions. Common evaluation metrics either provide bulk comparison (e.g., mean, standard deviation) or are sensitive to locational errors, where a modeled pattern is essentially correct, but a pointwise spatial comparison shows a poor correspondence (Bruland, *et al*., 2004; Hiemstra *et al*, 2006). A metric that evaluates both the spatial complexity of the distribution and its scaling properties would be useful for model development and refinement. Recent advances in lidar remote sensing of snow depth, combined with new fractal methods for characterizing scale relationships, provide a foundation from which to evaluate and improve model snow processes representations.

Tabler (1980) examined equilibrium snowdrift profiles over a range of length scales from 5 cm (drifts produced by 1:30-scale snow fence models) to 50 m (drifts behind full-sized, 3 m-tall snow fences). These profiles showed consistent drift geometry over the entire range of scales, leading to the conclusion that reduced-scale snow fence models provide accurate representations of full-scale fences. Further, the scale-invariant drift geometry suggests that a fractal model is appropriate for characterizing scaling relationships in snow drift patterns over length scales from 10 cm to 100 m (Deems *et al.*, 2006). The complexity of a fractal pattern is quantified by its fractal dimension (D), which describes the relative balance of the short- and long-range processes through which the pattern evolves. Natural systems tend to exhibit fractal patterns over specific scale ranges, with the changes in fractal dimension (scale breaks) indicating length scales at which the balance of driving processes changes.

Deems *et al*. (2006) examined the fractal scaling properties of snow depth distributions at several mountain study sites. Their results demonstrated fractal behavior over two distinct scale regions, separated by a relatively sharp break point. Fractal dimensions were consistent between sites, while the lag distance at which the scale break occurred differed by topographic relief and forest cover fraction. These results were consistent with other research (e.g., Shook and Gray, 1996; Kuchment and Gelfan, 1997). Scale breaks in the fractal distributions identify a length scale at which an important change in the governing processes occurs. This scaling information can aid in understanding process relationships and inform efforts to model the process dynamics. The power-law fractal relationships can be used to maintain appropriate spatial relationships when the fields are rescaled (Kuchment and Gelfan, 1997) and, in contrast to standard geostatistical models, have a physical justification for their use. Fractal dimensions derived from the power law exponent can be interpreted as measures of complexity, roughness, or autocorrelation, and thus are useful for comparing patterns from different sites or dates, and have potential as a metric for evaluating model performance.

From a process modeling perspective, the ability of a model to reproduce realistic fractal patterns over appropriate scale ranges is critical to the simulation of snow distributions for both model output and for input to subsequent model iterations. Successful simulation of fractal scaling behavior (i.e., fractal dimensions and scale break distances consistent with observations) would indicate that the model correctly represents processes and process interactions over the relevant scale ranges.

Physically based snow evolution models attempt to simulate the major processes and process interactions governing snow accumulation and melt; namely the interactions among precipitation, energy exchanges, and wind transport as a function of terrain, vegetation, and the existing snowpack. Recent developments in these models have resulted in more accurate process representations and greater model complexity (see

Liston, *et al.*, 2007). However, explicit modeling of fine-scale wind turbulence, necessary for modeling wind drifting patterns at the length scale of vegetation and topographic roughness elements (1 - 50 m), remains computationally prohibitive for seasonally evolving, spatially distributed models (e.g., Winstral *et al.*, 2002). Recently, Liston *et al.* (2007) implemented a subgrid algorithm in the SnowModel seasonal snow process model that forces the longitudinal profiles of lee snow drifts to conform to the equilibrium drift geometry defined by Tabler (1975). This sub-model simulates drift patterns resulting from fine-scale wind turbulence without the computational expense of modeling these wind fields explicitly. These drift patterns are particularly important at finer grid resolutions, where the snow depths are of similar magnitude to the grid element size (Liston *et al.*, 2007).

A variety of methods are used to validate distributed snow models, depending on project goals and model structure. Combinations of qualitative and quantitative measures are often employed. Hiemstra *et al.* (2002) analyzed snow patterns from air photos and used point-to-point comparisons with ground survey data to verify correct placement of ecologically important snow drifts in a treeline ecotone. They found that though the model output agreed well with air photos, the comparison with transect data was unsatisfactory. Based on sorted pointwise relationships (i.e., removing spatial information) they concluded the model was accurately simulating the statistical snow depth distribution, but modeled snow drifts were shifted from the observed by magnitudes on the same order as the model grid size (5 m), thereby delivering poor pointwise comparisons. In this case, conventional metrics highlighted model limitations, while the simulated patterns were quite realistic.

Pomeroy *et al.* (1997) applied their Distributed Blowing Snow Model (DBSM) at a 40 m resolution in an arctic environment, and compared domain-average snow water equivalent (SWE) estimates from model output and manual survey data. Though the domain-average modeled SWE was quite close to observed values (< 10%), the SWE

difference varied by land cover class, producing substantial but offsetting errors. As the authors note, the land cover class comparison is not able to resolve within-class snow depth variability, and thus is of limited use for evaluating model representation of specific process relationships. They cite the need for a time series of high-resolution ground data with which to verify model output and components.

Winstral and Marks (2002) compared modeled melt season SWE patterns with binary classified air photos (snow/no snow) to validate SWE accumulation at the basin scale. Additionally, they compared time series of modeled SWE to values measured at several meteorological station and snow course locations. This air photo validation method, though useful for examining spatial patterns during the melt season, provides only indirect information regarding the modeled representation of accumulation processes and process interactions; because the resulting patterns also include melt-rate distribution information (Liston, 1999).

None of these common spatial model validation techniques specifically examine the ability of the model to represent process interactions on multiple scales simultaneously. Fractal analyses of model output can inform development and validation efforts by allowing examination of characteristic scales of process relationships and scale-dependent changes in process dynamics. Several studies of ground and remotely-sensed data have characterized fractal properties of snow depth, building a literature base that allows initial investigations into the utility of fractal analysis as a model validation and evaluation tool (Shook and Gray, 1996; Kutchment and Gelfan, 2001; Deems *et al.*, 2006; Deems *et al.*, 2007).

In addition to using common model performance metrics, Essery *et al.* (1999) identified power-law scaling characteristics in output from the Prairie Blowing Snow Model (PBSM) coupled with a terrain windflow model, and compared the power-law derived Hausdorff (fractal) dimensions and cutoff length (scale break) to those presented by Shook and Gray (1996). They found the fractal slope of the model output was similar

to that reported by Shook and Gray (1996) from the same study site on a different date, though the modeled cutoff length was at 2 km instead of 500 m. Further, they found the fractal slope and cutoff length to be relatively insensitive to changes in model parameters that significantly affect the modeled total snow mass. However, the PBSM model as employed used a grid element size of 80 m, and therefore was not designed to represent smaller-scale processes (e.g., interaction of wind and vegetation). At this resolution, the PBSM will not simulate the change in fractal scaling observed at lags smaller than 50 m, but does suggest that a scale-dependent process change occurs near a lag of 2 km, a scale consistent with and possibly related to fractal changes in topographic distributions (see e.g., Klinkenberg and Goodchild, 1992).

In this study, we use variogram fractal analyses to test the ability of SnowModel (Liston and Elder, 2006a) to simulate complex snow depth patterns over two 1 km^2 domains in a midlatitude, mountain environment at a spatial grid resolution of 5 m. In order to explore the roles of different processes in defining snow depth patterns, the model is used to examine the sensitivity of fractal dimensions to model parameters.

6.2 Methods

6.2.1 Study Sites

The two 1 km^2 study sites were established as a part of the NASA Cold Land Processes Experiment (CLPX) in north-central Colorado, USA (Cline *et al.*, 2003; Figures 6.1 and 6.2). The Walton Creek site (40.4 N, 106.6 W) is characterized by a broad meadow environment, interspersed with small, dense stands of coniferous forest, low rolling topography, and deep snowpacks. The Buffalo Pass site (40.5 N, 106.7 W) has dense coniferous forest interspersed with open meadows, low rolling topography, and deep snowpacks (Cline *et al.*, 2003). Both sites are in a similar synoptic-scale terrain position, receiving high annual snowfall (typically over 1 m of SWE per year).

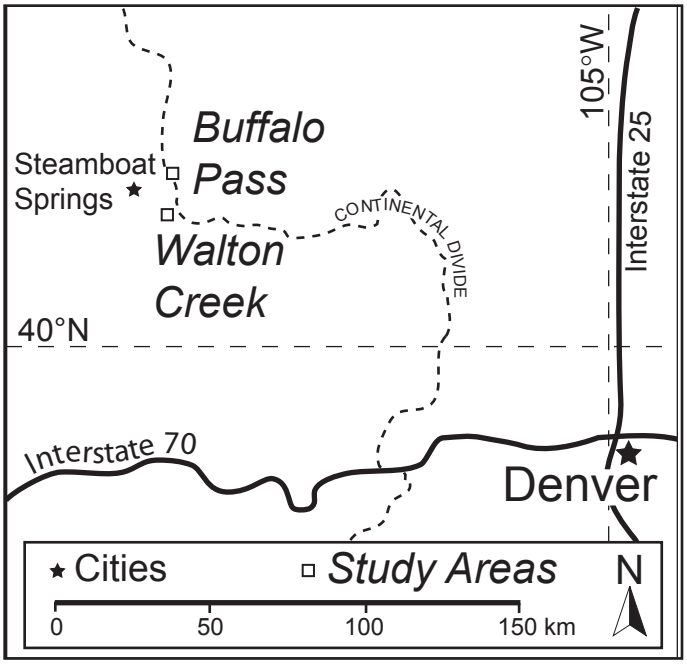

Figure 6.1. Locations of the Buffalo Pass (BP) and Walton Creek (WC) NASA CLPX Study areas, north-central Colorado, USA.

6.2.2 Snow Distribution Data

Distributed snow depth measurements were made via airborne lidar (Miller *et al.*, 2003). Two lidar datasets were used – one acquired on 9 April 2003 and the other on 19 September 2003. The last-return values from the September data provided ground surface ('bare earth') elevations, the September first-return data measured the terrain-plus-vegetation (vegetation topography) elevations, and the April last-return data provided snow surface elevations. A 1.5 m resolution DEM was produced from the bare earth point data using inverse-distance-weighting interpolation. The DEM elevations were then subtracted from the snow surface elevation points, producing a point dataset of snow depth estimates. This dataset was averaged to a 5 m grid to match the model resolution.

6.2.3 Model Summary

SnowModel consists of four sub-models: 1) MicroMet distributes micrometeorological data across the model domain from individual stations (Liston and

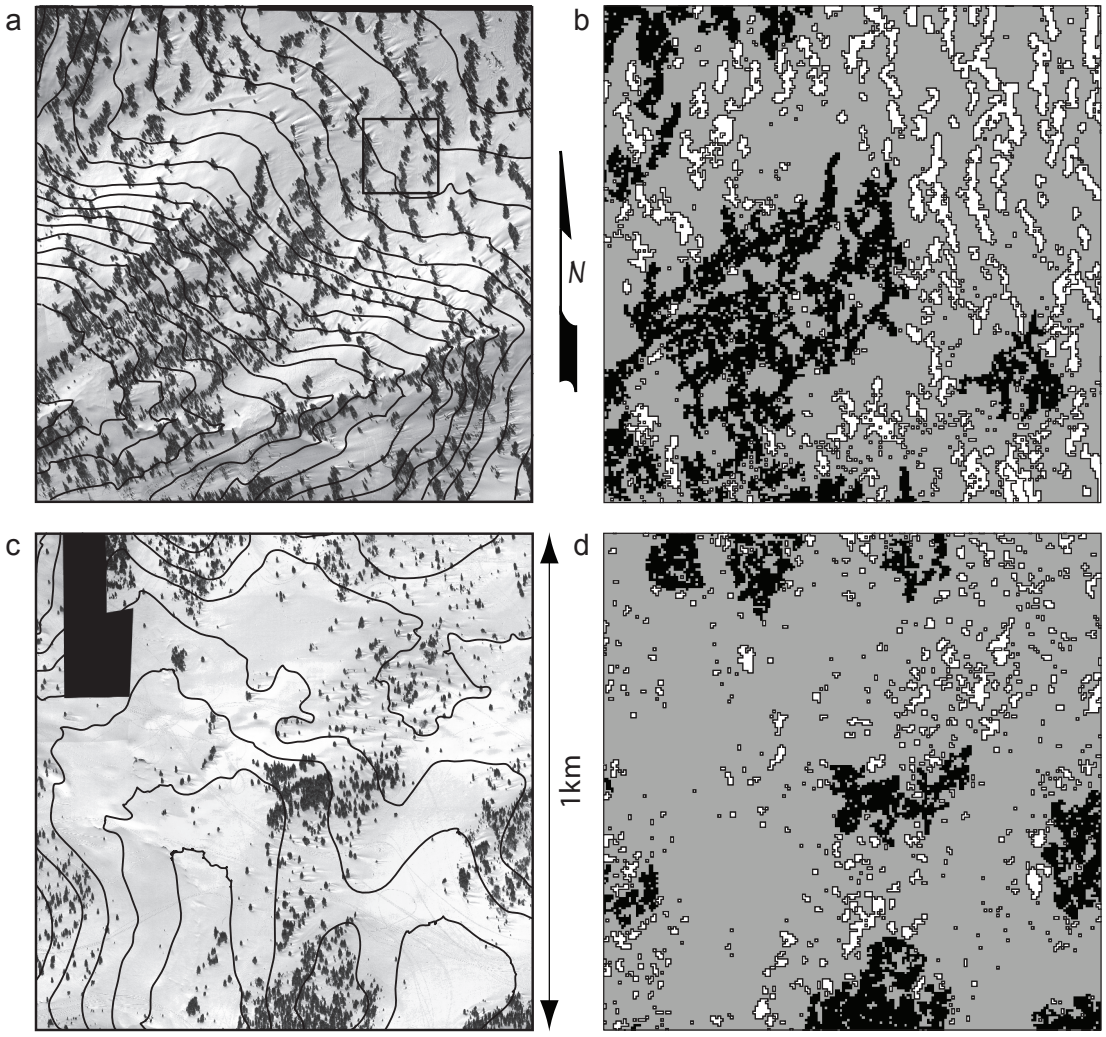

Figure 6.2. Orthophotographs of (a) BP and (c) WC study sites. Photos collected on 9 April, 2003, concurrent with lidar acquisition. Contour interval is 10 m. Panels (b) and (c) show vegetation classifications for both sites. Black represents areas of continuous forest cover, gray areas are classified as grass, and white areas are forest that has been converted to topography (veg-topo) to aid in simulating snow drifts around trees. The box in the NE corner of panel (a) outlines the area subset in Figures 8-10.

Elder, 2006b); 2) SnowTran-3D is a three-dimensional snow transport model for rough terrain (Liston and Sturm, 1998; Liston *et al*., 2007); 3) EnBal simulates the spatially distributed energy balance (Liston and Elder, 2006a); and 4) SnowPack evolves the internal snowcover structure (Liston and Elder, 2006a).

Recent improvements to SnowTran-3D include the addition of a routine to evolve the threshold friction velocity for wind transport, and the development of a sub-grid

algorithm that forces lee drifts to conform to empirical equilibrium drift profiles defined by Tabler (1975) (Liston *et al*., 2007). Tabler (1975) described 2-D equilibrium snow drift profiles with an empirical regression model using ground slopes up- and down-wind of an obstacle. The Tabler sub-model is a subgrid snow redistribution routine within SnowTran-3D that constrains snowdrifts in the lee of obstacles to fit that empirical equilibrium drift geometry. At each time step, snow is redistributed on a 1 m grid, and then re-gridded to the horizontal model resolution. This sub-model simulates fine-scale drift development without the computational expense of modeling complex wind behavior around small obstacles.

6.2.4 Driving Data

Data used to drive SnowModel were collected during the 2002/2003 CLPX field campaign. Measurements of air temperature, relative humidity, and wind speed and direction were recorded at micrometeorologic stations close to the center of each site. Incoming solar and longwave radiation were computed in the MicroMet sub-model, and included diffuse and direct-beam, solar, topographic, and cloud cover effects (Liston and Elder, 2006b). The remaining components of the snow surface energy balance were computed in the EnBal sub-model (Liston and Elder, 2006a).

Precipitation data were estimated from nearby SNOTEL station data. For the Walton Creek site, precipitation data from the Rabbit Ears SNOTEL site (ca. 8 km to the west) was decreased by a scalar factor (0.74) in order to match the accumulated precipitation depth to the lidar-derived SWE depth at the study site met station on 9 April 2003, the lidar survey date. This method assumes that sublimation losses are negligible, that there was no net loss of snow to wind transport, and that the met station location is representative of average SWE accumulation in the domain. At the Buffalo Pass site, the SNOTEL station is within the study site, so no adjustment was performed. Errors in precipitation measurement and subsequent rescaling could be an important and

unquantifiable source of error in the model results.

Topographic and vegetation data were derived from airborne lidar surveys of the study areas during snow-free conditions. The resulting lidar-derived 1.5 m horizontal resolution DEM was aggregated to the model grid size of 5 m. All lidar returns classified as "non-ground" were assumed to be vegetation. The DEM elevations were subtracted from the vegetation elevations to get vegetation height. If these heights were less than 1 m they were classified as grass, otherwise they were designated as conifer. In using this simple classification, we assume that the conifers of height 1 m or greater dominate the vegetation contribution to snow depth variability at these sites, however substantial areas of willow exist in the riparian areas at both sites, especially at Walton Creek. Willow areas will trap more drifting snow than grass, so it is possible that a more varied vegetation classification scheme would provide a more accurate representation of passive snow trapping in a variety of vegetation types.

SnowModel was originally designed to simulate snow/wind/terrain interactions in arctic environments, with vegetation serving as passive snow sinks, not topographic obstacles to the wind. In the midlatitude mountain domains where forest characteristics exert a strong influence on wind redistribution, the model requires some adaptation for simulating wind/vegetation interactions (Hiemstra *et al.*, 2002; 2006). Because the model typically treats vegetation as snow sinks with a specific snow holding depth, and not as roughness elements that interact with wind, some of the conifer stands were treated as topography by first manually examining the conifer distributions along with orthophotos showing snow drifts (Figure 6.2). Conifer heights that were either in small groups or were associated with significant snowdrift formation (as determined from orthophotos cotemporal with the snow-covered lidar data collections) were selected, smoothed with a 3x3 cell moving average window, and added to the DEM. Their classifications in the vegetation dataset were converted to grass. This method allows drift formation behind trees, and the lower snow holding capacity of the grass re-classification simulates scour

effects under the tree canopies. This vegetation/terrain manipulation is highly subjective, however, and could have a significant impact on modeled snow depth distributions.

6.2.5 Model Simulations

Three important model parameters were examined for their potential to affect spatial scaling behavior. Within SnowModel, terrain (profile) curvature is calculated over a length scale determined by the curvature length scale η, which effectively describes the size threshold for roughness elements that modify the wind field. This parameter is typically set to a distance equal to approximately half the wavelength of the dominant topographic features in the model domain (Liston and Elder, 2006b). In the domains used in this study, snow depth patterns are determined in part by wind scour and deposition around sparse meadow-edge tree stands and ribbon forest bands. In the interest of modeling these small-scale drift features, η values in the range of 5-50 m were used. The curvature is calculated by averaging the elevation differences between each grid cell and the surrounding cells at distance η along the N-S, E-W, NE-SW, and NW-SE directions (Liston and Elder, 2006b):

$$\Omega_c = \frac{1}{4}\left[\frac{z - \frac{1}{2}(z_W + z_E)}{2\eta} + \frac{z - \frac{1}{2}(z_S + z_N)}{2\eta} + \frac{z - \frac{1}{2}(z_{SW} + z_{NE})}{2\sqrt{2\eta}} + \frac{z - \frac{1}{2}(z_{NW} + z_{SE})}{2\sqrt{2\eta}}\right], \quad (6.1)$$

where z_N, z_{SW}, etc. are the grid cell elevations in a specific direction at distance η from the main grid cell with elevation z. The curvature is then scaled to $-0.5 \leq \Omega_c \leq 0.5$ for the entire domain. The terrain slope along the wind direction is calculated by (Liston and Elder, 2006b):

$$\Omega_s = \beta \cos(\theta - \xi), \quad (6.2)$$

where θ is the wind direction and ξ is the slope azimuth. The wind direction slope is also scaled to be between –0.5 and +0.5. The wind weighting factor W_W is used to modify the wind field based on the terrain slope and curvature (Liston and Elder, 2006b):

$$W_W = 1 + \gamma_s \Omega_s + \gamma_c \Omega_c . \quad (6.3)$$

The relative influence of slope and terrain curvature on the wind field are determined by the weighting parameters γ_s and γ_c (for slope and curvature, respectively) which control the wind speed acceleration on windward and convex slopes and the deceleration in lee and concave areas. The values of γ_s and γ_c are usually constrained such that $\gamma_s + \gamma_c = 1.0$, though this is not required. The wind speed at each grid cell (W) is modified by the wind weighting factor to produce the terrain wind speed W_t (Liston and Elder, 2006a):

$$W_t = W_W W . \quad (6.4)$$

SnowModel was run using a 5 m grid increment and an hourly time step from 1 October 2002 through 30 June 2003. Model outputs on 9 April 2003 were compared to the observed snow depth distributions derived from the 9 April 2003 lidar mission.

6.2.6 Model Validation

Model results were compared to the lidar-observed snow depth patterns using both conventional and variogram fractal analysis metrics. Snow depth means and standard deviations were evaluated along with point-wise spatial comparisons. To evaluate the ability of the model to represent multiscale process interactions, the fractal analysis procedure described in Deems *et al*. (2006) was followed. Omnidirectional semivariograms, $\gamma(r)$, were estimated from the model snow depth output and the lidar snow depth grids using 50 log-width bins:

$$\gamma(r_k) = \frac{1}{2(N_k)} \sum_{i=1}^{N_k} \{z_i - z_j\}^2 , \quad (6.5)$$

where r is the lag distance of bin k, N is the total number of pairs of points in the k^{th} bin, and z_i and z_j are the snow depth values at two different point locations i and j (Webster and Oliver, 2001).

Straight regions in each log-log variogram were identified visually, and each straight

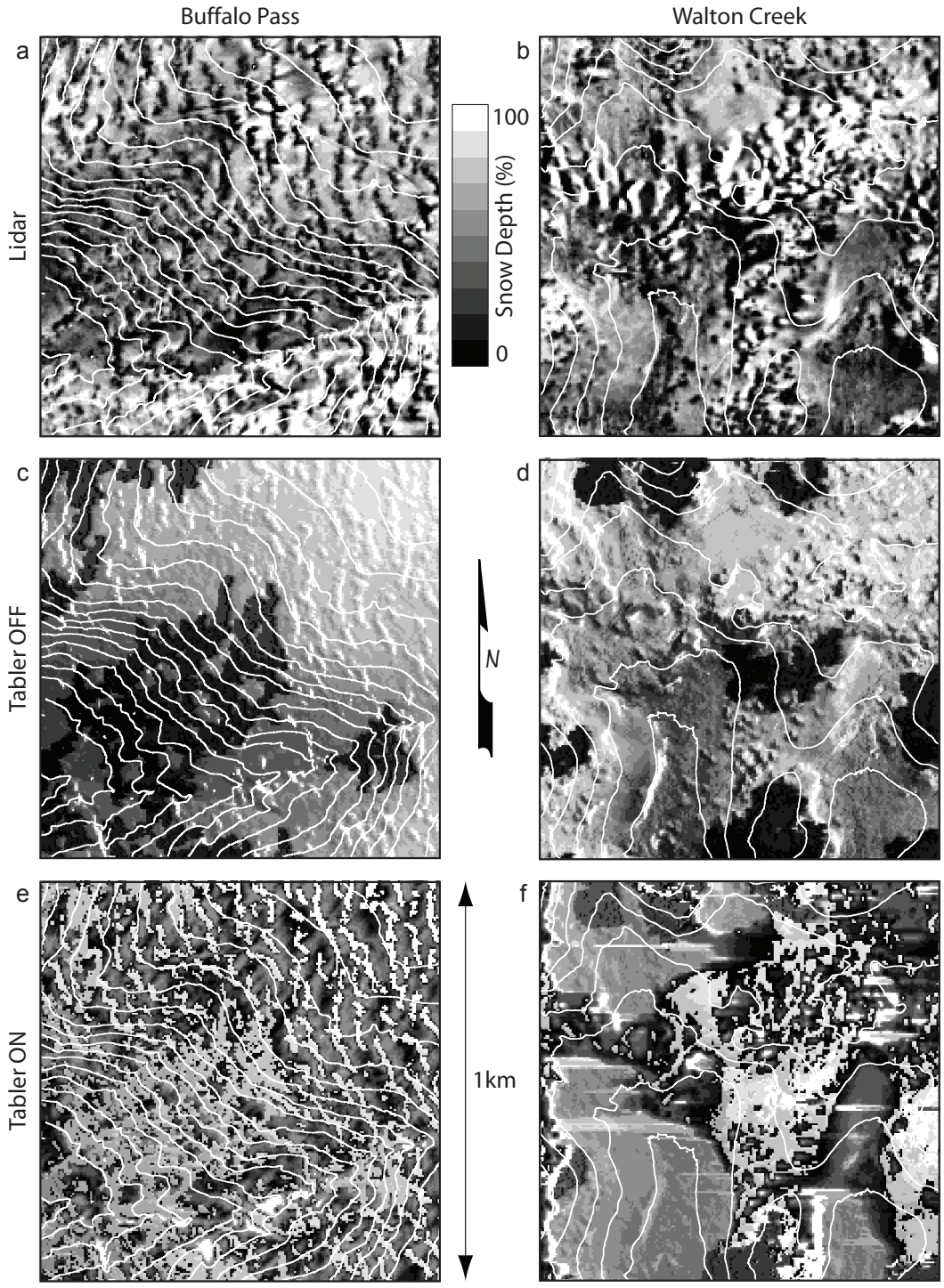

Figure 6.3. Lidar-observed snow depth (a, b) and simulated snow depth maps for the Buffalo Pass and Walton Creek sites, respectively. The simulations in panels (c) and (d) were run without the Tabler sub-grid model, while (e) and (f) were run using the Tabler sub-model. Snow depth is scaled as a percent of the maximum value in the domain. Contour interval is 10 m.

section was fit with a power function of the form:

$$\gamma(r) = ar^b. \quad (6.6)$$

The fractal dimensions (D) were derived from the power law exponents:

$$D = 3 - b/2 \quad (6.7)$$

(Klinkenberg and Goodchild, 1992). The η, γ_s, and γ_c parameters were varied in sequential runs to examine their influence on the simulated spatial snow depth patterns, as indexed by D values.

6.3 Results and Discussion

6.3.1 Model performance by conventional metrics

April 9 lidar-derived snow depth and example model outputs are shown in Figure 6.3. Without the Tabler sub-model (Figure 6.3c, d), the modeled spatial pattern is dominated by snow depth variations occurring on a distance scale commensurate with longer-range topographic variations. The short-range depth variations are tightly coupled with the forest stands that were converted to topographic roughness elements (vegetation-topography). With the Tabler sub-model engaged (Figure 6.3e, f), the model produces a greater degree of fine-scale depth patterns, leading to the initial conclusion that the Tabler model adds a new, potentially important source of short-range snow depth variation.

However, the current Tabler sub-model implementation appears to have some limitations in this mountain application. In the non-drift areas, the Tabler model allowed only a fraction of the precipitation to accumulate, and appears to be too efficient in moving snow downwind and out of the domain. This sub-grid redistribution model was designed to work in low-accumulation, wind-dominated environments, where snow accumulation is primarily confined to the drift zones, with substantial scour in the non-drift areas. The Tabler model is effectively a parameterization of fine scale wind effects, and several of its components are based on assumptions that, in its current

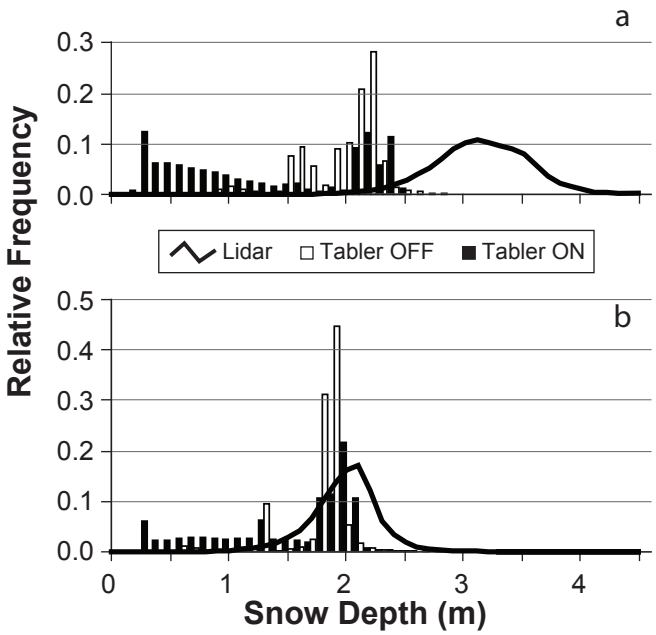

Figure 6.4. Snow depth histograms from (a) BP and (b) WC lidar measurements (observed) and modeled output with and without the Tabler sub-model.

implementation, appear to limit its application in deep snow environments.

Modeled and observed snow depth histograms and statistics (Figure 6.4; Table 6.1) indicate that the model underpredicts the snow depth distributions in both domains, and especially at the Buffalo Pass (BP) site. Mean snow depth at WC is about 10% low, while at BP the mean is underpredicted by 38%. Errors in precipitation measurements and estimates due to undercatch (e.g., Fassnacht, 2004) or extrapolation could have a pronounced effect on the mean snow depth. Running the model in assimilation mode, where SWE observations are used to rescale precipitation inputs, produced only a marginal improvement in overall depth. The large contiguous forest areas, which, when represented in SnowModel as snow sinks, must fill to capacity before snow transport

Table 6.1: Statistics for 9 April 2003 observed and modeled snow depth values.

	Lidar Snow Depth		**Modeled Snow Depth: Tabler OFF**		**Modeled Snow Depth: Tabler ON**	
	Mean	*SD*	*Mean*	*SD*	*Mean*	*SD*
Buffalo Pass	3.08	0.41	1.92	0.32	1.29	0.8
Walton Creek	1.93	0.30	1.73	0.27	1.48	0.61

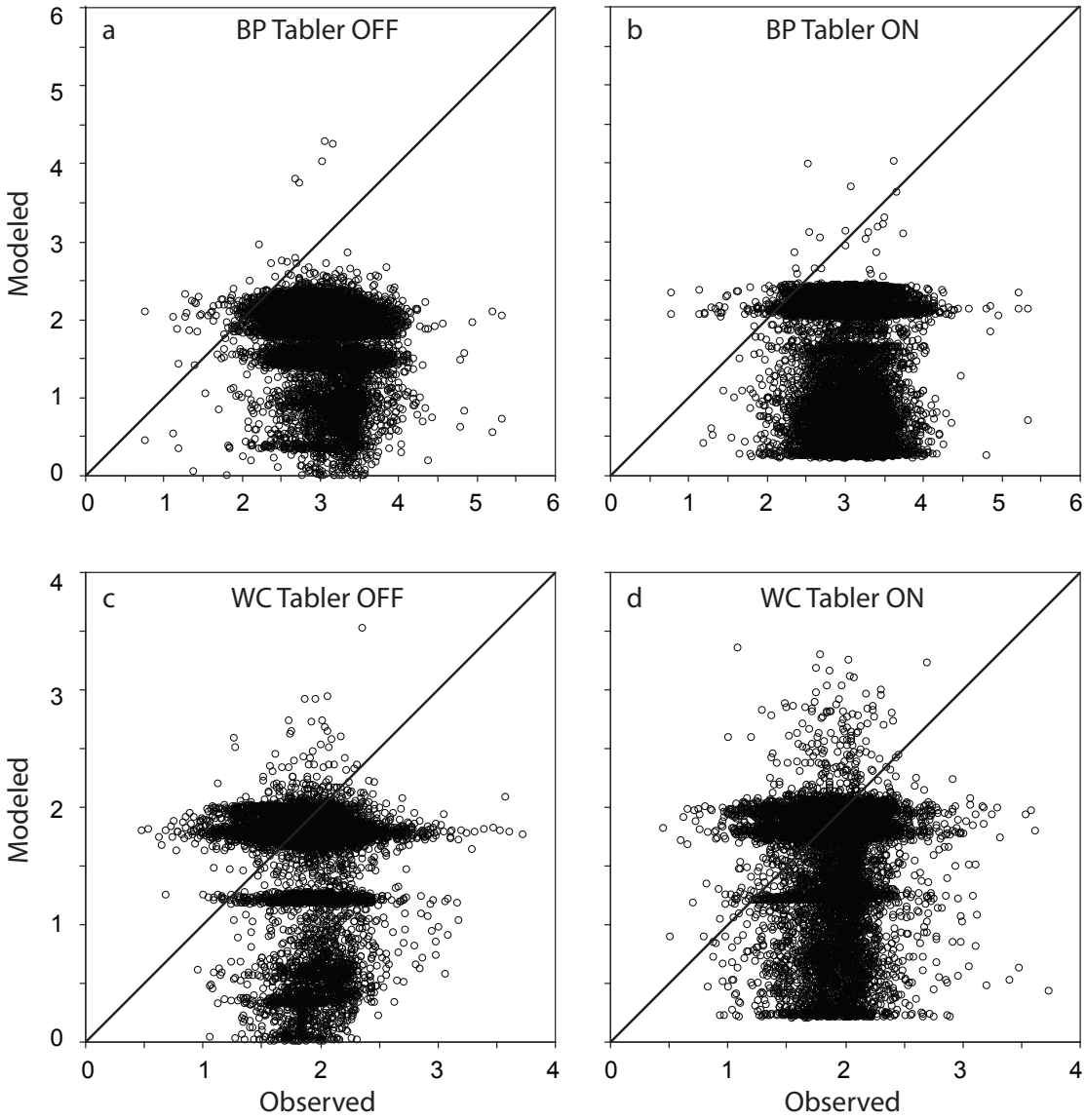

Figure 6.5. Modeled versus observed point snow depth values. (a) BP site, without Tabler sub-model; (b) BP site, with Tabler sub-model; (c) WC site, without Tabler sub-model; (d) WC site, with Tabler sub-model.

will occur, potentially limiting the amount of snow that can accumulate downwind. Comparison of average SWE values (not shown) indicates that the model overestimates snow density by about 5-10%, which contributes to the underprediction of snow depth. If the modeled average depths are recalculated using observed average density values, the depth underprediction decreases to 6% and 35% at WC and BP, respectively. Modeled snow depth standard deviations are similar to observed, though the modeled distributions are substantially narrower and peaked. With the Tabler routine engaged, modeled snow

depths exhibit much greater variance than observed and exhibit a pronounced negative skew. This high variance and the higher-than-observed proportions of zero and low snow depths are due to issues with the sub-grid redistribution described above.

Pointwise comparisons of modeled to observed snow depth (Figure 6.5) show generally poor correspondence with no clear evidence of a linear correlation. The scatterplots indicate that the modeled snow drift locations do not match the observations in most cases, and support the histogram evidence that the model underpredicts snow depth in the majority of locations. Horizontal features in the pointwise graphs suggest that the model preferentially accumulates snow to one or more depths. Some of these artifacts are related to fixed vegetation snow-holding capacities (0.25 m for grass, 5 m for trees), while some are due to difficulties of using the Tabler sub-model in this deep-snow environment. The output maps in Figure 6.3 (b, c) show large forest areas with consistent snow depths of about 1.5 m. These tree areas are snow sinks, and as such their only source of snow is precipitation. Wind redistribution plays a significant role in the two study areas, and therefore a major source of accumulation is not contributing to snow depths in forest areas. This issue was partially addressed by treating some of the vegetation as topographic roughness elements. The deepest modeled snow depths are in the lee of vegetation-topography obstacles, and though the modeled patterns are spatially less complex than observed, the model is clearly succeeding at placing snow drifts in physically realistic locations. This result suggests that the vegetation-topography approach to modeling wind/vegetation interaction is appropriate for applying SnowModel to these sites.

It is worth considering how the scale characteristics of the lidar snow depth datasets compare with those of other data sources commonly used for model evaluation. These data have at least three orders of magnitude greater point density across the domain than more readily acquirable manual depth surveys. The scale characteristics of the lidar data reveal spatially explicit snow depth variability that may be under-represented in

datasets with lower resolution or narrower extent. The snow depth variations mapped by the lidar are in fact produced by sets of processes operating at different scales (see e.g., Blöschl, 1999; Deems *et al.*, 2006). Apparent errors in the model output may be due to scale issues in the model process representations, especially if the model is designed to represent snow processes at scales larger than the resolution of the validation data. SnowModel is commonly run on a 30 m grid over domains covering several square kilometers, and therefore its design does not explicitly incorporate representations of fine-scale processes such as wind turbulence. When used to validate this implementation (5 m grid, 1 km^2 domain), the lidar snow depth data provide an opportunity to evaluate the ability of SnowModel to simulate snow depth patterns at fine and coarse scales simultaneously.

Le Quéré (2006) describes phases in the evolution of process models, wherein substantial changes in model capability and accuracy are driven by technological progress in observation of the modeled phenomena. In this context, the lidar snow depth data represent a high standard of validation that should be expected to highlight model deficiencies, and importantly, provide opportunities to guide further model refinements. One such opportunity is to exploit the resolution and extent of the lidar data to explore process scaling relationships through fractal analysis, and thereby evaluate process representation and guide future model development.

6.3.2 Model performance by fractal analysis

Examination of the visual texture of the output maps (Figure 6.3, a-f) indicates that the model represents fine-scale variations in snow depth that have a similar character or texture to those in the observed data. Thus, spatial patterns can be used to evaluate the model's process representations. Fractal analysis enables an evaluation of model predictions from a spatial pattern perspective, and quantifies scale relationships that are qualitatively evident in the visual texture of the modeled and observed snow depth maps.

Comparison of fractal dimensions can indicate if process representations produce an appropriate balance of short- and long-range variability, and comparison of scale break lengths shows whether changes in process balance occur at proper spatial scales (Deems *et al.*, 2006).

Indeed, log-log variograms show the model simulates fractal power-law snow depth distributions (Figure 6.6; Table 6.2). All of the model runs, however, have *D* values well above those observed in the lidar data at short lag ranges (2.7-2.8, vs. 2.4-2.46). This difference indicates that the modeled balance of short-range and long-range processes needs refinement. However, the model correctly simulates the variance at the shortest and longest lags – it is in the middle lag distances that the model underestimates the spatial variance. This underestimation is related to the lack of a scale break at around 20 m, as is evident in the lidar variogram. The scale break indicates a fundamental change in driving processes at that scale distance, whereas the model maintains a consistent process relationship at all scales at the BP site, and places a scale break at about 270 m at WC. While the observed scale break at 20 m has been interpreted as a shift from wind/vegetation to wind/terrain interactions (Deems *et al.*, 2006), the model scale break at 270 m is likely an artifact of the forest patch sizes representing snow sinks in the WC domain, which appear to be a substantial source of variation above that lag distance (see Figure 6.3d). A similar forest-patch pattern exists in the BP model output (Figure 6.3c), but the patch size and separations are larger than at WC, which would produce a scale break at a lag of around 500 m or more, where it would be buried in the noisy tail of the variogram.

When the Tabler sub-model is activated, the model output shows a scale break at a lag distance close to that of the lidar dataset, indicating that the model successfully represents an important process change at the 20 m scale (Figure 6.6). When the Tabler routine is disabled, the scale break is either nonexistent or is at a larger lag distance than observed in the lidar data. Using the Tabler routine effectively changes the process balance at short lag distances by redistributing snow to drift locations. This empirical drift-making

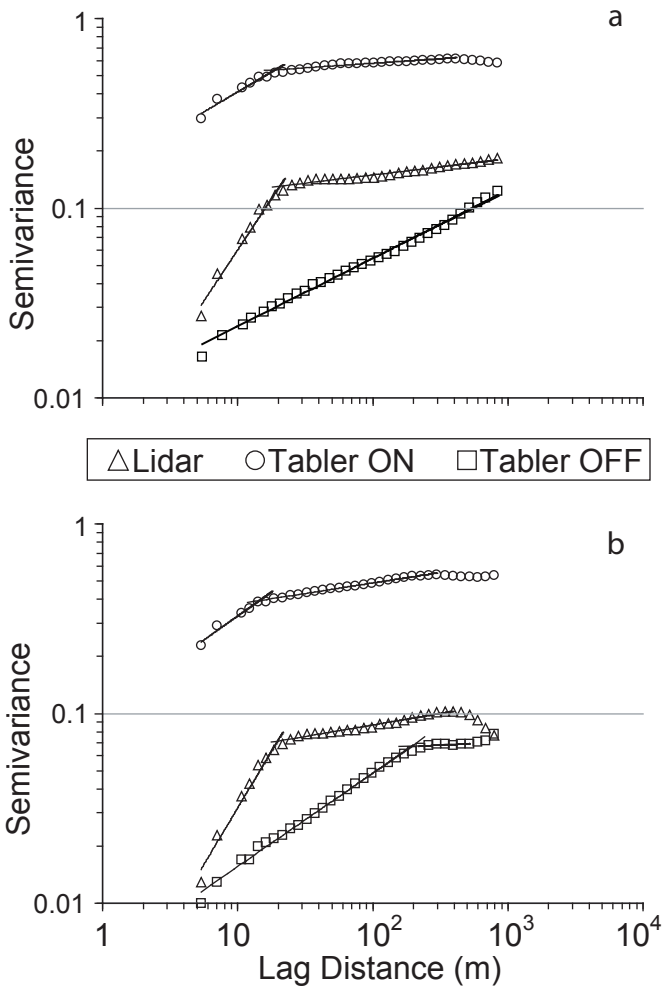

Figure 6.6. Log-log variograms of snow depth for (a) BP and (b) WC.

Table 6.2. Fractal dimensions (D) and scale break distances for observed and modeled snow depths.

	D	**Scale Break Distance (m)**
Buffalo Pass		
Lidar	2.46	21
Tabler ON	2.79	19
Tabler OFF	2.73-2.81	N/A
Walton Creek		
Lidar	2.40	20
Tabler ON	2.75	15
Tabler OFF	2.77-2.80	270

process is evidently superseded by the windflow simulation at a scale of about 20 m. Though the Tabler routine has difficulty simulating drift feature details in this deep-snow application as outlined above, its inclusion generates the scale break at an appropriate lag distance, which is an important result. The overall semivariance of the Tabler-On output is much higher than observed in the lidar data, likely due to the underestimation of snow depth. With greater baseline snow depths, the overall variance would decrease, and the Tabler-On and lidar variograms would be quite similar. As the Tabler sub-model is refined in future versions, it is likely to become an important component of the SnowModel simulation package.

The scale break generated by using the Tabler sub-model suggests that small-scale drift features are important in producing the scale break feature characteristic of the observed dataset, and that constraining the scaling of snow drifts behind obstacles drives the change in fractal pattern represented by the scale break. Though the modeled *D* values are much higher than those observed, they are consistent between sites, supporting the assertion of Deems *et al*. (2006) that the process balance determines the *D* value, while site-specific terrain and vegetation configurations affect the location of the scale break. This can be tested by altering the process relationships within the model by varying critical scaling parameters.

6.3.3 Fractal dimension sensitivity to model parameters

Various values of the model parameters η, γ_s, and γ_c were used to test their effects on the spatial pattern as indexed by the fractal dimension. Table 6.3 summarizes the range and combinations of model parameters examined. Varying these parameters resulted in virtually no effect on the bulk snow depth statistics, with only the range of modeled depth values showing any response. Varying η had only a modest effect on *D* (Figure 6.7b, d), while increasing γ_s with a corresponding decrease in γ_c strongly affected the resulting spatial distributions (Figure 6.7a, c). The γ_s and γ_c parameters directly affect the

Table 6.3. Model parameters and snow depth output statistics. Starred (*) datasets are examined in the wind field and snow depth subsets in Figures 8 -10.

	Model Parameters			Snow Depth Statistics						
Dataset/ Model Run	*η*	*ys*	*yc*	*min*	*avg*	*% avg*	*SD*	*range*	*max*	*D*
BP Lidar	N/A	N/A	N/A	0.1	3.10	N/A	0.42	5.61	5.71	2.46
***BP Run 1**	5	0.25	0.75	0.85	1.93	-0.38	0.28	2.26	3.11	2.73
BP Run 2	10	0.25	0.75	0.84	1.93	-0.38	0.29	2.95	3.79	2.76
BP Run 3	20	0.25	0.75	0.74	1.93	-0.38	0.29	3.59	4.33	2.76
BP Run 4	30	0.25	0.75	0.69	1.93	-0.38	0.29	3.99	4.68	2.75
BP Run 5	40	0.25	0.75	0.70	1.93	-0.38	0.29	4.14	4.84	2.75
***BP Run 6**	50	0.25	0.75	0.67	1.92	-0.38	0.29	4.30	4.97	2.75
***BP Run 7**	5	0.75	0.25	0.75	1.91	-0.38	0.32	5.81	6.56	2.81
BP Run 8	10	0.75	0.25	0.74	1.91	-0.38	0.32	5.96	6.70	2.81
BP Run 9	20	0.75	0.25	0.72	1.91	-0.38	0.32	6.18	6.90	2.81
BP Run 10	30	0.75	0.25	0.74	1.91	-0.38	0.32	6.28	7.02	2.81
BP Run 11	40	0.75	0.25	0.73	1.91	-0.38	0.32	6.39	7.12	2.81
BP Run 12	50	0.75	0.25	0.73	1.91	-0.38	0.32	6.41	7.14	2.81
BP Run 13	5	0.50	0.50	0.83	1.92	-0.38	0.30	3.78	4.61	2.78
BP Run 14	10	0.50	0.50	0.80	1.92	-0.38	0.31	4.18	4.98	2.78
BP Run 15	20	0.50	0.50	0.76	1.92	-0.38	0.30	4.63	5.39	2.78
BP Run 16	30	0.50	0.50	0.73	1.92	-0.38	0.30	4.94	5.67	2.78
BP Run 17	40	0.50	0.50	0.72	1.92	-0.38	0.31	5.14	5.86	2.78
BP Run 18	50	0.50	0.50	0.71	1.92	-0.38	0.30	5.22	5.93	2.79
WC Lidar	N/A	N/A	N/A	0.35	1.94	N/A	0.30	3.62	3.97	2.40
WC Run 1	5	0.25	0.75	0.50	1.70	-0.12	0.27	2.44	2.94	2.77
WC Run 2	10	0.25	0.75	0.45	1.70	-0.12	0.28	3.79	4.24	2.78
WC Run 3	20	0.25	0.75	0.43	1.70	-0.12	0.29	3.92	4.35	2.78
WC Run 4	30	0.25	0.75	0.42	1.70	-0.12	0.29	4.32	4.74	2.78
WC Run 5	40	0.25	0.75	0.39	1.70	-0.12	0.30	4.51	4.90	2.78
WC Run 6	50	0.25	0.75	0.36	1.70	-0.12	0.30	4.72	5.08	2.78
WC Run 7	5	0.5	0.5	0.47	1.69	-0.13	0.29	4.63	5.10	2.78
WC Run 8	10	0.5	0.5	0.45	1.69	-0.13	0.29	5.55	6.00	2.78
WC Run 9	20	0.5	0.5	0.42	1.69	-0.13	0.29	5.57	5.99	2.78
WC Run 10	30	0.5	0.5	0.41	1.69	-0.13	0.29	5.82	6.23	2.79
WC Run 11	40	0.5	0.5	0.39	1.70	-0.12	0.29	5.97	6.36	2.79
WC Run 12	50	0.5	0.5	0.40	1.70	-0.12	0.29	5.90	6.30	2.79
WC Run 13	5	0.75	0.25	0.46	1.69	-0.13	0.29	6.82	7.28	2.80
WC Run 14	10	0.75	0.25	0.46	1.70	-0.12	0.29	7.28	7.74	2.80
WC Run 15	20	0.75	0.25	0.43	1.69	-0.13	0.29	7.31	7.74	2.80
WC Run 16	30	0.75	0.25	0.42	1.69	-0.13	0.30	7.41	7.83	2.80
WC Run 17	40	0.75	0.25	0.42	1.70	-0.12	0.29	7.43	7.85	2.80
WC Run 18	50	0.75	0.25	0.41	1.70	-0.12	0.30	7.47	7.88	2.80

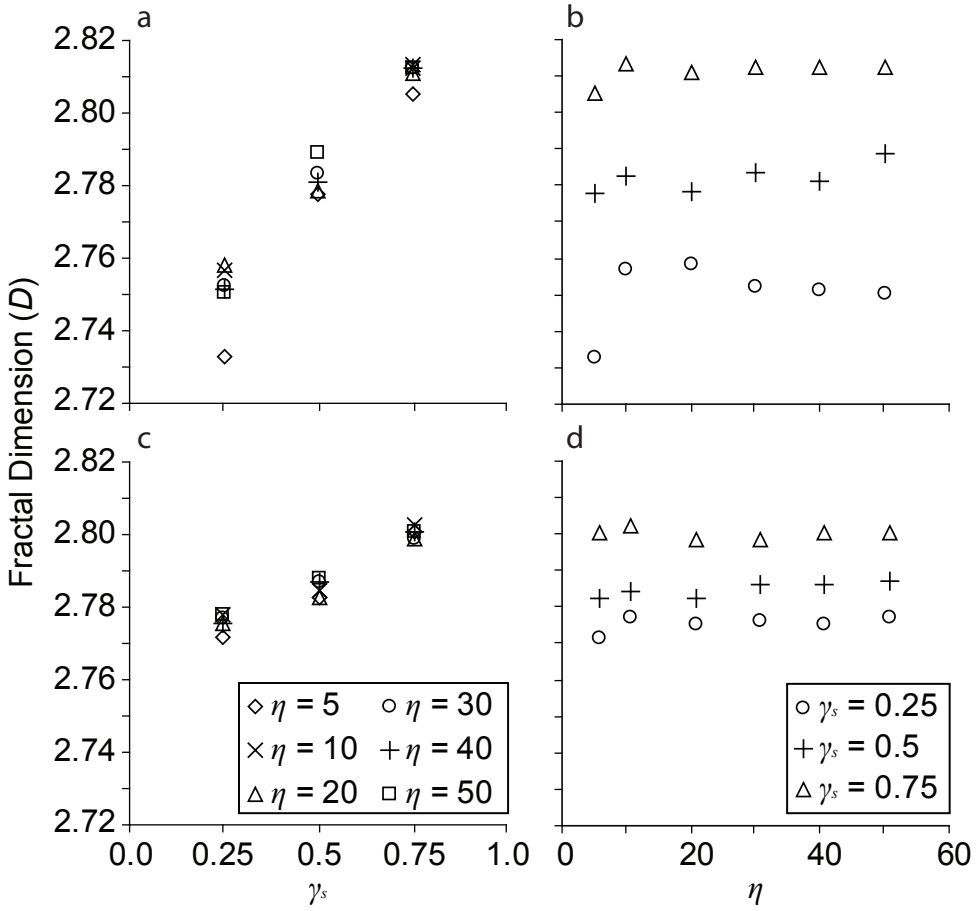

Figure 6.7. Fractal dimension (*D*) as a function of the curvature length scale (η) and slope weight (γ_s) model parameters for BP (a, b) and WC (c, d) sites.

modeled wind field, which in turn governs the patterns of snow erosion and deposition. *D* varies positively with γ_s, indicating that higher wind field dependence on terrain slope serves to increase short-range variability. The effect of changing γ_s is most pronounced at the BP site, where larger vegetation-topography elements exist, and therefore have a greater influence on the fractal properties of the entire domain. On the other hand, η has the secondary effect of determining the length scale over which the terrain curvature is calculated. Larger values will produce slightly smoother curvature fields, which can effectively mask small terrain or vegetation-topography features from the wind speed calculations.

Example wind field effects of changing the slope and curvature weights can be seen in Figures 6.8-10, which show a 30 x 30 m subset of the ribbon forest in the northeast

quadrant of the BP domain (see Figure 6.2a for subset location). In the first panel of each of these figures (a), the wind vector field is shown with the contoured vegetation-topography surface below, while the second panel (b) shows the modeled snow depths and vegetation-topography contours. It is evident that the rapid change in wind speed in the lee of the vegetation-topography obstacles allows wind-transported snow to be deposited, producing lee snowdrifts. The snow depth pattern varies with both the γ_s and η parameters. The greatest contrast in windspeeds in lee areas is produced by γ_s value of 0.75 (Figure 6.9a), and the modeled snow drifts are accordingly deeper and narrower than in the other two simulations. A high γ_s value also produces a stronger wind field overall which could potentially transport greater volumes of snow. This drift pattern produces higher variance over short distances than in the other simulations, resulting in higher *D* values, which indicate a rougher pattern and an increased dominance of short-range driving processes.

An increase in η from 5 m (Figure 6.8) to 50 m (Figure 6.10) has the effect of smoothing the wind field, and thus the smallest vegetation-topography features do not substantially impact the wind field. The resulting snow depth patterns show broader snow drifts than in either of the other two simulations. However, the difference in snow depths over short distances is greater in the simulations with high γ_s values, which consistently produce the highest *D* values. Because γ_s and γ_c were constrained to covary inversely, their effects are inseparable in this analysis, However, it is possible that γ_s has a greater impact than γ_c on the wind field in certain wind directions, as the terrain curvature at each grid cell is an average of the curvature in all directions, while the slope is calculated along the wind direction (Liston and Elder, 2006b).

Within the context of natural-system process-scale relationships, it is clear that interactions between snow, trees, and wind provides a dominant snow distribution mechanism driving process at 5-50 m length scales. The effects of changing the slope and curvature weights on the modeled wind field and resulting snow depth fractal

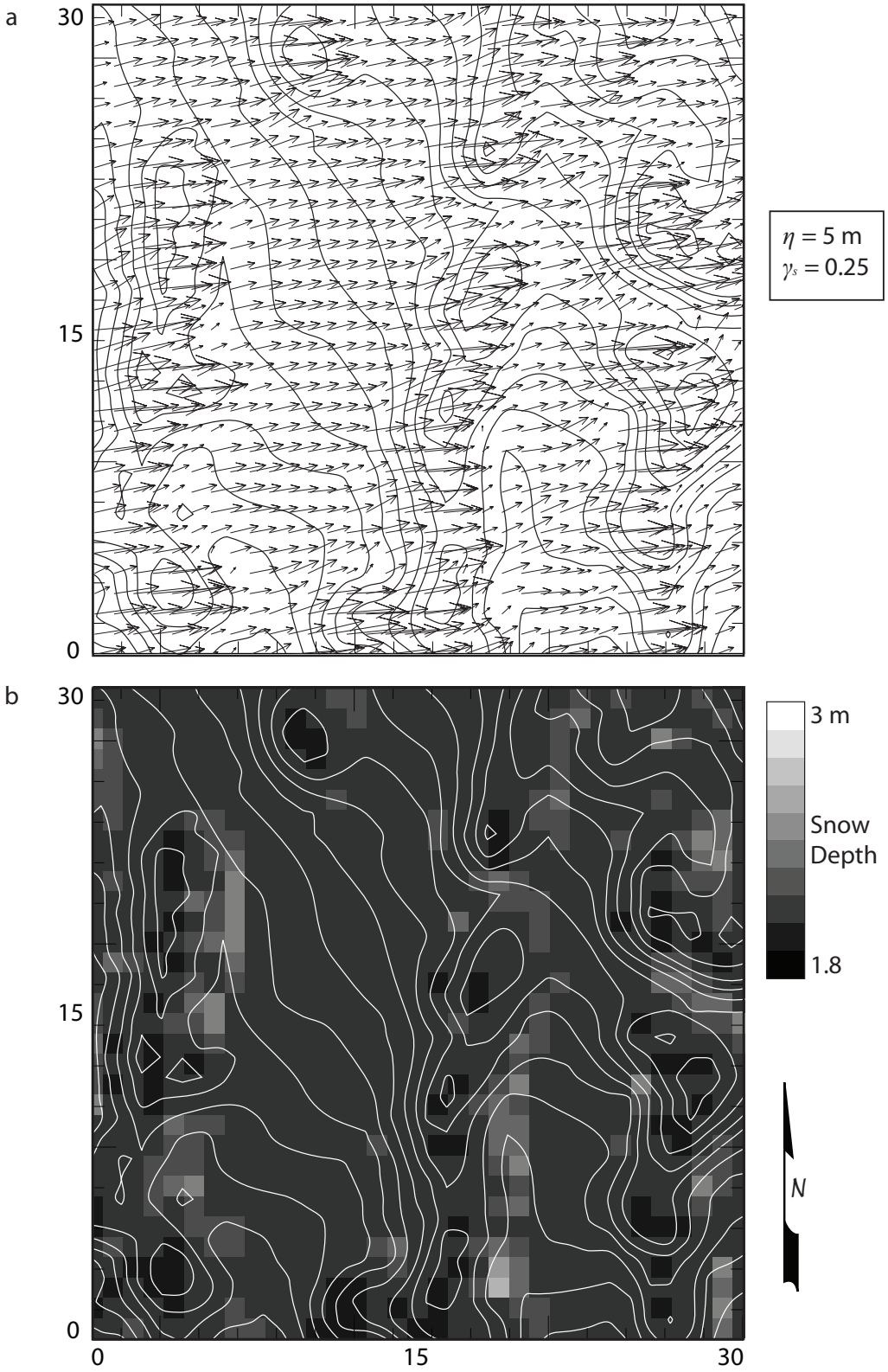

Figure 6.8. Modeled wind vectors (a) and snow depth (b) for a 30 x 30 m subset of the BP domain (see Figure 2a for the subset location). Model parameters: η = 5 m and γ_s = 0.25. Veg-topo contour interval is 2 m.

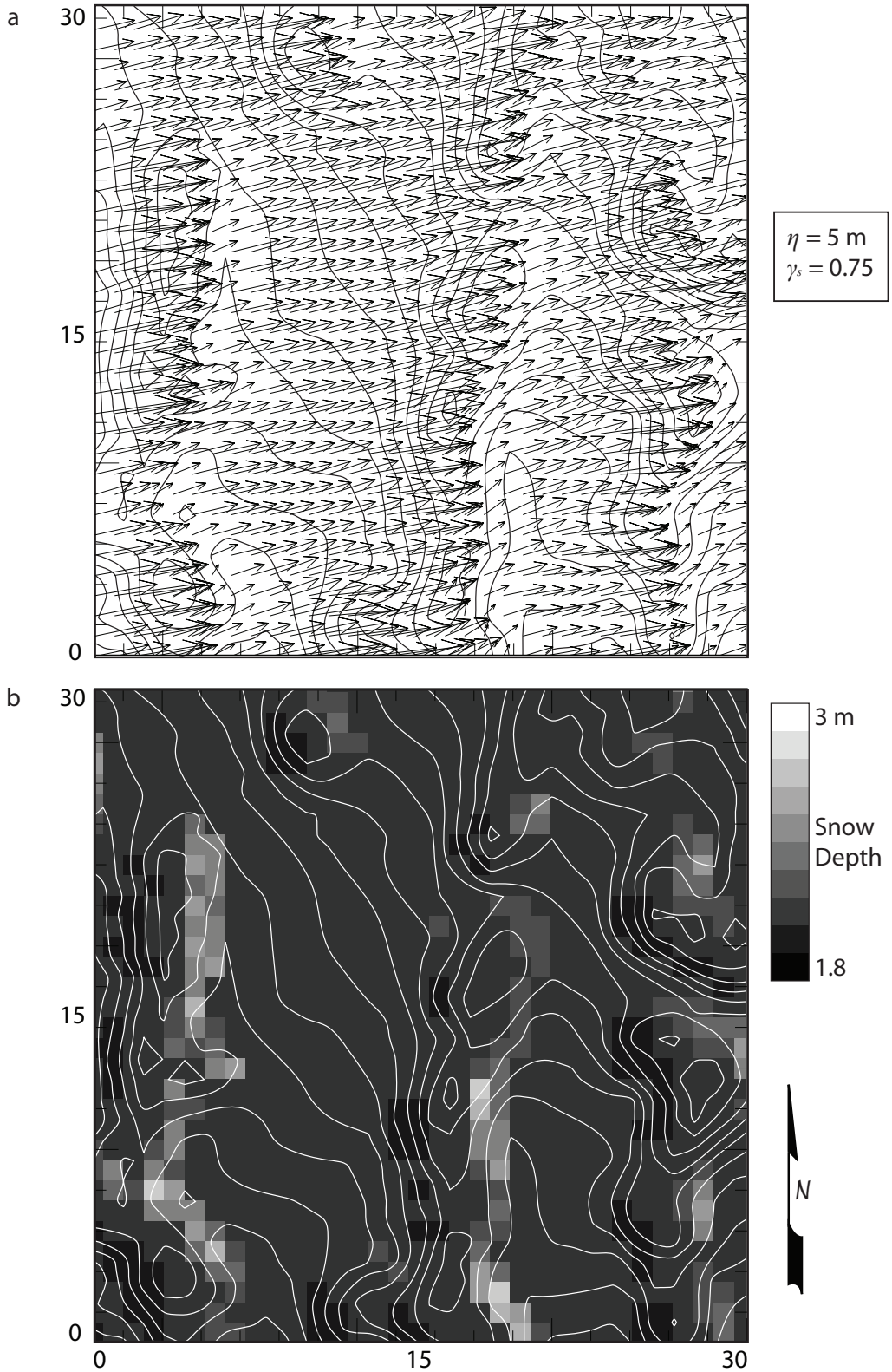

Figure 6.9. Modeled wind vectors (a) and snow depth (b) for a 30 x 30 m subset of the BP domain (see Figure 2a for the subset location). Model parameters: η = 5 m and γ_s = 0.75. Veg-topo contour interval is 2 m.

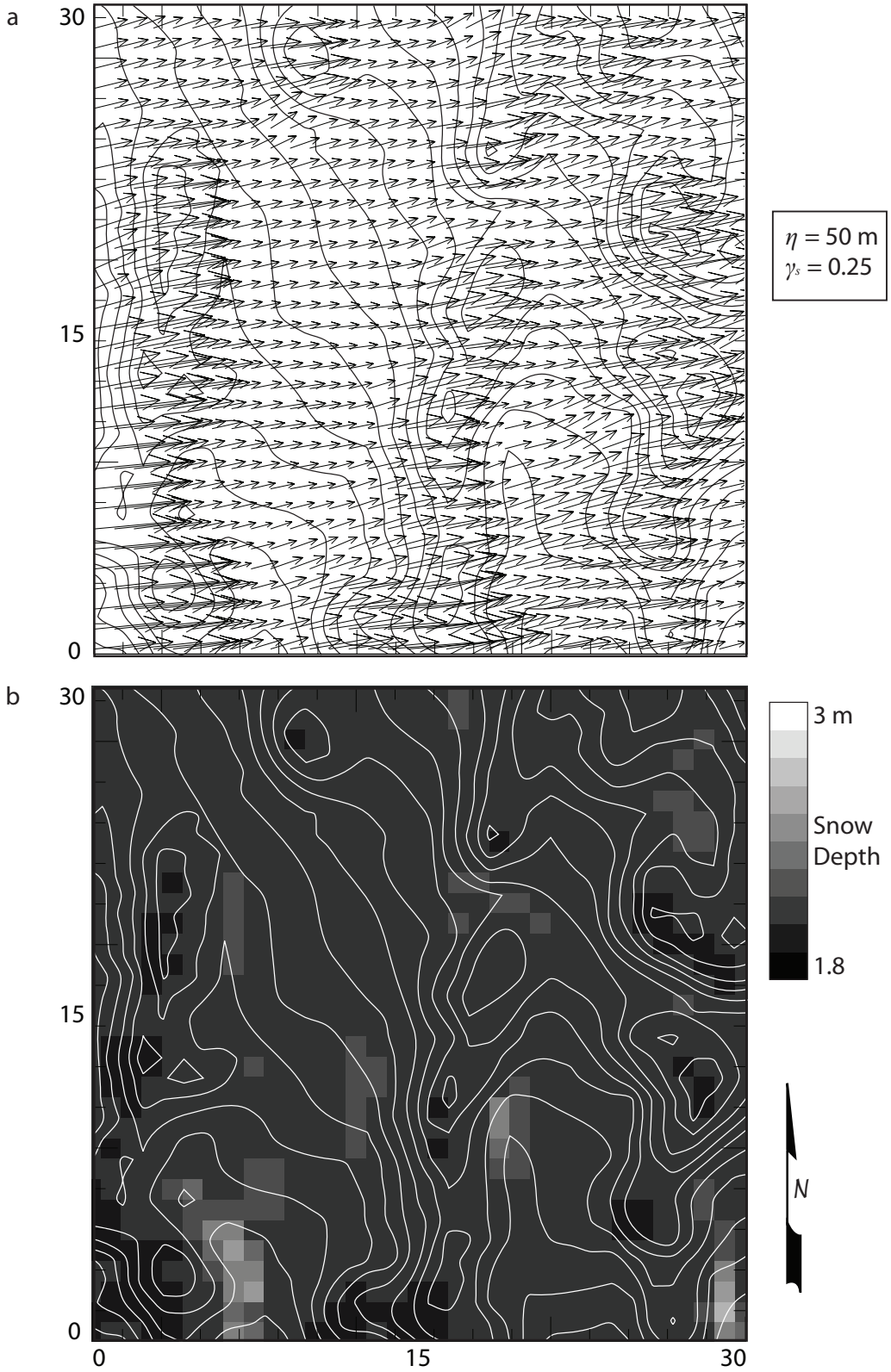

Figure 6.10. Modeled wind vectors (a) and snow depth (b) for a 30 x 30 m subset of the BP domain (see Figure 2a for the subset location). Model parameters: η = 50 m and γ_s = 0.25. Veg-topo contour interval is 2 m.

dimensions provide insight into how small-scale wind flow patterns could produce different snow-depth pattern complexity in different environments, or over time at a single site.

The slope and curvature weights, when combined with the representation of vegetation roughness elements as topography, provide a useful tool for exploring fractal scale relationships in spatial snow depth patterns. As development proceeds on this model, the fractal analysis methods can provide important metrics to guide parameter choices, with improvements in simulated fractal scaling properties indicating that realistic process relationships have been achieved. In midlatitude mountain environments, the vegetation distribution interacts with wind to produce profound effects on spatial snow depth distributions. In these simulations, the inclusion of vegetation roughness elements as terrain components proves to be necessary for simulation of small-scale drift features, and highlights the importance of scale effects in both process representation and input datasets.

6.4 Summary/Conclusions

Snow process models are important tools for exploring relationships among snow system variables, for predicting snow distributions in poorly sampled regions, and for developing input fields for larger-scale models. Spatial validation remains problematic, however, because conventional validation metrics use mean properties or are sensitive to spatial offsets in modeled and observed snow depth fields. This study examined fractal analysis as a supplementary tool to characterize measured and modeled spatial snow depth patterns.

The SnowModel snow evolution modeling system effectively simulates the fractal scaling structure observed in spatial snow depth distributions (e.g., Deems *et al.*, 2006), though with substantially higher fractal dimensions, indicating an imbalance in short- and long-range process components. Additionally, the model output does not show the scale

break at about a 20 m lag distance, as is seen in lidar-measured snow depth distributions. This is not unexpected, as the model is using the same process relationships regardless of scale, and therefore should produce a consistent power-law slope at all scales.

Applying the Tabler sub-grid redistribution model produces interesting, though ultimately imperfect results. With the Tabler sub-model engaged, the simulations show a fractal scale break at a lag distance very near that in the observed data, indicating that the change in process from the Tabler snow drift profile parameterization to wind field/ vegetation-terrain interaction occurs at a realistic length scale – an important result that highlights the role of drift geometry scaling in modeling of spatial snow distributions at scales from 5 to 1000 m. However, the snow depth mean and frequency distribution simulated with the Tabler model are different from observed, and unusual spatial snow depth features are produced. The Tabler sub-model needs further refinement for use in deep-snow environments, but will undoubtedly be a valuable model component in future versions.

The fractal analysis methods also allow investigation of the sensitivity of simulated spatial complexity to scalable model parameters. The fractal dimension appears to be a useful statistic for comparing model outputs from different process realizations, study sites, or temporal slices, as it provides a single number indexing spatial complexity and process scale balance. Therefore, we assert that fractal analysis can be used for evaluating model performance, process representation, and capability at high resolutions. However, conventional validation metrics remain important – if modeled results show realistic spatial scaling patterns but significantly under- or over-predict total SWE volume, the utility of the fractal metrics is limited. In turn, once model simulations produce fractal scaling characteristics consistent with observations, the model will be an important tool for exploring the process relationships that produce the fractal scale patterns. Processes can be introduced, removed, or their influence altered in order to better inform our understanding of the complex process interactions and their relative

importance.

Le Quéré (2006) describes the earth-system-model development process as consisting of several stages, with methodological advances informed by improved observation and validation techniques. Early in the model development sequence, model implementations produce results consistent with limited observations, but are constrained by incomplete knowledge of true process dynamics and variability. As observation techniques improve to provide a clearer picture of the natural system, model performance initially suffers, but the ensuing creativity and exploration of new process representations ultimately benefits the modeling effort and our understanding of the system. Snow evolution modeling is in a period of transition, and the lidar measurement and fractal analysis methods described here contribute to the ongoing model development objective. The lidar observations allow examination of model output at an unprecedented combination of resolution and extent, and enable the development of validation techniques such as fractal analysis that assess natural and modeled process interactions and complexity. Future refinements of SnowModel and other snow-cover evolution models will benefit from these types of investigations that stretch our understanding of natural systems and our ability to simulate system processes.

Snow depth patterns evolve due to multiscale process interactions. It is important for snow process models to be capable of representing all relevant scales of action appropriate to the chosen resolution and domain extent, otherwise the simulated spatial patterns will not contain the proper balance of fine- and coarse-scale variation. The results of this study introduce a tool and context for evaluating and validating scales of process representation in distributed snow models.

CHAPTER 7: CONCLUSIONS

Spatial snow distributions in midlatitude mountain environments are strongly and dynamically linked to many earth surface processes at many scales. The nature and specifics of these connections have seen much investigative interest, aiding understanding of the interactions between hydrologic, biologic, geologic, and atmospheric systems. Accurate and timely knowledge of spatial snow distributions provides important support for practical concerns, such as water supply and hydropower decision-making, as well as for investigations of land-atmosphere interaction or biogeochemical cycling. The broad and fundamental influences of seasonal snowpacks on proximal systems mandates accurate measurement and modeling of snow distributions and processes at many space and time scales.

However, snow properties are very difficult to measure due to their high variability in both space and time and the strong scale dependence of the measured variability. Subsequent extrapolation and modeling efforts are sensitive to the measurement and model scales relative to the snowpack process scales. Issues of scale are critical for ensuring that measurements and simulations of snow distributions are relevant and appropriate to the problem of interest.

To ensure that measurement and model scales are compatible with natural scales of variation in snow processes, knowledge or characterization of snow process scales is required. Recent advances in remote sensing using airborne lidar provide spatial snow depth data of sufficiently high resolution to allow an explicit examination of process scales over distances relevant to catchment hydrology.

7.1 Overview of Research

This research seeks to inform process, measurement, and model scale issues by using airborne lidar data, field observations, and modeled snow accumulation and redistribution processes to pursue three lines of inquiry. First, airborne lidar estimates of snow depth are explored as a data source for scale investigations of spatial snow depth distributions. Second, patterns and scales of spatial variability in snow depth are characterized and quantified using fractal analysis. Finally, the fractal analysis techniques are examined as a tool for verification of a distributed snow process model.

Through these lines of inquiry, this research advances the understanding of scale relationships in snow depth distributions by approaching the problems from the perspective of the mountain snow *system*, a complex and dynamic interaction of atmospheric and radiation balance driving variables with terrain and vegetation features. The complex, nonlinear, and scale-dependent behavior of the system interactions provides substantial challenges to a holistic approach. It is therefore necessary to search for measures, such as fractal dimensions, that provide information about the structure of the system and the complexity of its outputs. In this systems context, scale and process relationships are critical components for understanding or predicting the spatial or temporal changes in a single observable variable.

These investigations are structured by way of the following questions, examined sequentially in chapters 3 through 6: **(1)** Can airborne lidar surveys provide snow depth data with an accuracy, resolution, and extent suitable for addressing seasonal snow process scale questions? **(2)** Is fractal analysis an appropriate method for characterizing snow depth spatial variability and for exploring snow system interactions between terrain, vegetation, weather, and snowpack on the 1 to 1000 meter scale range? **(3)** Are observed scale properties of snow depth spatial pattern consistent, and can they be linked to scale patterns of vegetation or topography? **(4)** How well does a physically-based snow process model (SnowModel) represent the scale properties of wind-terrain/vegetation interaction?

The research presented here contributes several important advances. Airborne lidar can provide accurate, high resolution, and broad extent measurement of snow depths. The optical properties of snow contribute only about 1 cm to the overall elevation error budget for lidar systems operating at the 1064 nm wavelength, which is quite small compared to the order 10 cm errors due to the Global Positioning System (GPS) and Inertial Navigation System (INS) components of the survey systems. Therefore, elevation estimates of snow-covered laser targets are not expected to be any less accurate than snow-free targets. The higher albedo of snow-covered terrain compared to conventional terrestrial targets may actually increase the ground hit fraction in forested areas, or the fraction of laser pulses that successfully penetrate the forest canopy to measure the ground (or snow surface) elevation. These results help establish lidar snow depth retrieval as an increasingly important methodology for snow depth mapping in any terrain.

The high spatial resolution and broad extent of the lidar datasets allow an evaluation of fractal analysis techniques for characterizing and quantifying patterns and scales of spatial variability in snow depth. Log-log variograms of 9 April, 2003 lidar snow depth data from three Colorado mountain sites show two power-law fractal ranges separated by a distinct, site-dependent scale break. The fractal ranges indicate length scales over which driving process relationships are consistent, while the scale break is a lag distance at which those process relationships change fundamentally. This information directly describes the scales of action of snow accumulation, redistribution, and ablation processes, and informs scale considerations for measurement and modeling. These fractal scaling patterns appear to be interannually consistent, according to a comparison of data from two distinctly different snow seasons. This consistency suggests that snow depth scaling properties could be estimated based on site characteristics, and thus inform measurement and modeling design scale decisions.

The fractal characterization of process scale properties over the 1 to 1000 m scale

range subsequently permits an examination of modeled snow depth fields and an evaluation of simulated driving process relationships. The SnowModel seasonal snow cover evolution suite is shown to simulate fractal snow depth distributions, but with a different fractal dimension. The high *D* values indicate that the balance of processes in the model should be adjusted in order to produce a balance of short and long-range variability that is similar to the lidar snow depth patterns. Most revealing is that the modeled snow depth distributions do not display a scale break consistent with that observed in the lidar datasets, unless the Tabler sub-grid redistribution model is activated. Though the Tabler model, which forces lee snow drifts to match an empirical equilibrium drift geometry, causes an underestimation of domain average snow depth, it importantly produces a scale break at a realistic lag distance. Future implementations of the Tabler sub-model will be important for achieving accurate process representations. This result demonstrates that a process shift from wind/vegetation interaction to wind/topography interaction produces the observed scale break, and that this process shift can be successfully modeled. The fractal metrics provide important spatial scaling information that can inform model development and refinement. It is critical that snow models be capable of simulating realistic scale features in basin-scale snow depth distributions, both for increased output accuracy and for use in subsequent model iterations or as input for larger-scale land-atmosphere interaction simulations.

This research advances three important areas of snow hydrology measurement and modeling, with potentially significant implications. Airborne lidar mapping is shown to be an effective and accurate method for acquisition of spatial snow depth data, and moreover to have a unique combination of measurement capabilities. This technology is certain to gain broad application and influence in future studies and operational water resource management. Spatial snow distributions are shown to exhibit consistent fractal scaling properties, and an important process scale breakpoint is identified. This information will aid future measurement and modeling efforts by delineating the scale

ranges over which specific process variations may be treated explicitly. The fractal analysis techniques are shown to be an important new metric for evaluating model performance and design. When combined with conventional model validation metrics, fractal measures can add spatial pattern and scale considerations to the overall validation effort.

This investigation of scale relationships in snow depth distributions also contributes to an understanding of mountain snowpacks as a system composed of complex, multiscale process interactions. Conventional, reductionist investigations of individual system components provide fundamental knowledge of snow accumulation and ablation processes, but are limited in their ability to account for multiple, scale-dependent process interactions. Fractal analysis provides metrics that help to characterize the scale properties of the snow system seen through the spatial or temporal behavior of a single observable variable. Spatial snow depth patterns are a product of interactions among precipitation, terrain, vegetation, wind, energy balance, and metamorphic processes, related to each other through complex, interdependent linkages. The scale break and fractal dimension describe the complexity of snow depth patterns, and identify both length scales at which the interactions between processes change and scale ranges over which process relationships are consistent.

In support of measurement and modeling interests, process scale information from fractal analysis could be useful for developing strategies to sample variability relevant to the scale of interest, for identifying important processes over specific scale ranges, and for evaluating scale characteristics or biases of existing data or models. Future applications of fractal analysis techniques at narrower and wider scales, in different environments, and for different snow system variables will increase the utility and applicability of process scale information for measuring and modeling seasonal snow properties and distributions.

7.2 Future Investigations

Perhaps most importantly, this research invites a broad array of future investigations. Airborne lidar shows much promise for future snow depth mapping, with its high resolution, broad extent, high accuracy, and ability to map areas too dangerous or remote to sample manually. Lidar snow depth data are likely to play an important role in water supply and snow hydrology research and management in the near future.

Fractal scaling investigations, ideally using lidar snow depth data, could be expanded to different locations. The results of the current project indicate that fractal scaling properties of snow depth depend in large part on the physiographic and vegetation properties of the individual study site. The strength of this dependence could be evaluated and exploited by applying the fractal scale analysis to an array of sites comprising spectra of relief, forest cover, and snow climate (continentality). Of equal interest would be an exploration of the temporal evolution of the fractal snow depth distributions at a single site. The temporal study could evaluate the influence of individual storms and track the convergence of diverse early-season spatial patterns to the remarkably consistent end-of-winter distributions observed in this study and elsewhere.

The variogram fractal analysis techniques could also be applied to a wider range of length scales. Other scale breaks are likely to exist at different lag distances due to changes in the spatial pattern of other driving processes, for example wind turbulence and surface friction at finer scales and topography or vegetation assemblages at coarser scales. It is also an open question as to which snow property is most appropriate for scaling study over a given scale range. While snow depth appears to exhibit the primary mode of variation over the length scales examined in this project (1-1000 m), other variables may supersede depth in importance as the scale of observation changes. At shorter distances, surface roughness may deserve explicit treatment while snow depth appears to vary minimally. At longer distances, depth variations may average out, and snow-covered area or SWE may emerge to display the dominant variation.

Expansion of the fractal techniques to wider scale ranges is sure to encounter significant sampling challenges. In that light, snow process models may provide the best venue for studying scale effects. Inversely, use of process models to explore scale issues will have a positive influence on process model development, strengthening the ability to produce realistic simulations of spatial snow patterns. Fractal dimensions and scale break lengths, used as validation metrics, can inform modeled process representations, and provide quantitative criteria for model parameter choices. As snow process models develop the ability to simulate realistic spatial scale features, the models can in turn be used to explore the specific process dynamics that produce the scale features, increasing the understanding of the emergence of fractal patterns from complex systems.

This research has built upon well-established issues of scale in geographic sciences and snow hydrology, and applied techniques developed in other areas of geophysical research to quantify scale relationships in midlatitude mountain snowpacks. The combination of field measurements, remotely-sensed data, and snow process modeling is a well-established combination for addressing issues of scale and spatial variation in these highly dynamic environments. In this case, the high resolution of the lidar datasets allows the application of fractal analysis techniques at multiple sites and covering a wide range of scales that is difficult to cover using conventional, ground-based survey methods. The value of these contributions, however, lies mainly in the avenues opened for future research. In that respect this study represents merely the first in what is likely a series of investigations using the measurement, modeling, and analysis techniques applied here to spatial snow depth patterns. Studies of this nature, exploring process interrelationships between atmospheric, hydrologic, biologic, and geophysical systems, have tremendous potential for advancing the state of knowledge in hydrology specifically, and in earth system science in general.

REFERENCES

Bales, R. C., N. P. Molotch, T. H. Painter, M. D. Dettinger, R. Rice, and J. Dozier, 2006: Mountain hydrology of the western United States. *Water Resources Research*, **42**.

Balk, B. and K. Elder, 2000: Combining binary decision tree and geostatistical methods to estimate snow distribution in a mountain watershed. *Water Resources Research*, **36**, 13-26.

Baltsavias, E. P., 1999: Airborne laser scanning: Basic relations and formulas. *ISPRS Journal of Photogrammetry and Remote Sensing*, **54**, 199-214.

Barry, R. G., 1992: *Mountain Weather and Climate*. 2nd ed. Routledge, London, UK, 402 pp.

Birkeland, K. W., K. J. Hansen, and R. L. Brown, 1995: The spatial variability of snow resistance on potential avalanche slopes. *Journal of Glaciology*, **41**, 183-189.

Blöschl, G., 1999: Scaling issues in snow hydrology. *Hydrological Processes*, **13**, 2149-2175.

Blöschl, G. and R. Kirnbauer, 1992: An analysis of snowcover patterns in a small alpine catchment. *Hydrological Processes*, **6**, 99-109.

Blöschl, G., D. Gutknecht, and R. Kirnbauer, 1991: Distributed snowmelt simulations in an alpine catchment 2. Parameter study and model predictions. *Water Resources Research*, **27**, 3181-3188.

Brewer, J., L. Di Girolamo, J. AF Brewer, and L. Di Girolamo, 2006: Limitations of fractal dimension estimation algorithms with implications for cloud studies, *Atmospheric Research*, **82**, 433-454.

Brooks, P. D. and M. Williams, 1999: Snowpack controls on nitrogen cycling and export in seasonally snow-covered catchments. *Hydrological Processes*, **13**, 2177-2190.

Bruland, O., G. E. Liston, J. Vonk, K. Sand, and A. Killingtveit, 2004: Modelling the snow distribution at two high arctic sites in Svalbard, Norway, and at an alpine site in central Norway. *Nordic Hydrology*, **35**, 191-208.

Burrough, P., 1981: Fractal dimensions of landscapes and other environmental data. *Nature*, **294**, 240-242.

Burrough, P., 1993: "Fractals and geostatistical methods in landscape studies." *Fractals in Geography*, N. S. Lam and L. DeCola, Eds., Prentice-Hall: Englewood Cliffs, NJ, 87-121.

Cline, D., K. Elder, B. Davis, J. Hardy, G. Liston, D. Imel, S. Yueh, A. Gasiewski, G. Koh, R. Armstrong, and M. Parsons, 2003: An overview of the NASA Cold Lands Processes Field Experiment (CLPX-2002). *Proceedings of SPIE Volume: 4894 Microwave Remote Sensing of the Environment III*, C. D. Kummerow; J. Jiang; S. Uratuka, Eds., 361-372.

Cline, D., R. Armstrong, R. Davis, K. Elder, and G. Liston, cited Access 2001: NASA Cold Land Processes Field Experiment Plan. [Available online from http://www.nohrsc.nws.gov/~cline/clpx.html].

Conway, H. and J. Abrahamson, 1984: Snow stability index. *Journal of Glaciology*, **30**, 321-327.

Deems, J. S., K. J. Elder, and S. R. Fassnacht, 2007: Interannual consistency in fractal snow depth patterns at two Colorado mountain sites. *Journal of Hydrometeorology, in review*.

Deems, J. S., S. R. Fassnacht, and K. J. Elder, 2006: Fractal distribution of snow depth from LiDAR data. *Journal of Hydrometeorology*, **7**, 285-297.

Dozier, J. and T. Painter, 2004: Multispectral and hyperspectral remote sensing of alpine snow properties. *Annual Review of Earth and Planetary Sciences*, **32**, 465-494.

Dressler, K. A., G. H. Leavesley, R. C. Bales, and S. R. Fassnacht, 2006: Evaluation of gridded snow water equivalent and satellite snow cover products for mountain basins in a hydrologic model. *Hydrological Processes*, **20**, 673-688.

Elder, K. and A. Goodbody, cited Access 2004: CLPX-Ground: ISA Main Meteorological Data. [Available online from http://nsidc.org/data/clpx/].

Elder, K., J. Dozier, and J. Michaelsen, 1991: Snow accumulation and distribution in an alpine watershed. *Water Resources Research*, **27**, 1541-1552.

Elder, K., J. Michaelsen, and J. Dozier, 1995: Small basin modeling of snow water equivalence using binary regression tree methods. *Proceedings of the Symposium on Biogeochemistry of Seasonally Snow-Covered Catchments,* Boulder, CO, IAHS-AIHS and IUGG XX General Assembly, IAHS Publication 228,129-139.

Erickson, T. A., M. W. Williams, and A. Winstral, 2005: Persistence of topographic controls on the spatial distribution of snow in rugged mountain terrain, Colorado, United States. *Water Resources Research*, **41**, 1-17.

Essery, R., 2001: Spatial statistics of windflow and blowing-snow fluxes over complex topography. *Boundary-Layer Meteorology*, **100**, 131-147.

Essery, R., L. Li, and J. Pomeroy, 1999: A distributed model of blowing snow over complex terrain. *Hydrological Processes*, **13**, 2423-2438.

Fassnacht, S. R., 2004: Estimating alter-shielded gauge snowfall undercatch, snowpack sublimation, and blowing snow transport at six sites in the coterminous United States. *Hydrological Processes*, **18**, 3481-3492.

Fassnacht, S. R., K. A. Dressler, and R. C. Bales, 2003: Snow water equivalent interpolation for the Colorado River Basin from snow telemetry (SNOTEL) data. *Water Resources Research*, **39**, 1208-1218.

Gao, J. and Z. Xia, 1996: Fractals in physical geography. *Progress in Physical Geography*, **20**, 178-191.

Granger, R. J., J. W. Pomeroy, and J. Parviainen, 2002: Boundary-layer integration approach to advection of sensible heat to a patchy snow cover. *Hydrological Processes*, **16**, 3559-3569.

Groisman, P. and T. Davies, 2001: Snow cover and the climate system. *Snow Ecology*, H. Jones, Pomeroy, J.W., Walker, D.A., and R.W. Hoham, Eds.,Cambridge University Press: Cambridge, UK, 1-44.

Hiemstra, C., G. Liston, and W. Reiners, 2002: Snow redistribution by wind and interactions with vegetation at upper treeline in the Medicine Bow Mountains, Wyoming, U.S.A. *Arctic, Antarctic, & Alpine Research*, **34**, 262-273.

Hiemstra, C., G. E. Liston and W. Reiners, 2006: Observing, modelling, and validating snow redistribution by wind in a Wyoming upper treeline landscape. *Ecological Modelling*, **197**, 35-51.

Hopkinson, C., M. Sitar, L. Chasmer, C. Gynan, D. Agro, R.. Enter, J. Foster, N. Heels, C. Hoffman, J. Nillson, and R. StPierre, 2001: Mapping the spatial distribution of snowpack depth beneath a variable forest canopy using airborne laser altimetry. *Eastern Snow Conference*, Ottowa, Ontario, Canada, 253-264.

Hopkinson, C., M. Sitar, L. Chasmer, and P. Treitz, 2004: Mapping snowpack depth beneath forest canopies using airborne lidar. *Photogrammetric Engineering and Remote Sensing*, **70**, 323-330.

Jones, H. G., 1999: The ecology of snow-covered systems: a brief overview of nutrient cycling and life in the cold. *Hydrological Processes*, **13**, 2135-2147.

Jones, H. G., Pomeroy, J. W., Walker, D. A., Hoham, R. W., 2001: *Snow Ecology: An Interdisciplinary Examination of Snow-Covered Ecosystems*. Cambridge University Press: Cambridge, UK, 378 pp.

Klinkenberg, B. and M. F. Goodchild, 1992: The fractal properties of topography: a comparison of methods. *Earth Surface Processes & Landforms*, **17**, 217-234.

Kraus, K. and N. Pfeifer, 1998: Determination of terrain models in wooded areas with airborne laser scanner data. *ISPRS Journal of Photogrammetry and Remote Sensing*, **53**, 193-203.

Kuchment, L. S. and A. N. Gelfan, 1997: Statistical self-similarity of spatial snow accumulation variations and its application to snowmelt runoff models. *Russian Meteorology and Hydrology*, **7**, 53-60.

Kuchment, L. S. and A. N. Gelfan, 2001: Statistical self-similarity of spatial variations of snow cover: verification of the hypothesis and application in the snowmelt runoff generation models. *Hydrological Processes*, **15**, 3343-3355.

Lam, N. S. and L. DeCola, 1993: *Fractals in geography*. Blackburn Press: Caldwell, NJ, 308 pp.

Le Quéré, C., 2006: The unknown and the uncertain in earth system modeling. *Eos, Transactions, American Geophysical Union*, **87**(45), 496-497.

Lefsky, M. A., W. B. Cohen, G. G. Parker, and D. J. Harding, 2002: Lidar remote sensing for ecosystem studies. *BioScience*, **52**, 19-30.

Levin, S. A., 1992: The problem of pattern and scale in ecology. *Ecology*, **73**, 1943-1967.

Liston, G., 1995: Local advection of momentum, heat, and moisture during the melt of patchy snow covers. *Journal of Applied Meteorology*, **34**, 1705-1715.

Liston, G., 1999: Interrelationships among snow distribution, snowmelt, and snow cover depletion: Implications for atmospheric, hydrologic, and ecologic modeling. *Journal of Applied Meteorology*, **38**, 1474-1487.

Liston, G. and K. Elder, 2006a: A distributed snow-evolution modeling system (SnowModel). *Journal of Hydrometeorology*, **7**, 1259-1276.

Liston, G. and K. Elder, 2006b: A meteorological distribution system for high-resolution terrestrial modeling (MicroMet). *Journal of Hydrometeorology*, **7**, 217-234.

Liston, G., R. B. Haehnel, M. Sturm, C. A. Hiemstra, S. Berezovskaya, and R. D. Tabler, 2007: Simulating complex snow distributions in windy environments using SnowTran-3D. *Journal of Glaciology,* **181***, forthcoming*.

Liston, G. and M. Sturm, 1998: A snow-transport model for complex terrain. *Journal of Glaciology*, **44**, 498-516.

Liston, G. and M. Sturm, 2002: Winter precipitation patterns in arctic Alaska determined from a blowing-snow model and snow depth observations. *Journal of Hydrometeorology*, **3**, 646-659.

Litaor, M. I., T. R. Seastedt, and D. A. Walker, 2002: Spatial analysis of selected soil attributes across an alpine topographic/snow gradient. *Landscape Ecology*, **17**, 71-85.

Luce, C. H., D. G. Tarboton, and K. R. Cooley, 1998: The influence of the spatial distribution of snow on basin-averaged snowmelt. *Hydrological Processes*, **12**, 1671-1683.

Luce, C. H., D. G. Tarboton, and K. R. Cooley, 1999: Sub-grid parameterization of snow distribution for an energy and mass balance snow cover model. *Hydrological Processes*, **13**, 1921-1933.

Malamud, B. D. and D. L. Turcotte, 1999: Self-organized criticality applied to natural hazards. *Natural Hazards*, **20**, 93-116.

Mandelbrot, B., 1983: *The Fractal Geometry of Nature*. W.H. Freeman: San Francisco, CA, 468 pp.

Marchand, W. D. and A. Killingtveit, 2004: Statistical properties of spatial snowcover in mountainous catchments in Norway. *Nordic Hydrology*, **35**, 101-117.

Mark, D. M. and P. B. Aronson, 1984: Scale-dependent fractal dimensions of topographic surfaces: An empirical investigation, with applications in geomorphology and computer mapping. *Mathematical Geology*, **16**, 671-683.

Marks, D. and J. Dozier, 1992: Climate and Energy Exchange at the Snow Surface in the Alpine Region of the Sierra Nevada 2. Snow Cover Energy Balance. *Water Resources Research*, **28**, 3043-3054.

Matheron, G., 1963: Principles of geostatistics. *Economic Geology*, **58**, 1246-1266.

Miller, S. L., cited Access 2003: CLPX-Airborne: Infrared Orthophotography and LIDAR Topographic Mapping. [Available online from http://www.nsidc.org.].

Miller, S. L., K. J. Elder, D. Cline, R. E. Davis, and E. Ochs, 2003: Use of LIDAR for measuring snowpack depth. *Eos, Transactions, American Geophysical Union*, **84**(46) Fall Meeting Supplement, Abstract C42C-05.

Optech, I., cited Access 2006: ALTM 3100EA Specifications. [Available online from http://www.optech.ca/pdf/Brochures/ALTM3100EAwspecsfnl.pdf].

Pachepsky, Y., J. C. Ritchie, and D. Gimenez, 1997: Fractal modeling of airborne laser altimetry data. *Remote Sensing of Environment*, **61**, 150-161.

Pachepsky, Y. and J. Ritchie, 1998: Seasonal changes in fractal landscape surface roughness estimated from airborne laser altimetry data. *International Journal of Remote Sensing*, **19**, 2509-2516.

Pagano, T., P. Pasteris, M. Dettinger, D. Cayan, and K. Redmond, 2004: Water Year 2004: Western Water Managers Feel the Heat. *Eos*, *Transactions, American Geophysical Union*, **85**(40), 385-400.

Painter, T. H., J. Dozier, D. A. Roberts, R. E. Davis, and R. O. Green, 2003: Retrieval of subpixel snow-covered area and grain size from imaging spectrometer data. *Remote Sensing of Environment*, **85**, 64-77.

Painter, T. H., J. Dozier, C. McKenzie, and R. E. Davis: Retrieval of subpixel snow-covered area and grain size from MODIS reflectance data, *in preparation*.

Peters, O. and K. Christensen, 2002: Rain: relaxations in the sky. *Physical Review E*, **66**, 036120-1-036120-9.

Phillips, J. D., 1986: Spatial analysis of shoreline erosion, Delaware Bay, New Jersey. *Annals of the Association of American Geographers*, **76**, 50-62.

Phillips, J. D., 1999: *Earth surface systems: complexity, order, and scale.* Blackwell Publishing: Oxford ,UK, 180 pp.

Pomeroy, J. W., P. Marsh, and D. M. Gray, 1997: Application of a distributed blowing snow model to the arctic. *Hydrological Processes*, **11**, 1451-1464.

Poveda-Jaramillo, G. and C. E. Puente, 1993: Strange attractors in atmospheric boundary-layer turbulence. *Boundary-Layer Meteorology*, **64**, 175-197.

Purves, R. S., J. S. Barton, W. A. Mackaness, and D. E. Sugden, 1998: The development of a rule-based spatial model of wind transport and deposition of snow. *Annals of Glaciology*, **26**, 197-202.

Reutebach, S. E., R. J. McGaughey, A. H.-E., and W. W. Carson, 2003: Accuracy of a high-resolution lidar terrain model under a conifer forest canopy. *Canadian Journal of Remote Sensing*, **29**, 527-535.

Reutebuch, S. E., A. H.-E., and R. J. McGaughey, 2005: Light detection and ranging (LIDAR): An emerging tool for multiple resource inventory. *Journal of Forestry*, **103**, 286-292.

Roe, G. H., 2005: Orographic precipitation. *Annual Review of Earth & Planetary Sciences*, **33**, 645-676.

Romano, M., 2006: Merrick & Co., *Personal Communication*, August 9, 2006.

Rosenthal, W. and J. Dozier, 1996: Automated mapping of montane snow cover at subpixel resolution from the Landsat Thematic Mapper. *Water Resources Research*, **32**, 115-130.

Roth, R., 2007: Leica Geosystems, *Personal Communication,* May 7, 2007.

Serreze, M. C., M. P. Clark, and A. Frei, 2001: Characteristics of large snowfall events in the montane western United States as examined using snowpack telemetry (SNOTEL) data. *Water Resources Research*, **37**, 675-688.

Shook, K. and D. M. Gray, 1996: Small-scale spatial structure of shallow snowcovers. *Hydrological Processes*, **10**, 1283-1292.

Shook, K. and D. M. Gray, 1997: Synthesizing shallow seasonal snow covers. *Water Resources Research*, **33**, 419-426.

Shook, K., D. M. Gray, and J. W. Pomeroy, 1993: Temporal variation in snowcover area during melt in prairie and alpine environments. *Nordic Hydrology*, **24**, 183-198.

Sturm, M., McFadden, J. P., Liston, G. E., Chapin, F. S., III, Racine, C. H., Holmgren, J., 2001: Snow shrub interactions in arctic tundra: A hypothesis with climatic implications. *Journal of Climate*, **13**, 336-344.

Sun, W., G. Xu, P. Gong, S. Liang, W. AF Sun, G. Xu, P. Gong, and S. Liang, 2006: Fractal analysis of remotely sensed images: A review of methods and applications, *International Journal Of Remote Sensing,* **27**, 4963-4990.

Tabler, R. D., 1975: Predicting profiles of snowdrifts in topographic catchments. *43rd Annual Western Snow Conference*, San Diego, CA, 87-97.

Tabler, R., 1980: Self-similarity of wind profiles in blowing snow allows outdoor modeling. *Journal of Glaciology*, **26**, 421-434.

Tarboton, D. G., R. L. Bras, and I. Rodriguez-Iturbe, 1988: The fractal nature of river networks. *Water Resources Research*, **24**, 1317-1322.

Tobler, W. R., 1970: A computer model simulation of urban growth in the Detroit region. *Economic Geography*, **46**, 234-240.

Turcotte, D. L. and J. Huang, 1995: Fractal distributions in geology, scale invariance, and deterministic chaos. *in Fractals in the Earth Sciences*, C. Barton and P. L. Pointe, Eds., Plenum Press: New York, NY, 1-40.

Webster, R. and M. Oliver, 2001: *Geostatistics for Environmental Scientists*, John Wiley and Sons: Chichester, England, 271 pp.

Wehr, A. and U. Lohr, 1999: Airborne laser scanning - an introduction and overview. *ISPRS Journal of Photogrammetry and Remote Sensing*, **54**, 68-82.

Wen, R. and R. Sinding-Larsen, 1997: Uncertainty in fractal dimension estimated from power spectra and variograms. *Mathematical Geology*, **29**, 727-753.

Winstral, A. and D. Marks, 2002: Simulating wind fields and snow redistribution using terrain-based parameters to model snow accumulation and melt over a semi-arid mountain catchment. *Hydrological Processes*, **16**, 3585-3603.

Winstral, A., K. Elder, and R. E. Davis, 2002: Spatial snow modeling of wind-redistributed snow using terrain-based parameters. *Journal of Hydrometeorology*, **3**, 524-538.